2012-05-07

Water and Carbon Balances of Deciduous and Evergreen Broadleaf Trees from a Subtropical Cloud Forest in Southwest China

Yongjiang Zhang
University of Miami, zhangyj@bio.miami.edu

UNIVERSITY OF MIAMI

WATER AND CARBON BALANCES OF DECIDUOUS AND EVERGREEN BROADLEAF TREES FROM A SUBTROPICAL CLOUD FOREST IN SOUTHWEST CHINA

By

Yongjiang Zhang

A DISSERTATION

Submitted to the Faculty
of the University of Miami
in partial fulfillment of the requirements for
the degree of Doctor of Philosophy

Coral Gables, Florida

May 2012

UNIVERSITY OF MIAMI

A dissertation submitted in partial fulfillment of
the requirements for the degree of
Doctor of Philosophy

WATER AND CARBON BALANCES OF DECIDUOUS AND EVERGREEN BROADLEAF TREES FROM A SUBTROPICAL CLOUD FOREST IN SOUTHWEST CHINA

Yongjiang Zhang

Approved:

_____
Guillermo Goldstein, Ph.D.
Professor of Biology

_____
Terri A. Scandura, Ph.D.
Dean of the Graduate School

_____
Donald L. DeAngelis, Ph.D.
Professor of Biology

_____
David P. Janos, Ph.D.
Professor of Biology

_____
David W. Lee, Ph.D.
Professor of Biology
Florida International University

ZHANG, YONGJIANG (Ph.D., Biology)

Water and Carbon Balances of Deciduous and Evergreen Broadleaf Trees from a Subtropical Cloud Forest in Southwest China (May 2012)

Abstract of a dissertation at the University of Miami.

Dissertation supervised by Professor Guillermo Goldstein.
No. of pages in text. (145)

Evergreen and deciduous trees are conspicuous growth forms across most forest ecosystems around the world. The competition or coexistence between deciduous and evergreen tree species is an old but important ecological topic. The relative advantages of being deciduous or evergreen and the environmental constraints on tree and ecosystem level carbon assimilation in subtropical forests are poorly understood. Evergreen broadleaf trees dominate the forests from elevations of 1000 to 2600 m in the subtropical area of Southwest China, while the subtropical forests from Southeast China at similar elevations are dominated by deciduous trees. The eco-physiological mechanism in explaining this distribution pattern is an interesting topic that has not yet been studied. The objectives of this dissertation were (1) to understand the difference in daily water use and photosynthesis between subtropical evergreen and deciduous tree species, (2) to understand the environmental constraints on the leaf and ecosystem level carbon assimilation of the subtropical forests in Southwest China, (3) to understand the tradeoffs in water relations and carbon assimilation between being deciduous and evergreen in the subtropics, and (4) to determine the annual carbon balance of evergreen and deciduous

trees in the subtropics of Southwest China, which may partially explain the dominance of evergreen trees at the high elevations of this region.

Tree hydraulic and photosynthetic traits, diurnal and seasonal dynamics in the water use and carbon assimilation of evergreen and deciduous trees from a subtropical montane cloud forest in Southwest China were studied from 2008 to 2011. Environmental conditions (temperature, rainfall, daytime fog, photosynthetic photon flux density etc.) and ecosystem level water and carbon exchange were also recorded. These forests are characterized by a summer with high precipitation and a dry mild winter. The long duration of fog and frequent rain during the summer is an important characteristic of the forest. I found that (1) the deciduous species had significantly higher stem hydraulic conductivity, greater stem capacitance, higher midday stem water potential, and higher midday stomatal conductance than the evergreen species, (2) the evergreen cloud forest buffered the effects of seasonal water deficits and rainfall anomalies by using soil water storage and ground water at depth, and by lowering the leaf and canopy water loss rates, (3) the evergreen species maintained high carbon assimilation (5.4 to 8.8 μmol m^{-2} s^{-1}) during the winter, and the net ecosystem carbon gain was higher in the winter than in the summer, (4) the most common deciduous species in the forest extended their leaf life spans and used red senescing leaves to assimilate a considerable amount of carbon during part of the winter season.

I concluded that (1) the considerable carbon gain by the evergreen broadleaf trees in the winter/dry season results in a higher yearly carbon gain than for the deciduous species, which partially explains the dominance of evergreen trees in the subtropical forests of Southwest China; (2) the low temperatures in the winter do not limit, while the longtime

duration of cloud cover and leaf wetness during the summer strongly constrains, the tree and ecosystem level carbon gain, which weakens the advantages of deciduous species by having higher photosynthetic rates compared to the evergreen species during the summer; (3) extending the carbon assimilation period of a deciduous species into the winter months suggests that being evergreen is more competitive than being deciduous in subtropical forests of Southwest China. Therefore, the results of my dissertation provide a potential explanation for the dominance of evergreen trees in the subtropical forests in Southwest China. Substantial carbon uptake during the winter/dry season also allows this subtropical cloud forest to be one of the largest carbon sinks among old-growth forests in the world, suggesting the importance of subtropical forests in the global carbon cycle.

The presence of cloud forests in the subtopics of China is not known or very little known to the international academic community. This dissertation puts the Chinese cloud forests in the world map and provides a mechanistic understanding of the selective pressures operating in subtropical cloud forests. The results of this dissertation also reveal the hydraulic and photosynthetic adaptations of evergreen and deciduous tree species growing in subtropical cloud forests.

DEDICATION

I would like to dedicate this dissertation to my grandparents, my parents, my sister, my girlfriend and all my good friends.

ACKNOWLEDGEMENTS

This dissertation represents an international cooperative project between the Department of Biology at the University of Miami (UM) and the Xishuangbanna Tropical Botanical Garden (XTBG) of the Chinese Academy of Sciences (CAS). I would like to express my deepest gratitude to all the people from XTBG and UM who made this international cooperative project happen, especially Dr. Jin Chen, the director of XTBG, and Dr. Ted Fleming, the previous Interim Chair of the Department of Biology at UM. I finished another dissertation project entitled *The relationship between plant water relations and photosynthesis, and the influence of environmental factors* in parallel to partially fulfill the requirements for a Ph. D. in Ecology from the CAS. I would never have been able to finish my dissertations without the guidance of my advisor, co-advisor and committee members from UM and XTBG, support from my family, and help from my good friends.

First of all, I would like to give my utmost gratitude to my advisor, Dr. Guillermo Goldstein. His wisdom, knowledge, experience and passion in scientific research inspired and motivated me. He was continuously giving me guidance and encouragement during every step of my Ph. D. study. I also would like to give thanks from deep of my heart to the co-advisor of this dissertation, Dr. Kun-Fang Cao from XTBG. His commitment to the highest standards was always motivating me. He was continuously giving me supervision and support during the whole time of my Ph. D. study. I am also grateful to my committee members, Drs. David P. Janos, David W. Lee, Donald L. DeAngelis, and Jack B. Fisher, who gave me many instructive suggestions for improving this research project and were always willing to help whenever I needed it.

I would like to thank the Ailaoshan Station for Subtropical Ecosystem Studies for providing the climate data and logistic support, and Dr. Yi-Ping Zhang and Zheng-Hong Tan from XTBG for providing the eddy covariance data. I also thank the Biogeochemistry Laboratory of the XTBG for the determination of nutrient and soluble sugar concentrations.

My sincere thanks also go to Mr. Yang Qiuyun, Mr. Ma Hong, Mr. Fu Xuwei, Mr. Zeng Xiaodong, Mr. Ai Ke, Mr. Qi Jinhua, Mr. Luo Xin, Mr. Li Xinde, and Mr. Liu Yuhong for their assistance in the field work. Without their help, it is impossible for me to finish the field measurements in a mist cloud forest on a remote Mountain.

This dissertation also reflects the discussion and cooperation with some inspiring plant biologists I met during my graduate study. Their intelligence and passion inspired me, and I learned a lot from them. They are Drs. Fabian G. Scholz, Sandra J. Bucci, Frederick C. Meinzer, Noel Michel Holbrook, Timothy J. Brodribb, and Lawren Sack.

I am heartily thankful to all my good friends in Miami, Xishugangbanna, and Ailaoshan for their material and spiritual support during my Ph.D. study. They are Randol Villalobos-Vega, Ana Salazar, Eric Manzané, Guangyou Hao, Zihao Li, Zuwen He, Ming Tu, Jiang Jiang, Shijian Yang, Shuai Li, Liang Song, Huan Fan, Jinhua Qi, Xin Luo, Xinde Li etc.

This dissertation research was supported by a National Science Foundation of China grant (30670320). My study and research in UM and XTBG also were supported by the Department of Biology at UM, the Eco-physiological group at XTBG, and the Anness Fellowship from the College of Arts and Sciences at UM. My research in Brazil and

Argentina was supported by National Science Foundation grants (0296174 and 0322051) and a CONICET grant from Argentina (PIP-112-200801-01703).

Last but not least, I would like to thank my family and my girlfriend for their support. They were always encouraging me with their best wishes, and sharing the good times and the bad moments with me.

TABLE OF CONTENTS

LIST OF FIGURES

Page

LIST OF TABLES

Page

LIST OF ABBREVIATIONS

Variable	Abbreviation	Unit
Anthocyanin reflectance index	ARI	
Apparent quantum yield	AQY	
Carotene concentration per mass	Car	mg g^{-1}
Chlorophyll a concentration	Chl *a*	mg g^{-1}
Chlorophyll b concentration	Chl *b*	mg g^{-1}
Chlorophyll concentration	Chl *a*+*b*	mg g^{-1}
Dark respiration	R_d	mol m^{-2} s^{-1}
Hydraulic capacitance	C	kg m^{-3} MPa^{-1}
Intrinsic water use efficiency	A/g_s	mol mol^{-1}
Leaf hydraulic conductance per area	K_{leaf}	mmol m^{-2} s^{-1} MPa^{-1}
Leaf lethal temperature	LT_{50}	^oC
Leaf mass per area	LMA	g m^{-2}
Leaf nitrogen concentration per mass	N	g kg^{-1}
Leaf phosphorus concentration per mass	P	g kg^{-1}
Leaf relative water content	RWC	%
Leaf water potential	Ψ_L	MPa
Light compensation point	LCP	μmol m^{-2} s^{-1}
Light saturation point	LSP	μmol m^{-2} s^{-1}
Light-saturated CO2 assimilation	A_{max}	μmol m^{-2} s^{-1}

Normalized difference vegetation index	NDVI	
Photochemical efficiency of Photosystem I	P_m	
Photochemical efficiency of Photosystem II	F_v/F_m	
Photosynthetic photon flux density	PPFD	mol m^{-2} s^{-1}
Sapwood specific hydraulic conductivity	K_s	kg m^{-1} s^{-1} MPa^{-1}
Stem hydraulic conductivity	K_h	kg m s^{-1} MPa^{-1}
Stem water potential	Ψ_{ST}	MPa
Stomatal conductance	g_s	mol m^{-2} s^{-1}
Vapor pressure deficit	VPD	kPa

CHAPTER 1

Introduction

Evergreen and deciduous trees are conspicuous growth forms across most forest ecosystems around the world. Some forests are evergreen-dominated, others are deciduous-dominated and there are some forests where both deciduous and evergreen trees coexist. The competition or coexistence between deciduous and evergreen tree species, where one became dominant, as well as the global and regional pattern in distribution of evergreen and deciduous forests, are old ecological topics that have interested and attracted many ecologists, biogeographers, and global modelers (Kikuzawa 1991; Aerts 1995; Eamus 1999; Givnish 2002). China has a special distribution pattern of evergreen and deciduous forests in the subtropical area; evergreen broadleaf trees dominate the forests from elevations of 1000 to 2600 m in the subtropical area of Southwest China, while deciduous trees dominate the subtropical forests with similar elevations in Southeast China (Wu 1980). The eco-physiological mechanisms that explain the distribution pattern form an interesting topic that has not yet been studied. The objective of this dissertation was to understand the water and carbon balances of evergreen and deciduous trees from a subtropical cloud forest in Southwest China, as well as the environmental constraints on carbon assimilation of the subtropical cloud forest, which may provide a potential explanation for the dominance of evergreen trees at the high elevations of subtropical Southwest China.

Distribution of evergreen and deciduous forests

At a global scale, evergreen broadleaf trees dominate low latitude tropical rainforests and some non-seasonal cloud forests; deciduous trees dominate temperate forests in mid-latitude and some tropical and subtropical seasonal dry regions of the northern hemisphere, while evergreen conifers dominate many boreal forests at high latitudes. As annual precipitation decreases, and the seasonality of precipitation increases, in general the proportion of deciduous species in the forest increases (Frankie *et al*. 1974; Medina 1984). In the subtropical montane area of Southeast China, evergreen broadleaf trees characterize low elevation forests, deciduous trees dominate mid-elevation forests (ranging from 1000 to 2000 m in elevation; Fig. 1.1), while evergreen conifer trees dominate the forests at high elevations. However, in the subtropical montane area of Southwest China, forests dominated by evergreen broadleaf tree species are in direct contact with the forests characterized by evergreen conifer trees or elfin forests, depending on elevation, and there is no deciduous forest zone between them. Warmer winters and smaller annual temperature fluctuations of Southwest China are thought to be the climatic determinants for this conspicuously different pattern of forest type distribution between Southeast and Southwest China. However, how these environmental factors influence the water and carbon balances of the deciduous and evergreen broadleaf species in certain habitats of subtropical China, and how deciduous and evergreen broad-leaf trees adapt to certain environments has not yet been studied.

Ecology of evergreen and deciduous species

Deciduous trees, a conspicuous growth form, are defined as trees that remain completely leafless for a certain period of time during the year (for a review see: Kikuzawa and Lechowicz, 2011). The deciduous habit of tree species originated in the Cretaceous period when angiosperms spread from low latitude to mid-latitude regions (Axelrod 1966). The deciduous habit of plants is thought to be an adaptation to the seasonal low temperatures in the mid-latitude region of the northern hemisphere. In the southern hemisphere, where the seasonality is relatively weak, a deciduous forest zone does not exist. The deciduous habit may be an adaptation to seasonal drought, consistent with the dominance of deciduous species in some tropical and subtropical seasonal dry forests.

The major advantages of evergreen leaves for woody plants are: (1) a longer period for carbon capture; (2) lower amortized costs of leaf construction; (3) lower amortized cost of replacing nutrients; and (4) tougher leaf laminas that can better endure herbivore pressure. On the other hand the potential advantages of deciduous leaves for woody plants are: (1) higher photosynthetic rates per unit leaf mass due to higher leaf nitrogen content and specific leaf area; (2) lower root cost during the unfavorable season compared to evergreen species; and (3) no leaf respiration during the unfavorable season (Givnish 2002). According to the studies by Reich *et al*. (1991; 1992; 1997), leaf life span is negatively correlated with photosynthetic rate per unit leaf mass. Strong negative relationships were also found between leaf life span and specific leaf area, as well as between leaf life span and leaf nitrogen content (Wright *et al*. 2004).

Effects of low temperatures on plant water and carbon balances

Low temperatures may influence photosynthesis by increasing photoinhibition (Sevanto *et al*. 2006; Miyazawa 2007) and impairing enzyme activities (Hammel 1967). Photoinhibition is the decrease of photosynthetic rates when leaves are exposed to high light that exceeds the photon requirement for photosynthesis (Osmond 1994; Long, Humpheries & Falkowski 1994). Low temperatures commonly result in photoinhibition and photooxidation because low temperatures affect light utilization more than light absorption (Long, Humpheries & Falkowski 1994; Germino & Smith 1999; 2000; Miyazawa *et al*. 2007). Photon capture and transfer of excitation energy are less affected by low temperatures than electron transport and the enzyme activity of the Calvin-Benson Cycle. Therefore, low temperatures may induce photoinhibition even under normal or low light conditions. However, photosynthetic depression could be compensated by greater incoming solar radiation during the winter. In a temperate deciduous forest, winter CO_2 assimilation of the understory evergreen trees is a large portion of the yearly CO_2 assimilation due to an increase in sunlight reaching the understorey during the winter (Miyazawa & Kikuzawa 2005).

In habitats with frequent subzero temperatures, freeze-thaw cycles induce embolism (blocking of xylem vessels by air bubbles) in the xylem vessels (Hammel 1967; Sperry & Sullivan 1992; Davis *et al*. 1999; Cavender-Bares & Holbrook 2001; Pittermann & Sperry 2006). During freezing, air dissolved in the xylem sap comes out from the water/ice as air bubbles. Then, during the thaw process when the tension is re-established, these air bubbles will grow and cause embolism. Since evergreen broad-leaf species from cold climates are actively transpiring during the winter when night air

temperatures are below the equilibrium freezing temperatures of the xylem tissue, they have to recover from embolism after the freeze-thaw cycles in stem and leaf tissues. Embolism caused by freeze-thaw cycles in the winter will lower the stem hydraulic conductivity, which may limit the photosynthetic gas exchange. In a Japanese cool temperate forest, Taneda & Tateno (2005) found that evergreen broad-leafed trees with substantial decreases in hydraulic conductivity assimilate negligible CO_2 during the winter, while species that could maintain substantial stem long distance water transport efficiency maintain positive CO_2 assimilation (Taneda & Tateno 2005).

Effects of water deficits on plant water and carbon balances

Water deficits limit photosynthesis as a consequence of low stomatal conductance (Brodribb & Holbrook 2004b; Zhang *et al*. 2009) and/or Calvin Cycle impairment (Flexas *et al*. 2001; Oliveira & Penuelas 2004). Down-regulation in stomatal conductance is a common strategy that trees use to avoid further water loss when exposed to water deficits (Schulze *et al*. 1987). However, down-regulation in stomatal conductance slows leaf CO_2 uptake, and therefore has a cost in terms of carbon balance (Brodribb & Holbrook 2004; Zhang *et al*. 2009). Trees also may decrease total leaf area (Breda *et al*. 2006), or decrease the leaf area to sapwood area ratio (McDowell *et al*. 2002; Zhang *et al*. 2009) to reduce transpirational water loss during water deficits. These hydraulic adjustments decrease total leaf area for photosynthesis, which may lead to carbon imbalance and tree dieback (Zhang *et al*. 2009). Drought deciduousness is also an adaptation to avoid the effects of seasonal water deficits (Kikuzawa & Lechowicz 2011).

Water deficits may also cause embolism in stem xylem (Pockman *et al*. 1995; Sperry 1995; Tyree & Zimmermann 2002), impairing long distance water transport and gas exchange. According to the cohesion-tension theory (Dixon & Joly 1894), transpiration in the leaf surface generates tension and draws water from the roots to the canopy leaves through the continuous water column in the xylem vessels. Cavitation is the breakage of the continuous water column and filling of the xylem vessel with air bubbles when the air enters the vessel through the pores in the pit membrane (Pockman *et al*. 1995; Sperry 1995; Tyree & Zimmermann 2002). When the plants are subjected to water deficits, the tension in the xylem vessel becomes very high (or the water potential becomes very negative), and cavitation may occur. The occurrence of cavitations will result in blockage of water columns (embolisms) and dysfunction of the xylem vessels for long distance water transport (Tyree & Sperry 1989). Choat *et al*. (2005) suggested that deciduous species are more vulnerable to cavitation induced by water deficits than coexisting evergreen broadleaf species in an Australian dry forest.

Effects of cloud cover on tree carbon balance

Cloud cover or fog persistence influences photosynthesis of plants in two ways. On one hand, cloud cover limits carbon gain and tree growth by reducing incoming light (Hollinger *et al*., 1994; Mulkey *et al*. 1996; Kellomäki & Wang 2000; Graham *et al.* 2003; Zhang *et al*. 2011). Artificial increases in light levels on trees in a Panamanian tropical rainforest increased leaf CO_2 uptake and tree growth (Graham *et al*. 2003). Some eddy flux studies suggest that cloud cover greatly influences day to day and year to year variations in net ecosystem carbon gain (Hollinger *et al*., 1994; Kellomäki & Wang 2000;

Zhang *et al*. 2011). On the other hand, cloud cover has the potential to reduce leaf photodamage during the winter because low temperatures and high light levels increase photoinhibiton. In addition, low cloud cover provides more constant regimes and enhances the daily carbon gain of understorey species (Johnson & Smith 2006).

Coordination between stem and leaf hydraulics

In the water transport pathway of plants from soil to atmosphere, stems contribute substantially to the whole tree hydraulic resistance because many trees are tall. However, leaves are an important hydraulic bottleneck, representing about 30% of whole plant resistance for a range of life forms (Sack *et al*. 2003). The proportion can be as high as 80% in some species during peak transpiration (Nardini & Salleo 2000; Brodribb *et al*. 2002). As well, leaves are more vulnerable to embolism than stems in several tree species (Bucci *et al*. 2003; Brodribb & Holbrook 2003; Brodribb *et al*. 2003; Woodruff *et al*. 2007; Hao *et al*. 2008; Zhang *et al*. 2009). Diurnal decreases in leaf hydraulic conductance (K_{leaf}) during the morning and an increase in K_{leaf} during the afternoon and evening are observed in some temperate and tropical trees, suggesting the occurrence of embolism formation and refilling on a daily basis (Bucci *et al*. 2003; Brodribb & Holbrook 2004a).

There is coordination between leaf and stem hydraulics, meaning that the resistances of water transport in stems and leaves vary in such a way that water movement up to the site of transpiration is efficient and embolisms in stems are avoided. Embolism repair is more difficult in stems than in leaves (Bucci *et al*. 2003; Brodribb & Holbrook 2004a). The stomatal regulation is a key process linking gas exchange,

transpiration, and stem water status (Brodribb *et al*. 2003; Brodribb & Holbrook 2004b). The sensitivity of stomata to environment changes (*e.g*. change in air vapor pressure deficit; VPD) is thought to be significantly adaptive (Brodribb & Jordan 2008). Stomata closing under certain circumstances could prevent further drops of water potential (xylem tension), embolism formation, and consequently a catastrophic drop in stem hydraulic conductivity. Diurnal regulation of K_{leaf} also can have some adaptive significance in the control of stem water potentials (Brodribb & Holbrook 2004a). The reversible loss of hydraulic conductivity in the leaf lamina may be an adaptive means of amplifying the evaporative demand signal to the stomata in order to expedite a stomatal response.

Although it is hypothesized that deciduous species are more hydraulically efficient than evergreen broad-leaf species, the pattern is still not clear. No clear correlation has been established between hydraulic architecture and leaf life span. Some studies showed that deciduous species were more hydraulically efficient than evergreen broad-leaf species (Gartner *et al*. 1990; Sobrado 1993; 1997; Choat *et al*. 2005), while others reported the opposite (Goldstein *et al*. 1987; 1990). According to the strong negative relationship found between wood density and capacitance (Scholz *et al*. 2007), deciduous species are expected to have higher capacitance due to their lower wood density compared to evergreen broadleaf species (Choat *et al*. 2005). Trees with relatively larger internal water storages have higher capacities for buffering water deficits than those with smaller water storages.

Introduction to the subtropics in China, and the study site

The subtropical forests in Southwest China are located south of the Tibetan (Xizang) Plateau (with average elevation of 4000 m; Fig. 1.2) and the Yun-Gui Plateau and south to the tropical belt located at the border with Burma, Laos and Vietnam. The Tibetan plateau prevents cold fronts from moving south and, therefore, the minimum temperatures during the winter at high elevations can drop to about -5 ^{o}C (2460 m). The subtropical forests to the east, however, are not protected by the Tibetan plateau and the temperatures can drop to about –11^{o}C (elevation 1000 m). The east side is also more influenced by cold continental winds in the winter, while the Southwest is sheltered by mountains and the Plateaus.

The evergreen broadleaved forest studied is located in a montane area (Ailaoshan; Ailao Mountain) in Southwest China, 23^{o}35'-24^{o}44'N, 100^{o}54'-101^{o}30'E, ranging from 1100 m (or 1300 m) to about 2600 m in elevation. This site has a subtropical climate, with an annual average temperature of 11.3 ^{o}C and annual average precipitation of 1931 mm (Ailaoshan Station for Subtropical Evergreen Broadleaf Forest Ecosystem Studies; 24°32′N, 101°01′E, elevation 2460 m; Qiu & Xie 1998). High precipitation in Southwest China results from the blocking of the Southwestern Monsoon from the India Ocean by the mountains in this region and the Tibetan Plateau. However, the precipitation is seasonal, and during 3 months of the year the monthly precipitation is less than 50 mm (Fig. 3). The dry season coincides with the winter (Fig. 1.3). The average temperature of the warmest and coldest month is 11.6 ^{o}C and 5.4 ^{o}C, respectively (Fig. 1.3; elevation 2460 m). Compared to typical temperate climates, seasonal and diurnal variations in temperatures of this region are relatively small.

The forests on Ailao Mountain are dominated by evergreen Fagaceae, associated with evergreen Lauraceae, Theaceae, etc. Deciduous trees are rare, with a few species scattered in the forests (Aceraceae, Staphyleaceae, Styracaceae; Table 1.1; Fig. 1.4). Ten evergreen and five deciduous species from the forests were chosen for this dissertation study (Table 1.2; Table 1.3). The growth rhythms of the forests on Ailao Moutain are more similar to those of the tropical forests than to those of temperate forests. Plants flower and bear fruit almost all year. In eastern China at the same latitude (around 24^{o} N), the mountains usually have evergreen broadleaf forests at low elevations, deciduous forests in the middle (elevations from 1000 to 2000 m) and conifer forests at higher elevations.

Objectives of this dissertation

The general objective of this dissertation was to understand the water and carbon balances of evergreen and deciduous trees in the subtropics of Southwest China, which may partially explain the dominance of evergreen trees at the high elevations of the subtropical Southwest China, as well as the tradeoffs in water relations and carbon assimilation between being deciduous and evergreen in the subtropics. The specific objectives of this study were:

1. To assess the difference in daily water use and carbon assimilation between evergreen and deciduous species from a subtropical montane cloud forest in Southwest China (Chapter 2);

2. To determine the effects of seasonal water deficits and drought years on the water and carbon balances of the evergreen trees species from the cloud forest (Chapter 3);

3. To determine the effects of cloud cover and seasonal low temperatures on leaf and ecosystem level carbon balances of the cloud forest (Chapter 4);

4. To determine whether deciduous species from the cloud forest extend leaf life spans into the winter months to utilize the great incoming solar radiation during the fall and winter (Chapter 5).

Table 1.1 The relative dominance, density, frequency, and importance value of common evergreen and deciduous broadleaf species in typical evergreen broad-leaved forests on Ailao Moutain (elevation 2400-2600). E stands for evergreen, while D stands for deciduous. (Data source: Qiu & Xie 1998)

Species	E/D	Dominance %	Density %	Frequency %	Importance Value
Castanopsis wattii A. Camus	E	23.7	4.6	100.0	128.3
Lithocarpus xylocarpus Markgr.	E	14.5	6.3	94.7	115.5
Schima noronhae Reinw. ex Blume	E	9.9	5.9	94.7	110.5
Lithocarpus jingdongensis Y.C.Hsu & H.J.Qian	E	17.9	6.1	84.2	108.2
Vaccinium delavayi Franch.	E	2.4	15.6	73.7	91.7
Manglietia insignis Blume	E	2.0	2.6	84.2	88.8
Machilus viridis Hand.-Mazz.	E	1.8	2.2	78.9	82.9
Camellia forrestii Cohen-Stuart	E	0.5	5.4	63.2	69.1
Hartia sinensis Dunn	E	3.1	4.8	57.9	65.8
Eurya yunnanensis P.S.Hsu	E	<0.1	1.9	63.2	65.1
Eriobotrya bengalensis Hook. f.	E	1.2	4.7	57.9	63.8
Illicium macranthum A.C. Smith	E	0.7	1.3	47.4	49.4
Litsea elongata Benth. & Hook.f.	E	0.3	1.8	42.1	43.7
Neolitsea polycarpa H. Liou	E	0.4	0.3	26.3	27.0
Styrax perkinsiae Rehder	D	0.8	1.6	36.8	39.2
Lyonia ovalifolia Drude var. *ovalifolia*	D	2.0	1.3	26.3	29.6
Tapiscia yunnanensis Oliv.	D	0.5	0.6	15.8	16.5
Acanthopanax evodiifolius Franch.	D	0.6	0.3	15.8	16.5
Acer amplum Rehder var. *jianshuiense* W.P.Fang	D	<0.1	0.1	5.3	5.4
Betula luminifera H. Winkl.	D	0.1	<0.1	5.3	5.4
Acer heptalobum Diels	D	<0.1	<0.1	5.3	1.3

Table 1.2 Fifteen broadleaf tree species studied in this dissertation

Species	Family
Evergreen	
Lithocarpus jingdongensis Y.C. Hsu & H.J. Qian	Fagaceae
Symplocos sumuntia D. Don	Symplocaceae
Schima noronhae Reinw. ex Blume	Theaceae
Vaccinium delavayi Franch	Vacciniaceae
Manglietia insignis Blume	Magonoliaceae
Lithocarpus hypoviridis Y.C. Hsu, B.S. Sun & H.J. Qian	Fagaceae
Ternstroemia gymnanthera Sprague	Theaceae
Lyonia ovalifolia Drude var. *lanceolata* Hand.-Mazz.	Ericaceae
Hartia sinensis Dunn	Theaceae
Illicium macranthum A.C. Smith	Illiciaceae
Deciduous	
Lyonia ovalifolia Drude var. *ovalifolia*	Ericaceae
Betula alnoides Hamilt.	Betulaceae
Populus yunnanensis Dode	Salicaceae
Alnus nepalensis D. Don	Betulaceae
Clethra brammeriana Hand.-Mazz.	Clethraceae

Table 1.3 Tree species studied in different chapters of this dissertation

Species	Chapter 2	Chapter 3	Chapter 4	Chapter 5
Evergreen				
Lithocarpus jingdongensis	√	√	√	
Symplocos sumuntia	√	√	√	
Schima noronhae	√	√	√	
Vaccinium delavayi	√	√	√	
Manglietia insignis	√	√	√	
Lithocarpus hypoviridis	√	√	√	
Ternstroemia gymnanthera	√	√	√	
Lyonia ovalifolia var. *lanceolata*	√		√	
Hartia sinensis	√	√	√	
Illicium macranthum	√	√	√	
Deciduous				
Lyonia ovalifolia var. *ovalifolia*	√		√	√
Betula alnoides	√		√	√
Populus yunnanensis	√		√	√
Alnus nepalensis			√	√
Clethra brammeriana	√		√	√

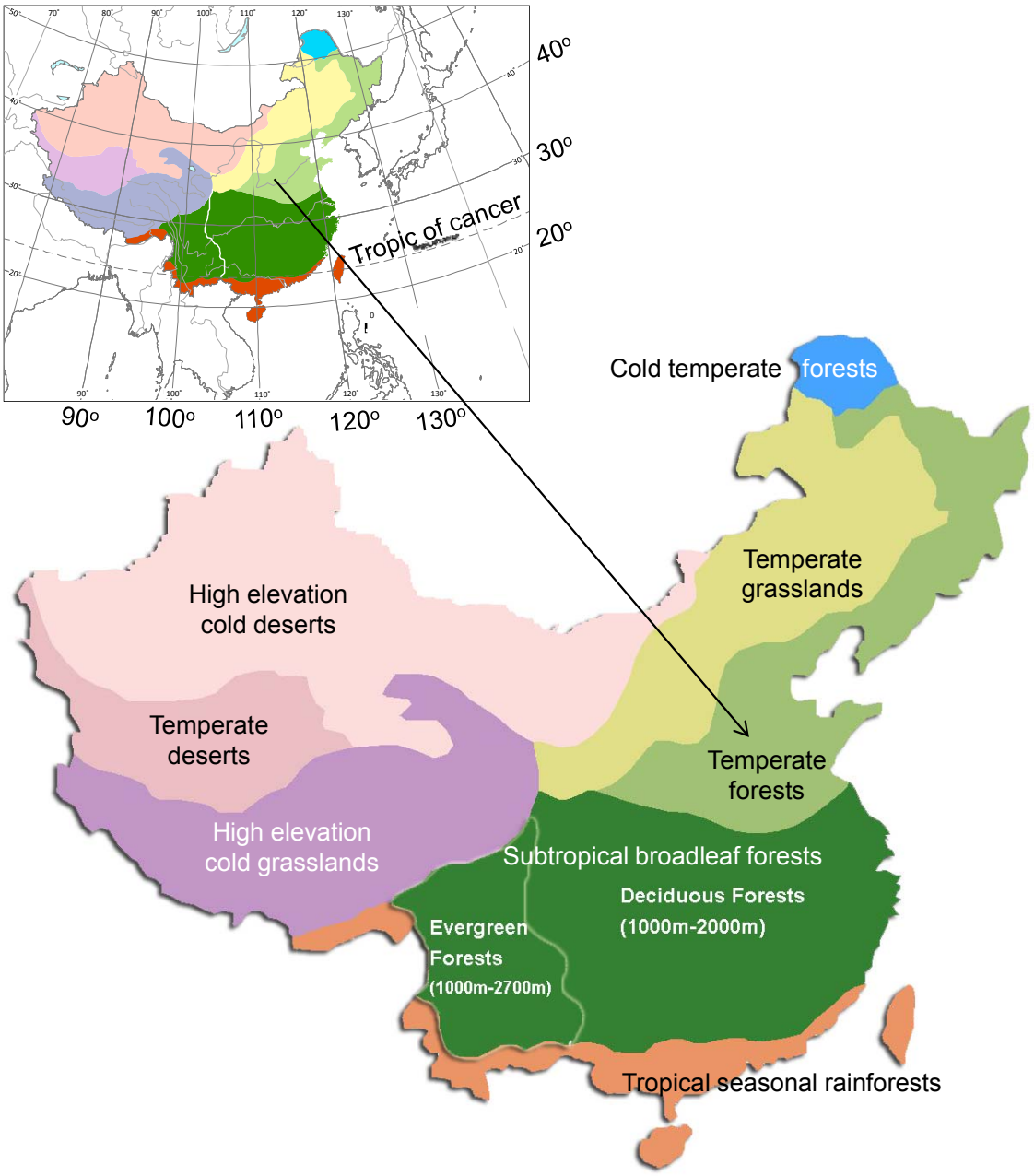

Figure 1.1 A vegetation map of China according to Wu (1980).

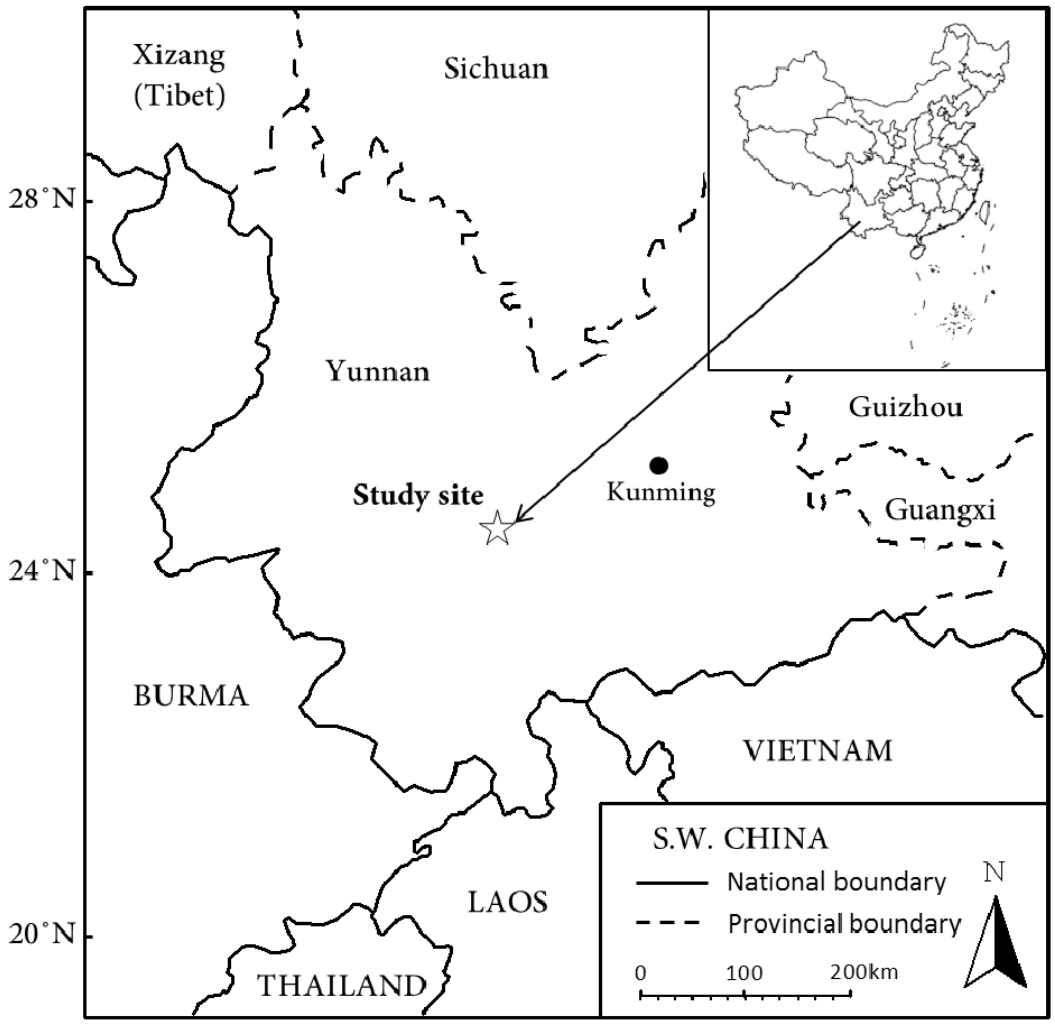

Figure 1.2 The location of the study site: Ailaoshan Station for Subtropical Forest Ecosystem Studies (24°32′N, 101°01′E) in Yunnan Province, Southwest China.

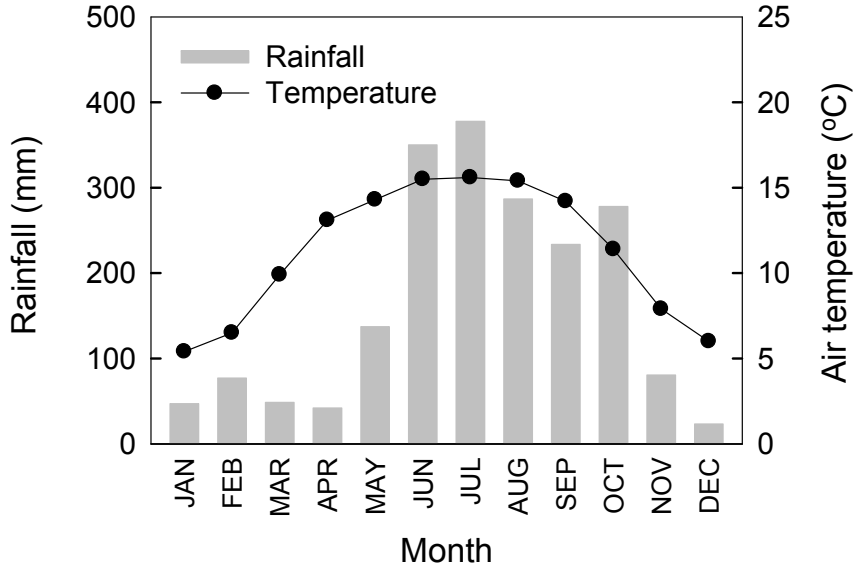

Figure 1.3 Monthly precipitation and monthly mean air temperature of the study site (Ailaoshan Station for Subtropical Forest Ecosystem Studies; elevation 2460 m; 5 year average; data source: Qiu & Xie 1998).

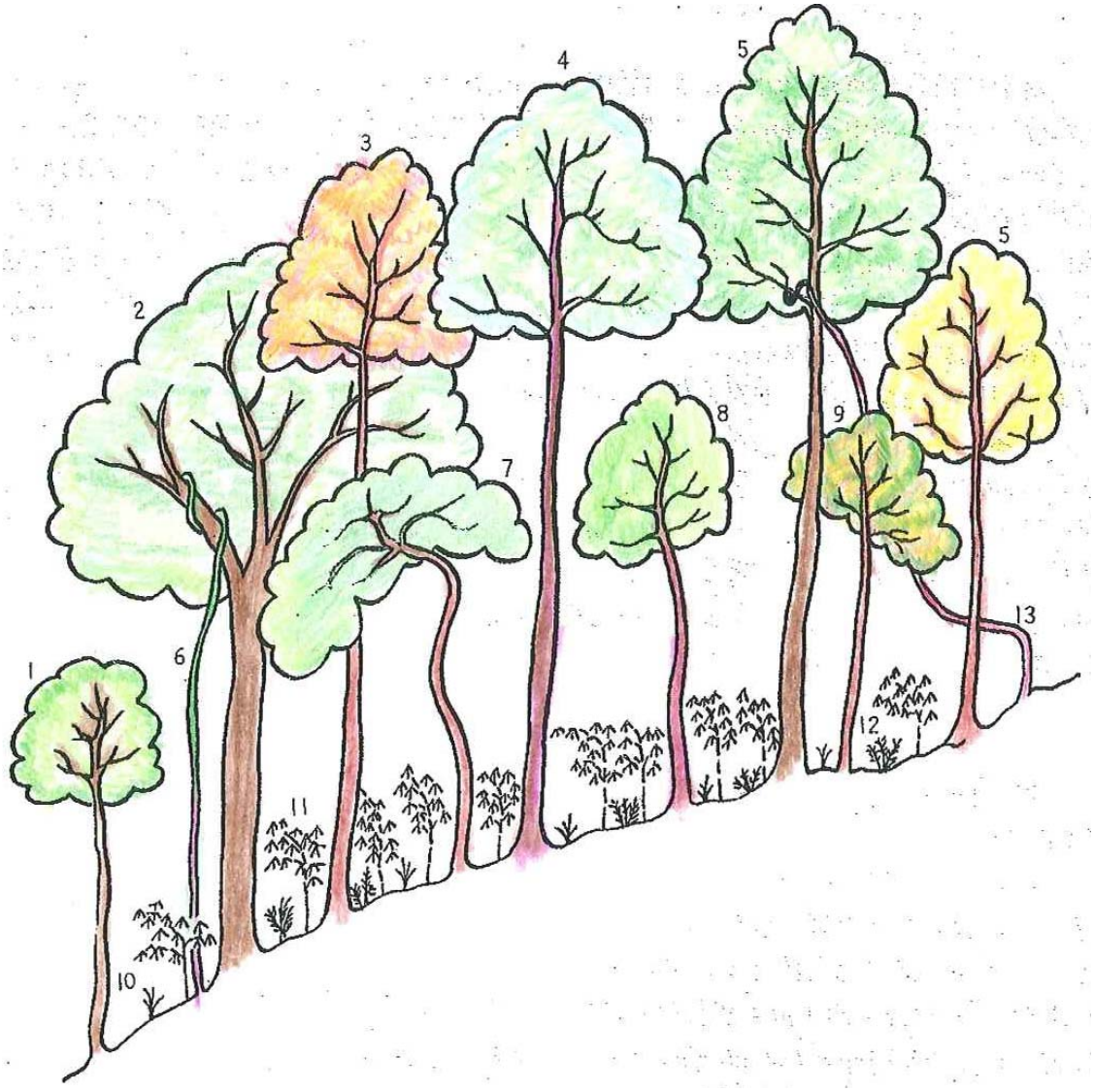

Figure 1.4 A diagram depicting the forest composition of an evergreen broadleaf forest on Ailao Mountain (elevation 2500 m). 1. *Illicium macranthum* 2 *Castanopsis wattii* 3. *Acer heptalobum* 4. *Schima noronhae* 5. *Lithocarpus xylocarpus* 6. *Rosa longicuspis* Bertol. 7. *Eurya obliquifolia* Hemsl. 8. *Neolitsea polycarpa 9. Lindera thomsonii* Allen 10. *Carex teinogyna* Boott 11. *Sinarundinaria nitida* (Mitford) Nakai 12. *Plagiogyria communis* Ching13. *Kadsura coccinea* (Lem.) A.C.Sm. Adapted from Qiu & Xie 1998.

CHAPTER 2

Midday stomatal conductance is more related to stem than to leaf water status in subtropical deciduous and evergreen broadleaf trees

Summary

Midday depressions in stomatal conductance (g_s) and photosynthesis are common in plants. The aim of this study was to understand the hydraulic determinants of midday g_s, the coordination between leaf and stem hydraulics, and whether regulation of midday g_s differed between deciduous and evergreen broadleaf tree species in a subtropical cloud forest of SW China. We investigated leaf and stem hydraulics, midday leaf and stem water potentials, as well as midday g_s of co-occurring deciduous and evergreen tree species. Midday g_s was positively correlated with midday stem water potential across both groups of species, while no relationship between midday g_s and midday leaf water potential was found. Species with higher stem hydraulic conductivity and greater daily reliance on stem hydraulic capacitance were able to maintain higher stem water potential and consequently higher g_s at midday than species with lower stem hydraulic conductivity and lower stem hydraulic capacitance. Deciduous species exhibited significantly higher stem hydraulic conductivity and greater reliance on stem capacitance, and consequently had higher stem water potential and g_s at midday than evergreen species. Our results suggest that midday g_s is more associated with midday stem than with leaf water status, and that the functional significance of stomatal regulation in the broadleaf tree species is mainly preventing stem xylem dysfunction.

Background

Midday depression in photosynthetic gas exchange is commonly observed in plants (Tenhunen, Pearcy & Lange 1987; Koch, Amthor & Goulden 1994; Kosugi & Matsuo 2006; Tucci *et al*. 2010), and down-regulation of stomatal conductance (g_s) is one of the major contributing factors (Schulze *et al*. 1974; Raschke & Resemann 1986; Iio *et al*. 2004; Grassi *et al*. 2009). Although the trigger of stomatal closure is not fully-understood, leaf water potential (Ψ_L) is one of the major factors in stomatal regulation because stomatal aperture directly responds to guard cell turgor (Franks *et al*. 1995). However, the interspecific relationship between midday Ψ_L and midday g_s has not been well established, and the mechanism by which stomata respond to and control Ψ_L is unclear (Brodribb & Holbrook 2003; Meinzer *et al*. 2009). Notably, the ability of a plant to maintain high Ψ_L during active transpiration is related to the plant hydraulic system: those species with high water transport efficiency would be able to replace transpirational water loss quickly and therefore maintain high Ψ_L. Consequently, a positive relationship between water transport efficiency and maximum photosynthetic rate has been found in different plant taxonomic groups and different ecosystems (Brodribb & Feild 2000; Santiago *et al*. 2004; Broddribb, Feild & Jordan 2007; Campanello, Gatti & Goldstein 2008; Zhang & Cao 2009).The midday g_s of a plant could also be related to plant hydraulic characteristics: plants with higher water transport efficiency at midday can maintain better leaf water status during this daytime period, and consequently experience less depression in midday g_s. However, this hydraulic determinant of midday g_s has not been well investigated.

Stomatal regulation is responsible for controlling the stem xylem water potential during the day (Meinzer *et al*. 2009). Decreased g_s at midday slows down further water loss; consequently, it has an adaptive significance in protecting the plant vascular system from xylem dysfunction. Recent studies have shown that diurnal depression in leaf hydraulic conductance is common in many plant species (Bucci *et al*. 2003; Brodribb & Holbrook 2004a; Zhang *et al*. 2009; Johnson *et al*. 2009; 2011b; Zufferey *et al*. 2011), while a diurnal decrease in stem hydraulic conductivity is rare. Since leaf hydraulic conductance decreases and recovers diurnally in many species, the major function of stomatal regulation is not likely to be protection of the leaf hydraulic system from dysfunction in those species. Rather, the significance of diurnal stomatal regulation is probably to maintain Ψ_{ST} in the range that will avoid stem xylem embolism during the day (Meinzer *et al*. 2009). In fact, midday depression in K_{leaf} itself is thought to be a mechanism to magnify the signal triggered by water deficits, resulting in rapid stomatal closure (Brodribb & Holbrook 2004b), which slows down further dehydration of stems and roots. Under the assumption that the down-regulation in K_{leaf} and g_s is mainly to prevent stem xylem dysfunction, we suggest that midday g_s should be more related to Ψ_{ST} rather than to Ψ_L.

The relationship between g_s and Ψ_{ST} could be mediated by stem hydraulic capacitance (Meinzer *et al*. 2008; Meinzer *et al*. 2009). Stem water storage plays an important role in mitigating diurnal water deficits caused by transpirational water loss (Goldstein *et al*. 1998; Scholz *et al*. 2007), and may reduce diurnal fluctuation in Ψ_{ST} (Meinzer *et al*. 2008). Stem hydraulic capacitance strongly determines the midday stem and leaf water status (Meinzer *et al*. 2003; 2008; Sholz *et al*. 2007), and consequently

trees with higher water storage capacities are able to maintain maximum transpiration rates for a longer period of time during the day than trees with lower water storage capacities (Goldstein *et al*. 1998). Therefore, stem hydraulic capacitance needs to be considered in analyzing the relationship between midday g_s and leaf/stem water potentials. Notably, two deciduous species were reported to have higher stem hydraulic capacitance than two co-occurring evergreen species in an Australian seasonally dry rainforest (Choat *et al*. 2005). If this difference in hydraulic capacitance between deciduous and evergreen species reflects a general pattern acrosss other types of ecosystems, deciduous species with potentially higher hydraulic capacitance may maintain higher midday leaf and stem water potentials, and consequently higher midday g_s than evergreen species.

We studied leaf and stem hydraulics, midday stem and leaf water status, and midday leaf g_s of 14 co-occurring broadleaf tree species (ten evergreen and four deciduous species) in a subtropical cloud forest with abundant moisture in SW China. The objectives of the present study were (1) to understand the hydraulic determinants of midday depression in photosynthetic gas exchange, (2) to assess the hydraulic regulation of midday stem and leaf water potentials, and (3) to explore the difference in midday hydraulic and stomatal performance between deciduous and evergreen broadleaf tree species.

Materials and methods

Study site

This study was carried out in an evergreen broadleaf forest at the Ailaoshan Station for Subtropical Evergreen Broadleaf Forest Ecosystem Studies (24°32′N, 101°01′E, elevation 2460 m), located on Ailao Mountain, Jingdong County, Yunnan Province, SW China. The station is a member of the Chinese Ecosystem Research Network (CERN), and a member of the Chinese National Ecosystem Observation and Research Network (CEORN). Average annual temperature at the study site is 11.3 ^{o}C and average annual precipitation is 1931 mm (Qiu & Xie 1998). Because of abundant moisture and persistent cloud cover, this forest has also been named subtropical cloud forest. The soils of the study site are loamy yellow-brown soils. The surface soil layer (0-15 cm) contains 12.15% organic matter, 0.42% total N, and 0.16% total P (Qiu & Xie 1998). All of the physiological measurements were carried out at the end of the rainy season (September to early November) in 2011. We performed the measurements in this time period because soil water potentials still were close to zero, while sunny days were frequent enough to complete the measurements. Sunny days are rare in the middle of the rainy season owing to frequent rain and fog events. Fourteen co-occurring broadleaf tree species were selected, including ten evergreen species, and four deciduous species (Table 2.1). Sun-exposed trees (2 to 3-m-high) on the forest edge were used to perform the physiological measurements to avoid shading effects.

Leaf and stem water potentials and stomatal conductance

For each species, six newest fully-developed mature leaves from sun-exposed terminal branches of different individuals were selected to measure leaf water potential (Ψ_L) and stomatal conductance (g_s). Leaf water potential was measured with a pressure chamber (PMS, Albany, OR, USA). Stem xylem water potential (Ψ_{ST}) was estimated by measuring the water potential of a non-transpiring (bagged) leaf (Begg & Turner 1970; Nardini, Tyree & Salleo 2001, Sack, Cowan & Holbrook 2003; Bucci *et al*. 2004). Six sun-exposed mature leaves per species were pre-bagged at late afternoon of the previous day for Ψ_{ST} measurement. Predawn samples were collected from the tree in the field at 600 to 700h, while midday samples were collected at 1230 to 1430 h.

Daily maximum and midday leaf stomatal conductance (g_s) was measured with a portable photosynthesis measurement system (LI-6400, LI-COR, Nebraska, USA) under ambient conditions on typical sunny days. Daily maximum stomatal conductance was measured at 900 to 1100 h, while minimum/midday g_s was measured at 1230 to 1430 h. Ambient temperature was around 19 ^{o}C in the morning, and was around 22 ^{o}C during the midday period. Ambient atmospheric vapor pressure deficit (VPD) was around 0.9 kPa in the morning, and 1.4 kPa at midday.

Stem relative water content and capacitance

For stem relative water content (RWC) measurement, stem sections about 15 cm long (n = 6) were cut from different individuals in the field, immediately sealed in a plastic bag, and then transported to the laboratory. Stem samples were collected between 600 and 700 h and again between 1230 and 1430 h. A segment about 5-cm-long was cut from the

middle of the stem section and used to determine the RWC. After determining the fresh weight (FW), the segment was submerged under water for about 48 h for rehydration. After determining the saturated weight (SW), the stem segment was oven-dried for 48 h to determine the dry weight (DW). Stem RWC was then calculated as:

$$RWC = (FW - DW) / (SW - DW) \times 100\% \quad (2.1)$$

Stem hydraulic capacitance over the Ψ_{ST} range during the day (C_{day}) was determined as:

$$C_{day} = \Delta RWC / \Delta\Psi = (RWC_p - RWC_m) / (\Psi_{ST\text{-}p} - \Psi_{ST\text{-}m}) \quad (2.2)$$

Where RWCp is the predawn stem RWC, RWC_m is the midday stem RWC, $\Psi_{ST\text{-}p}$ is the predawn stem water potential, and $\Psi_{ST\text{-}m}$ is the midday stem water potential. Since all the midday $\Psi_{ST\text{-}m}$ were quite high, and more positive than the typical stem tissue turgor loss point of trees (Meinzer *et al*. 2008), it was assumed that stem tissue did not lose turgor during the midday. Stem C_{day} was then normalized to weight of water per volume per MPa (kg m^{-3} Mpa^{-1}) by multiplying the weight of water at saturation per unit sapwood volume. Since stem C_{day} used in the present study is measured over the range of Ψ_{ST} during the day, it is a measure of daily reliance on capacitance, and not necessarily comparable to the hydraulic capacitance as determined in other studies (*e.g.* Meinzer *et al*. 2003).

Wood density

Wood (sapwood) density of terminal branches was measured for six individuals per species. Stem section samples were taken from the terminal branches, sealed in plastic bags, and transported to the laboratory immediately. After removing the bark and pith with a razor blade, the cores were weighed, placed in water in a small graduated cylinder

to determine the volume, and then oven-dried to a constant mass and weighed again to obtain the dry mass. Density was then determined by dividing the dry mass by the volume of the sample.

Stem hydraulic conductivity and leaf hydraulic conductance

Stem hydraulic conductivity was measured using a hydraulic conductivity measurement system (Tyree & Sperry 1989). Branches about 1.5 m long were cut from the trees (n = 6) in the early morning, placed in black plastic bags, and then transported to the lab for measurements. Immediately after arriving at the laboratory, stem segments about 70-cm-long were re-cut under water and attached to the hydraulic conductivity measurement system (Tyree & Sperry 1989). The downstream ends of the stems were connected to measuring pipettes and the flow rates were volumetrically monitored. Following a short equilibration period, water flow generated by a constant hydraulic head of 70 cm, was measured. Distilled/de-gassed water was used as the perfusion fluid. Hydraulic conductivity (kg m $s^{-1}MPa^{-1}$) was calculated as:

$$K_h = J_v / (\Delta P / \Delta X) \quad (2.3)$$

Where J_v is the flow rate through the stem segment (kg s^{-1}; converted from ml s^{-1}) and $\Delta P/\Delta X$ is the pressure gradient across the stem segment (MPa m^{-1}). Specific hydraulic conductivity (K_s; kg m^{-1} $s^{-1}MPa^{-1}$) was obtained as the ratio of K_h and the cross-sectional area of the active xylem. Active xylem area was distinguished from heartwood by pushing dye through the stem sections.

Midday leaf hydraulic conductance (K_{leaf}) was measured with the *in situ* evaporation method (Sellin & Kupper 2007; Sack, Cowan & Holbrook 2003) at 1230 to 1430 h. Leaf

transpiration rate (E) was measured with the portable photosynthetic measurement system (LI-6400, LI-COR, Nebraska, USA) under ambient conditions. Measurements were done within 1 or 2 minutes after leaves were enclosed in the cuvette to minimize the difference in environmental conditions between the cuvette and ambient atmosphere. The driving force was the difference between stem water potential (Ψ_{ST}) and leaf water potential (Ψ_L), measured as described above. Midday K_{leaf} was then calculated as:

$$K_{leaf} = E / \Delta\Psi = E / (\Psi_{ST}-\Psi_L) \quad (2.4)$$

This method may have a disadvantage because the environmental conditions of the enclosed cuvette could be slightly different from the field conditions (Sellin & Kupper 2007), but it also has an advantage in avoiding the effects of detaching the leaves from the plants.

Data analysis

The differences between maximum and midday g_s, between midday Ψ_{ST} and Ψ_L, and between predawn and midday stem RWC were tested by One-way ANOVA. The differences in mean stem capacitance, K_s, midday stem or leaf water potential, as well as midday and maximum g_s between evergreen and deciduous species were tested by Mann-Whitney U tests. Linear or exponential regressions were fitted to the relationships among functional traits (as shown in the Figures).

Results

Eleven of the fourteen broadleaf tree species significantly down-regulated leaf stomatal conductance (g_s) at midday, while three species did not show a significant midday decrease in g_s compared with daily maximum g_s (Fig. 2.1a). Deciduous species had significantly higher maximum and midday g_s, compared with evergreen species (Fig. 2.1a; Table 2.2). Midday leaf water potential (Ψ_L) of the 14 tree species ranged from -0.55 to -1.84 MPa, while midday stem water potential (Ψ_{ST}) ranged from -0.12 to -0.50 MPa (Fig. 2.1b). The deciduous tree species had significantly lower midday Ψ_L, but significantly higher Ψ_{ST} than the evergreen species (Fig. 2.1b; Table 2.2). Midday Ψ_L was significantly more negative than Ψ_{ST} in all the species (Fig. 2.1b). All 14 species showed midday declines in stem RWC, but these were only significant in eight of the species (Fig. 2.1c).

No significant correlation was found between midday g_s and midday Ψ_L across species (Fig. 2.2a). In contrast, a significant, positive correlation was found between midday g_s and midday Ψ_{ST} (Fig. 2.2b). Midday Ψ_{ST} and midday Ψ_L were not significantly correlated (data not shown). Midday g_s and daily maximum g_s were positively correlated with stem xylem area specific hydraulic conductivity (K_s; Fig. 2.2c; 2.2d). Deciduous species had significantly higher K_s than the evergreen species (Fig. 2.2c; Table 2.2).

Midday Ψ_{ST} was positively correlated with stem hydraulic capacitance over the Ψ_{ST} range during the day (C_{day}; Fig. 2.3a), negatively correlated with wood density (Fig. 3b), and positively correlated with K_s (Fig. 2.3c) across the 14 tree species. On the other hand, Ψ_L was negatively correlated with C_{day} (Fig. 2.4a) and change in stem RWC

(predawn RWC – midday RWC; Fig. 2.4b), and positively associated with midday leaf hydraulic conductance (Fig. 4c).

Discussion

In spite of the commonness of midday depression in stomatal conductance (g_s) and its impact on leaf photosynthetic gas exchange and plant productivity, the hydraulic determinants of midday g_s are not well understood. Previous studies have focused on the role of hydraulics in determining maximum g_s and photosynthetic rate (Brodribb & Field 2000; Santiago *et al*. 2004; Broddribb, Feild & Jordan 2007; Campanello, Gatti & Goldstein 2008; Zhang & Cao 2009), but not in maintaining g_s at midday. By studying the interspecific correlations among stem specific hydraulic conductivity (K_s), daily reliance on hydraulic capacitance, midday stem xylem water potential (Ψ_{ST}), leaf water potential (Ψ_L), and g_s in 14 co-occurring broadleaf species, our study reveals some insights concerning the hydraulic determinants of midday g_s, the coordination between stem and leaf hydraulics, and the adaptive significance of midday depression in g_s. Different tree species may have different rooting depth, and may experience different soil water potentials, which will influence stomatal behavior. However, our measurements were performed at the end of the rainy season when water potentials of the different soil layers were close to zero. Therefore, species-specific difference in g_s should be explained by species-specific functional traits rather than soil water availability in the rooting zone.

Hydraulic determinants of midday stomatal conductance

Our results suggest that midday g_s of the 14 broadleaf species studied was more closely related to midday stem water status than to leaf water status. That is, species with a greater capacity to avoid high stem water deficits during periods of higher transpiration were able to maintain higher midday g_s than species with lower hydraulic capacity. On the other hand, the close relationship between Ψ_{ST} and g_s suggests that the primary functional significance of stomatal closure during the day is probably to protect the stem xylem rather than the leaf hydraulic system, although the direct internal signal that triggers stomatal closure probably involves leaf level traits such as guard cell turgor (Franks *et al*. 1995) or leaf hydraulic conductance (K_{leaf}) (Brodribb & Holbrook 2003).

Several studies have shown that diurnal decrease and recovery in leaf hydraulic conductance is common in plants (Bucci *et al*. 2003; Brodribb & Holbrook 2004a; Zhang *et al*. 2009; Johnson *et al*. 2009a; 2011b; Zufferey *et al*. 2011), and that embolism is the main process explaining the decrease in K_{leaf} (Lo Gullo *et al*. 2003; Woodruff *et al*. 2007; Johnson *et al*. 2009b; Johnson *et al*. 2011a). The lack of coordination between midday g_s and midday Ψ_L in the present study was consistent with the diurnal decline and recovery in K_{leaf} reported in several species and suggests that stomatal regulation of Ψ_L does not avoid embolism in leaves of the species studied. Embolism refilling in leaves with relatively smaller xylem vessels than those of stems will cost less energy because the hydrostatic pressures required for embolism refilling depend upon the conduit size (Hack & Sperry 2003), and also leaf xylem is in close proximity to the sugars recently produced by photosynthesis, which apparently are required for embolism refilling under negative pressure (Zwieniecki & Holbrook 2009; Nardini, Lo Gullo & Salleo 2011). Embolism in

either the petiole or leaf lamina introduces a hydraulic bottleneck between leaf and stem, which would inhibit further water loss from the stem (Zufferrey *et al*. 2011). In addition, stomatal closure is closely coordinated with the initiation of leaf cavitation (Brodribb & Holbrook 2003; Brodribb *et al*. 2003, Brodribb & Holbrook 2004b), and leaf cavitation may amplify the signal of water deficits to further stimulate stomatal closure to inhibit further water loss from stems (Brodribb & Holbrook 2004b). Therefore, both stomatal closure and K_{leaf} down-regulation appear to be involved in maintaining Ψ_{ST} within a safe range to avoid xylem dysfunction, and regulation of K_{leaf} probably linked Ψ_{ST} and g_s in the studied species.

Determinants of midday leaf and stem water potentials

The maintenance of high stem water potential during active transpiration appears to be related to both hydraulic conductivity and stem water storage. The positive correlation between daily reliance on hydraulic capacitance (C_{day}) and midday Ψs_T in this study agrees with the positive effects of hydraulic capacitance on Ψs_T found in previous studies (Meinzer *et al*. 2003; 2008; 2009), suggesting the generality of this coordination, and the importance of stem water storage in maintaining better stem water status during periods of active transpiration. Stem water storage may only contribute a small fraction to the total daily transpiration (Kobayashi & Tanaka 2001; Phillips *et al*. 2003; Meinzer *et al*. 2003); however, it can play an important role in dampening diurnal fluctuations in Ψ_{ST} (Meinzer *et al*. 2008). Stem hydraulic conductivity (K_s) also was correlated strongly with midday Ψ_{ST}, suggesting that the efficiency of the water transport system from root to the stem also plays a role in buffering diurnal fluctuations in stem water status. Therefore,

stem water status during periods of active transpiration is a function of both the water transport efficiency upstream and the transient release of water from internal storage pools.

In contrast to Ψ_{ST}, midday Ψ_L was negatively related to C_{day} across species: species with higher stem hydraulic capacitance showed more negative midday Ψ_L. This was consistent with the negative relationship between daily change in RWC and midday Ψ_L indicating that species withdrawing more stored water from their stems tended to have more negative values of midday Ψ_L than species withdrawing less stored stem water. This relationship could be explained by an indirect linkage: high C_{day} allows higher Ψ_{ST}, and since stomatal regulation mainly protects the stem xylem from embolism, higher Ψ_{ST} promotes maintenance of higher g_s, but the greater transpiration associated with higher g_s results in a greater drop in Ψ across the hydraulic resistance of the leaf. Partial loss of K_{leaf} in response to the transpiration-induced decline in Ψ_L would amplify the difference between Ψ_{ST} and Ψ_L unless transpiration was limited by reduced g_s. The relationship between capacitance and Ψ_L observed here is contrary to the result from a study in a Brazilian savanna, which reported a positive relationship between stem hydraulic capacitance and midday Ψ_L (Scholz *et al*. 2007). This is probably because the study of Scholz *et al*. was performed during the pronounced dry season when g_s is more depressed at midday compared to the present study, which would bring leaf and stem Ψ closer to equilibrium. In contrast, midday g_s of the trees in the present study was relatively high (ranging from 0.08 to 0.34 mol m^{-2} s^{-1}), which would prevent equilibrium between stem and leaf Ψ.

Comparison between evergreen and deciduous species

Evergreen and deciduous species showed convergent relationships between midday Ψ_{ST} and both stem capacitance and midday g_s. However, deciduous species were able to maintain higher midday Ψ_{ST}, and higher midday g_s due to their higher C_{day} and higher K_s, compared with the evergreen species. This result is consistent with those from a previous study, showing lower wood density and higher capacitance in deciduous species than co-occurring evergreen species (Choat *et al*. 2005). Higher midday g_s in deciduous species should allow higher midday CO_2 assimilation and consequently higher daily carbon gain per unit leaf area compared to evergreen species.

Notably, in spite of higher Ψ_{ST} and g_s, deciduous species showed significantly lower midday Ψ_L than the evergreen species, suggesting that higher Ψ_{ST} does not necessarily result in higher Ψ_L, and high Ψ_L is not necessary for maintaining high midday g_s in these species. This agrees with the result that midday g_s was more related to Ψ_{ST} than to Ψ_L across species in the present study. Deciduous species may maintain high g_s during the midday at the expense of embolism in their leaves. Although diurnal embolism was not studied in the present study, deciduous species showed lower midday K_{leaf} than evergreen species, which, combined with higher midday g_s and transpiration rate contributed to substantially lower midday Ψ_L than in evergreen species. In addition, although deciduous species showed significantly higher C_{day}, K_s, midday Ψ_{ST} and g_s than evergreen species, evergreen and deciduous species showed overlap in these functional traits, suggesting that these two phenological groups operate along a shared continuum of functional traits.

In conclusion, we found that midday g_s was more closely associated with midday stem water status than with leaf water status, suggesting that the functional significance of stomatal regulation in the species studied is mainly prevention of stem xylem dysfunction. The ability of species to avoid stem hydraulic dysfunction during periods of active transpiration was related to both stem hydraulic conductivity and reliance on stem hydraulic capacitance.

Table 2.1 Fourteen broadleaf tree species studied in Chapter 2, their species code used, family and leaf phenology

Species	Code	Family	Leaf phenology
Lithocarpus jingdongensis Y.C.Hsu & H.J.Qian	LJ	Fagaceae	Evergreen
Symplocos sumuntia D. Don	SS	Symplocaceae	Evergreen
Schima noronhae Reinw. ex Blume	SN	Theaceae	Evergreen
Vaccinium delavayi Franch	VD	Vacciniaceae	Evergreen
Manglietia insignis Blume	MI	Magonoliaceae	Evergreen
Lithocarpus hypoviridis Y.C. Hsu, B.S. Sun & H.J. Qian	LH	Fagaceae	Evergreen
Ternstroemia gymnanthera Sprague	TG	Theaceae	Evergreen
Lyonia ovalifolia Drude var. *lanceolata* Hand.-Mazz.	LOv	Ericaceae	Evergreen
Hartia sinensis Dunn	HS	Theaceae	Evergreen
Illicium macranthum A.C. Smith	IM	Illiciaceae	Evergreen
Betula alnoides Hamilt.	BA	Betulaceae	Deciduous
Populus yunnanensis Dode	PY	Salicaceae	Deciduous
Lyonia ovalifolia Drude var. *ovalifolia*	LO	Ericaceae	Deciduous
*Clethra brammeriana*Hand.-Mazz.	CB	Clethraceae	Deciduous

Table 2.2 The mean stem capacitance over the Ψ_{ST} during the day (C_{day}), specific hydraulic conductivity (Ks), midday stem water potential (Ψ_{ST}) or leaf water potential Ψ_L, as well as midday and maximum stomatal conductance (g_s) of evergreen and deciduous species. The data are means ± SE. The *P* values are from Mann-Whitney U test between evergreen and deciduous species

	C_{day} kg m^{-3} MPa^{-1}	K_s kg m^{-1} s^{-1} MPa^{-1}	Midday Ψ_{ST} MPa	Midday Ψ_L MPa	Midday g_s mol m^{-2} s^{-1}	Maximum g_s mol m^{-2} s^{-1}
Evergreen	94±23	1.38±0.12	-0.31±0.03	-0.79±0.06	0.11±0.01	0.19±0.02
Deciduous	324±115	2.48±0.44	-0.16±0.02	-1.56±0.22	0.21±0.04	0.27±0.02
P	0.011	0.016	0.016	0.024	0.005	0.016

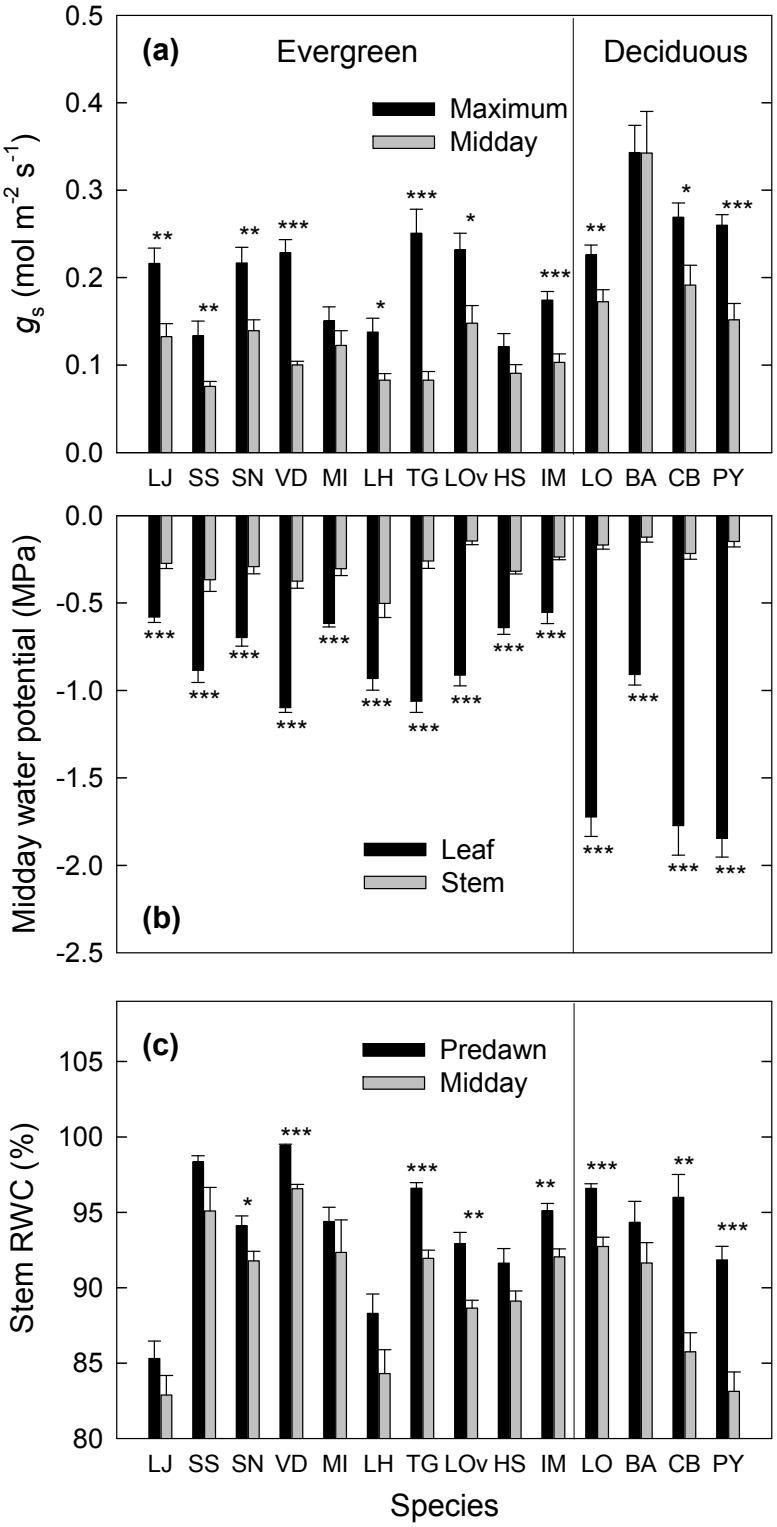

Figure 2.1 (a) Daily maximum and midday leaf stomatal conductance (g_s); (b) midday leaf water potential and midday stem water potential; and (c) predawn and midday stem relative water content (RWC) of 14 broadleaf tree species from Ailao Mountain. * $P < 0.05$; ** $P < 0.01$; *** $P < 0.001$.

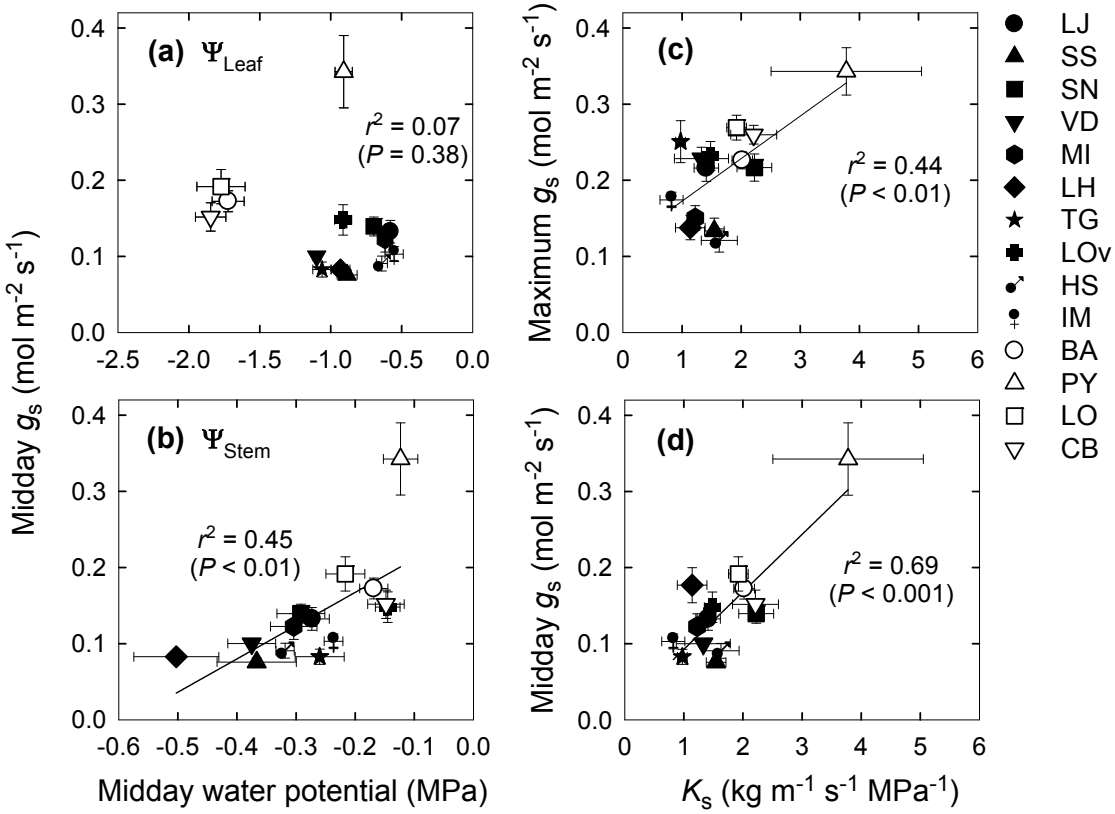

Figure 2.2 (a) Midday leaf stomatal conductance (g_s) in relation to midday leaf water potential (a), and midday stem water potential (b); and stem xylem area specific hydraulic conductance in relation to daily maximum g_s and midday g_s across species. Solid lines are linear regressions fitted to the data.

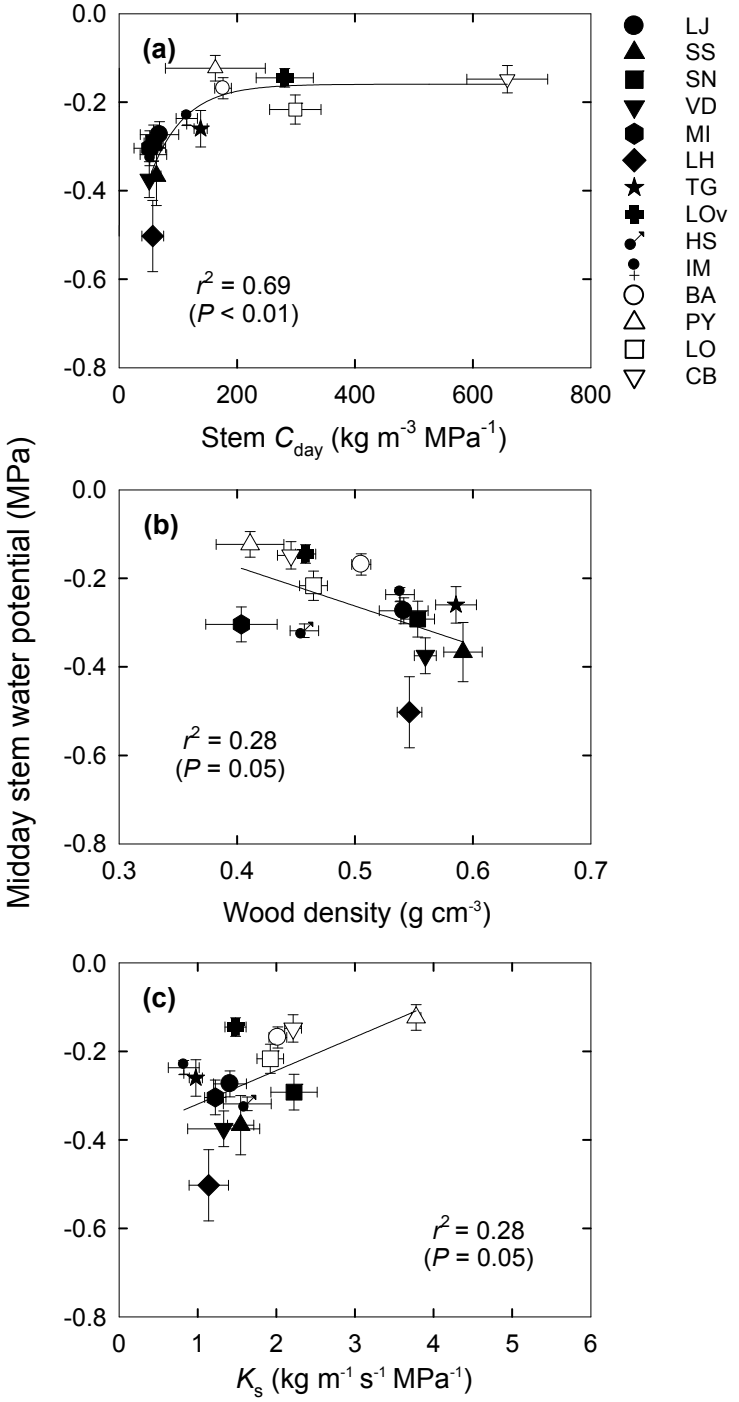

Figure 2.3 Midday stem water potential in relation to stem hydraulic capacitance over the Ψ_{ST} range during the day (C_{day}; a), wood density (b), and stem xylem area specific hydraulic conductance (c). Solid lines are linear (b; c) or exponential (a) regressions fitted to the data.

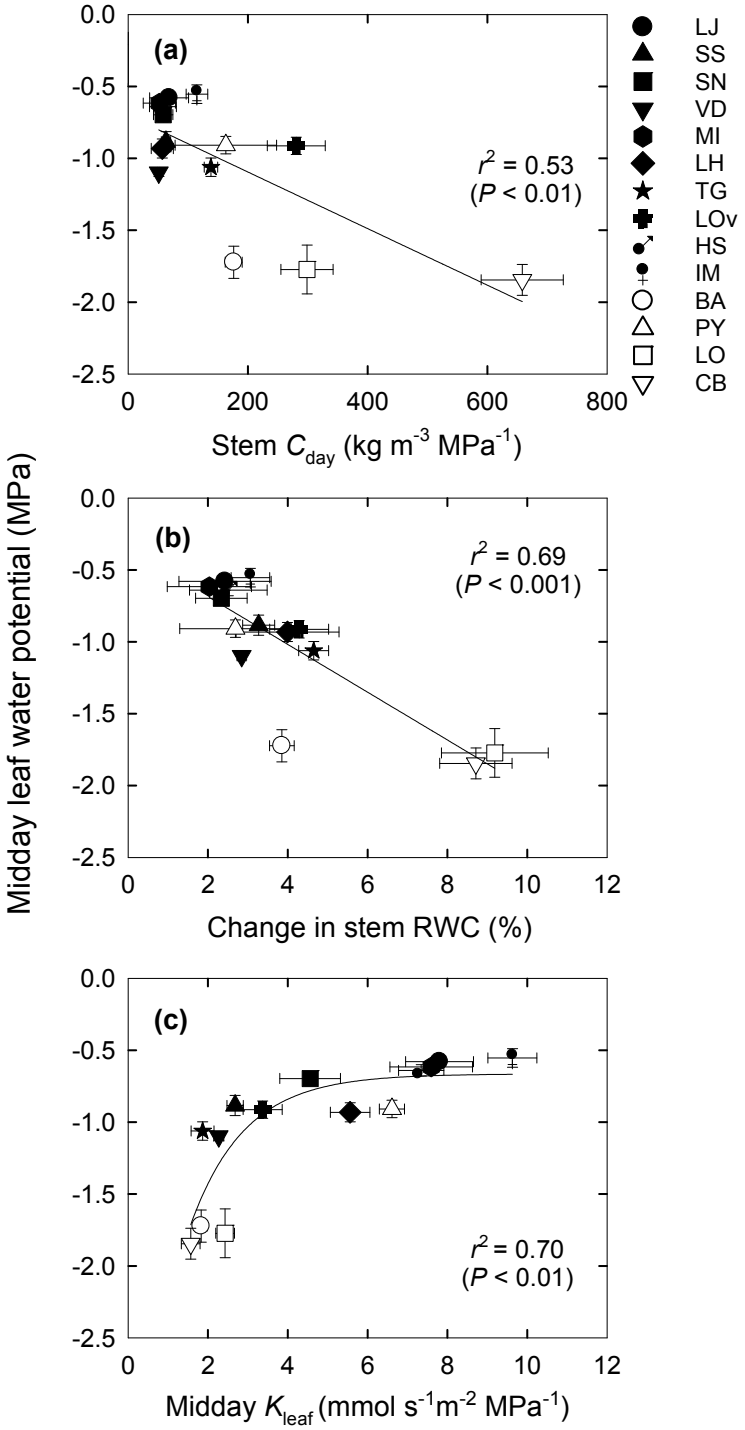

Figure 2.4 Midday leaf water potential in relation to stem hydraulic capacitance over the Ψ_{ST} range during the day (C_{day}; a), change in stem relative water content (b), and midday leaf hydraulic conductance (c). Solid lines are linear (a; b) or exponential (c) regressions fitted to the data.

CHAPTER 3

Homeostasis of water and carbon balances in an Asian subtropical cloud forest during the 2010 rainfall anomaly

Summary

Southwestern China experienced the most severe rainfall anomaly in a century during the 2010 dry season. In order to understand the response of subtropical forests to rainfall anomalies, we studied leaf physiology, soil water status, canopy conductance, and ecosystem carbon exchange of a primary subtropical cloud forest in SW China during the normal 2009 dry season and the 2010 rainfall anomaly. Soil water storages of the primary forest and some secondary forest/shrub-land in this region also were compared. Trees in the primary cloud forest were not water-deficient either during the 2009 or 2010 dry season (predawn leaf water potentials > -0.4 MPa). Minimum leaf water potential, which ranged from –0.7 to -1.2 MPa, did not differ between the 2009 and 2010 dry seasons. The homeostasis in minimum water potential in 2010, despite a substantial decrease in soil water content and the substantial lowering of the water table, was probably a consequence of decreased stomatal and canopy conductance. Down-regulation of transpiration incurred a small cost in carbon uptake at leaf and ecosystem levels. Although net ecosystem CO_2 assimilation decreased from that of the 2009 dry season by 116 g m^{-2} $month^{-1}$ in the last month of the 2010 dry season, the forest was still a carbon sink even during the driest period of the 2010 rainfall anomaly. Our results provide evidence that some Asian subtropical forests can buffer the effects of severe rainfall anomalies by using soil water storage and ground water at depth, and by lowering

stomatal and canopy conductance. The considerable carbon gain by the evergreen broadleaf trees in the dry seasons also partially explains the dominance of evergreen trees in the subtropical forests of SW China, and the large carbon sink function of these ecosystems.

Background

Water availability is a major environmental factor that strongly limits the primary production of terrestrial ecosystems on a global scale (Lieth 1975). Intense and/or prolonged droughts greatly influence the structure, composition, dynamics and productivity of forest ecosystems (Krishnan *et al*. 2006; Mueller *et al*. 2005; Engelbrecht *et al*. 2007; Granier *et al*. 2007). Although drought is a frequently-recurring event in many terrestrial ecosystems, such ecosystems may or may not be able to resist drought events in the future as their frequency, strength, and duration will increase according to global circulation model predictions (Trenberth 1999; Easterling *et al*. 2000). Increased drought strength and frequency may induce tree dieback (Allen 2009; Allen 2010), may change species composition of the ecosystem (Condit *et al*. 1998; Jentsch *et al*. 2007), and may convert forests to savannas (Bachelet *et al*. 2001). On the other hand, tree dieback and the eventual loss of forest stands induced by droughts may further accelerate global climate change (Raming *et al*. 2010). Understanding the responses of different ecosystems to severe drought events is necessary for predicting the interaction between vegetation and climate in the future, and is necessary for developing effective strategies of land use management.

During the dry season or severe drought events, trees and forests may use different mechanisms to mitigate against increased water deficits. In the short term, trees could down-regulate stomatal conductance (Schulze *et al*. 1987), refill embolized xylem (Bucci *et al*. 2003), and use water storage in stems to buffer water deficits (Borchert 1994; Goldstein *et al*. 1998; Scholze *et al*. 2007; Meinzer *et al*. 2009). In the long term, trees may decrease total leaf area (Breda *et al*., 2006), modify their hydraulic architecture (e.g. the leaf area to sapwood area ratio; McDowell *et al*. 2002; Zhang *et al*. 2009), and increase investments in the root system for enhancing water uptake (Leuschner *et al*. 2001). Drought deciduousness is also an adaptation to avoid the effects of seasonal water deficits (Kikuzawa & Lechowicz 2011). Soil water storage and ground water storage may serve as buffers for rainfall shortage in dry seasons and severe droughts. Soil water storage capacity is an important factor in determining ecosystem production and species distributions (Lacambra *et al*. 2010; Piedallu 2011). The capacity is mainly determined by soil depth, soil porosity, organic matter content, and root development (Hursh 1943; Madsen *et al*. 2008; Geroy *et al*. 2011). Different vegetation types may differ in soil water storage capacity.

Several regions of the world experienced the worst drought (rainfall anomaly) of a century in 2010, including the Amazon region (Lewis *et al*. 2011) and Southwest China (Qiu 2010; Stone 2010; Zang *et al*. 2010). The 2010 drought in the Amazon caused a larger scale tree dieback than the 2005 “once in a century” drought (Marengo *et al*. 2008), based on satellite imagery (Lewis *et al*. 2011). The 2010 drought also turned the Amazon forest from a carbon sink into a carbon source (Lewis *et al*. 2011). The 2010 SW China drought severely affected the regional agriculture and economy (Qiu 2010; Stone 2010;

Zang *et al*. 2010). This severe drought might induce tree dieback and weaken the carbon sink function of the subtropical and tropical forests in this region. However, the effects of this rainfall anomaly on forest ecosystems in SW China were not assessed.

In spite of a pronounced dry season, the subtropical forests in SW China are dominated by evergreen broadleaf trees (Wu 1980). This suggests that the evergreen trees assimilate carbon in the dry season and outcompete deciduous tree species, a likely phenomenon that needs verification. However, an increase in duration and strength of droughts in the future may change the forest composition by favoring deciduous species, and reverse the carbon sink function. We studied the dry season leaf level, tree level, and ecosystem level performances of an evergreen broadleaf cloud forest from subtropical SW China, as well as the responses of this forest to the 2010 rainfall anomaly. This forest was within an area experiencing the highest rainfall deficits in SW China during the 2010 rainfall anomaly (Zang *et al*. 2010). The aims of this study were (1) to assess the dry season performance in terms of water and carbon balances and the impact of the 2010 rainfall anomaly on a subtropical cloud forest in SW China; (2) to understand the responses at leaf and ecosystem levels of the primary forests in this region to the rainfall anomaly, and (3) to understand the mechanisms that trees and the forest ecosystem may use to mitigate the negative effects of rainfall anomalies.

Materials and methods

Study site

We conducted this research in a primary cloud forest at the Ailaoshan Station for Subtropical Evergreen Broadleaf Forest Ecosystem Studies (24°32′N, 101°01′E, elevation 2460 m), located on Ailao Mountain, Jingdong County, Yunnan Province, SW China. This mountain stretches for 500 KM, ranging from 23^{o} 35’ to 24^{o}44’N, and from 100^{o} 54’ to 101^{o}30’E. Its forest is dominated by evergreen broadleaf trees, with some deciduous species scattered in the forest. Of the few deciduous species, most of them grow at the edge of the forest stands and in gaps, while only about two or three are late successional species interspersed with evergreen trees. The deciduous species remain leafless for 5 to 6 months. The evergreen broadleaf forests on this mountain are located on the upper part of the water catchment areas that provide water for agricultural lands in nearby areas (Qiu & Xie 1998). The station is affiliated with Xishugangbanna Tropical Botanical Garden, Chinese Academy of Sciences, and is a member of the Chinese Ecosystem Research Network (CERN), and also the Chinese National Ecosystem Observation and Research Network (CEORN). Annual average temperature at the study site is 11.3 ^{o}C and annual average precipitation is 1931 mm (5 year averages; Qiu & Xie 1998). Because of abundant moisture and persistent cloud cover, this forest has been considered to be a subtropical cloud forest. The soils of the study site are loamy yellow brown soils. The surface soil layer (0-15 cm) contains 12.15% organic matter, 0.42% total N, and 0.16% total P (Qiu & Xie 1998). More than 85% of rain falls in the wet season from May to October or November. Therefore, there is an obvious dry season

from December to April. We compared the leaf level, individual level and ecosystem level water relations and gas exchange of the cloud forest during the 2010 rainfall anomaly with those in a year with normal rainfall (2005, 2009 or 2011). Nine dominant evergreen tree species in the primary forest were selected for the present study (Table 3.1). All the physiological measurements were performed on sunny days.

Soil and leaf water potentials and soil water storage capacity

Soil water potential was estimated using measured soil water content and the soil moisture releasing curves for different soil layers of this forest (the relationship between soil water potential and soil water content; unpublished data, YJZ) in April 2009 and April 2010. In 2010, soil water content was determined for three sites in the primary forest on April 15th, while in 2009, soil water content was determined for one site on April 15th, as the regular dynamic monitoring of the Ailaoshan Station for Subtropical Evergreen Broadleaf Forest Ecosystem Studies. Predawn and midday leaf water potentials were measured with a pressure chamber (PMS, Corvallis, OR, USA) in April 2009 and 2010. Predawn leaf samples were collected from trees in the field at 600 to 700 h, while midday samples were collected at 1230 to 1430 h.

Soil water storage capacities of a primary forest and a secondary *Yushania-Pteridium* shrub-land formed after logging and burning also were estimated based on soil porosity (Sun *et al*. 2006; CERN Science Commission 2007) compared with secondary forests in this region (Peng *et al*. 2005). Three sites in the primary forest, and three in the secondary shrub-land were chosen for soil water storage capacity measurements.

Leaf gas exchange measurements

Leaf maximum (light saturated) photosynthetic rate (CO_2 assimilation; A_{max}) and stomatal conductance (g_s) were monitored at the end of the dry season in 2009 and in 2010 with a Li6400 portable photosynthesis system (Li-Cor Inc., Lincoln, NE, USA). Sun-exposed trees (2-3 m high) at the forest edge were used for gas exchange measurements to avoid shading effects. Six sun-exposed leaves per species and from different individuals were chosen for the gas exchange measurement. A_{max} was measured under a saturation photosynthetic photon flux density (PPFD; 1200 μmol m^{-2} s^{-1}), ambient temperature, ambient relative humidity, and ambient CO_2 concentration. Leaf intrinsic water use efficiency was calculated as A/g_s.

Tree sap flow measurement

Xylem sap flow was monitored with a heat dissipation sap flow measurement system (Grainer 1985; Grainer 1987). Ten trees from 9 species in the forest were selected for sap flow measurements. Two cylindrical probes (20 mm long; 2 mm diameter) were inserted horizontally into the south facing side of the trees at breast height. Irregular sections of tree stems were avoided. The upper probe was continuously heated by a constant current power supply, while the lower reference probe (about 15 cm lower than the upper probe) remained unheated. Temperature differences between two probes were measured every 10 seconds, and 30 minute averages were recorded by a datalogger (CR1000, Campbell Scientific, USA). Sap flux densities were calculated using the empirical function developed by Granier (1987). Tree sap flux densities from typical sunny days in April

2010, and in April 2011 were compared. The sap flow monitoring was started in late 2009, thus data for April 2009 were not available.

Tree growth and canopy leaf area index

Tree circumferential growth at breast height of 102 trees from the primary forest was monitored using stainless steel dendrometer bands installed ~1.5-m-high aboveground. Irregular sections of tree stems were avoided. Data were collected monthly from July 2009 to December 2010. Annual total circumference increments in 2009 and 2010 were compared. Stem growth was not standardized by the initial stem diameter because our purpose was to compare stem growth of the same individuals in two continuous years. Canopy leaf area index was measured by a LAI-2000 canopy analyzer (Li-Cor Inc., Lincoln, NE, USA) in April 2005 and April 2010. Leaf area index measurements are part of the regular forest dynamics monitoring work by the Ailaoshan Station conducted every 5 years. Eight sites in the forest were chosen for these measurements, at 0800, 1200, 1600 on sunny days at each site, and the daily averages were used to represent the LAI of each site.

Ecosystem carbon assimilation and canopy conductance

Ecosystem carbon assimilation and canopy conductance were estimated from eddy flux data. The eddy flux system was installed above the canopy on a canopy tower, at a height of 34 m. The flux system included a CSAT3 three-dimensional sonic anemometer (Campbell Scientific Inc., Logan, UT, USA), and a Li-7500 open-path CO_2/H_2O infrared gas analyzer (Li-Cor Inc., Lincoln, NE, USA). Measurements were recorded every 0.1

sec with a CR5000 datalogger (Campbell Scientific Inc., Logan, UT, USA). Air humidity and temperature (HMP45C, Vaisala, Helsinki, Finland), wind speed (A100R, Vector Instruments, Denhighshire, UK), soil heat flux (HFP01, HukseFlux, Delft, Netherlands) were also recorded every 30 min. Data processing and calculations were described by Tan *et al*. 2011, while canopy conductance was calculated as in Li *et al*. 2006.

Data analysis

The differences in mean leaf A_{max}, g_s, water use efficiency between April 2009 and April 2010 were tested by the Mann-Whitney U tests because homogeneity of variance was not satisfied. The differences in canopy leaf area index and in tree annual circumferential growth at breast height between April 2005 (or 2009) and April 2010, were tested by one-way ANOVA. The relationship between daily average canopy conductance and daily average VPD were fitted with an exponential equation ($y = a + b \times e^{-c \times x}$).

Results

The rainfall in the 2010 dry season was a historical minimum at the Ailaoshan Station, 274 mm lower than the inter-annual average (Fig. 3.1a). The length of the dry season was also longer than the previous dry season and extended four months into the previous year (Fig. 3.1b). The normal dry season can extend one or two months into the previous year. However, for simplicity we denote the dry season year with the year containing most of the dry months. The rapid decrease of the ground water table started in August 2009 for the 2010 dry season, about 3 months earlier than the rapid decrease of the water table in 2007 and 2008. The ground water table in 2010 also reached the lowest recorded value

since the initiation of water table monitoring in 2007 (Fig. 3.1c). The water potentials of the surface soils (0-10 and 10-30 cm) were substantially lower in April 2010 (end of the dry season) than in April 2009, but the deeper soil layers differed little in water potential between April 2009 and April 2010 (Fig. 3.2). Water potential at the surface soil layer (0-10 cm) reached -0.58 MPa in April 2010. Soils deeper than 10 cm maintained water potentials higher than –0.5 MPa in April 2010. There were fewer rain events during the first 15 days of April in 2010 than in 2009 (Fig. 3.3a). There were 12 days with daily average air VPD higher than 0.8 KPa during the first 15 days of April 2010 (Fig. 3.3b). The maximum daily average VPD in April 2010 was also higher than that in April 2009 (Fig. 3b). Air VPD tended to decrease after April 15th, when frequent rains started (Fig. 3.3a).

Predawn leaf water potentials of all the 9 evergreen tree species studied were less (more positive) than –0.4 MPa in April 2010 (Fig. 3.4a). Three tree species had significantly lower predawn leaf water potentials in April 2010, compared to the values in April 2009, consistent with the lower ground water table height (Fig. 3.1c), and lower soil water potentials (Fig. 3.2) observed in 2010. Daily minimum water potentials were similar between 2009 and 2010 dry seasons (Fig. 3.4b). Only one species had a lower midday leaf water potential in April 2010 than that in April 2009 (Fig. 3.4b).

Two of the nine tree species had lower leaf maximum CO_2 assimilation (photosynthetic rate; A_{max}) in April 2010 than in April 2009, while the rest of the species did not differ significantly in A_{max} between two dry seasons (Fig. 3.5a). However, all the species except *Lithocarpus hypoviridis* exhibited significantly lower stomatal conductance (g_s) in April 2010 than that in April 2009 (Fig. 3.5b). Consequently, intrinsic

water use efficiency (A/g_s) of all the tree species was higher in April 2010 than in April 2009 (Fig. 3.5c). Average tree sap flux density of the 10 trees was also reduced in April 2010 compared to the same period of 2011 (Fig. 3.6).

The relationship between canopy conductance and ecosystem net CO_2 assimilation (Fig. 3.7b) was similar to the relationship between leaf g_s and A_{max} (Fig. 3.7a). As g_s or canopy conductance increased, A_{max} or net ecosystem net CO_2 assimilation also increased. When g_s reached 1.3 mol m^{-2} s^{-1} or canopy conductance reached 1 cm s^{-1}, both A_{max} and net ecosystem net CO_2 assimilation of the forest remained constant with increasing conductance (Fig. 3.7). Many of the points from April 2009 fell into the asymptotic portion of the relationship, when CO_2 assimilation did not tend to increase as stomatal/canopy conductance increased (Fig. 3.7).

Daily average canopy conductance decreased as daily average air VPD increased, and the relationship was well described by an exponential decay equation (Fig. 8). In a large number of days during the 2010 dry season, the VPD remained at high levels, and canopy conductance remained very low (Fig. 3.8).

The daily net ecosystem CO_2 assimilation on typical sunny days of April 2010 was lower than that in the dry season of 2009 (Fig. 3.9a). Net ecosystem CO_2 assimilation on sunny days of the 2010 dry season showed higher midday depression than in the 2009 dry season (Fig. 3.9b). The monthly carbon assimilation in 2010 April was about two thirds of that in 2009, whereas the carbon assimilation was still high (193 g CO_2 m^{-2} $month^{-1}$; Fig. 3.8b). Canopy leaf area indices between April 2005 and April 2010 did not differ statistically (Fig. 3.9c). Tree circumferential growth at breast height was lower in 2010 than in 2009, but not significantly so (Fig. 3.9d).

The soil water storage, particularly noncapillary water storage (the portion that is available for plant use) in the evergreen broadleaf cloud forest soils on Mount Ailao was higher than that of the secondary *Yushania-Pteridium* shrub land in Mount Ailao, as well as higher than that of other secondary forests in this region (Fig. 3.10).

Discussion

Our study revealed that the evergreen trees in subtropical SW China maintained good water status and considerable carbon assimilation during the 2009 dry season, and during the 2010 severe rainfall anomaly. Homeostasis in minimum water potentials can help explain that, despite a rainfall anomaly, the subtropical cloud forests in SW China maintained high soil water contents and high carbon assimilation rates. The dry season CO_2 assimilation of the evergreen species is advantageous for the carbon balance of those species compared to the deciduous species that remain leafless in the dry seasons, and may help to explain why the subtropical forests in SW China are dominated by evergreen species (Wu 1980). Our results provide evidence that primary evergreen subtropical forests could buffer the effects of the most severe rainfall anomaly in a century, and could limit the negative effects of rainfall shortages on forest carbon assimilation and tree growth by using soil water storage, and by increasing water use efficiency.

Limited impact of the dry season and the rainfall anomaly

Trees of the 9 evergreen species studied in the cloud forest did not experience water deficits, either in the 2009 dry season or in the 2010 rainfall anomaly. In consequence, the trees and the ecosystem maintained considerable carbon assimilation in the 2009 dry

season and during the 2010 rainfall anomaly, while nearly all deciduous species were leafless or partially leafless. Deciduousness is an adaptation to unfavorable seasons (Kikuzawa & Lechowicz 2011), therefore some tropical and subtropical ecosystems with strong rainfall seasonality and without underground water are dominated by deciduous species (Givnish 2002). The limited impact of seasonal water deficits and the 2010 rainfall anomaly on forest carbon assimilation also help to explain the high carbon sink function of this old-growth subtropical cloud forest (Tan *et al*. 2011).

The 2010 rainfall anomaly substantially decreased the water loss rates of the trees, but the leaf area index and carbon assimilation were relatively less affected. Stomatal conductance (g_s), tree sap flux density and canopy conductance on sunny days were significantly lower in the 2010 dry season than in the 2009 dry season. Some tropical and subtropical forests partially drop leaves to decrease canopy transpiration to conserve water during droughts (Breda *et al*. 2006). However, absence of leaf area index differences between 2005 and 2010 dry seasons suggests that the 2010 rainfall anomaly did not result in substantial leaf drop. Despite significant decreases in g_s, the maximum leaf photosynthetic capacity of most species did not decrease during the 2010 rainfall anomaly, compared to the 2009 dry season. However, a lower maximum g_s resulted in higher sensitivity of carbon assimilation to changes in stomatal/canopy conductance during the day (the leaves operated on the linear portion of the A-g_s relationship, Fig. 3.7). As a consequence, there was a larger photosynthetic midday depression in 2010 than in 2009, which resulted in a lower daily carbon assimilation on sunny days (Fig. 3.9a). The 2010 Amazon rainfall anomaly shifted the carbon balance of the Amazon forest from carbon sink to carbon source (Lewis *et al*. 2011), while the studied subtropical cloud

forest was still a carbon sink in the driest period of the 2010 rainfall anomaly (Fig. 3.10). The tree growth of the cloud forest was negatively affected, but not significantly. All of this suggests that the 2010 rainfall anomaly had a limited impact on physiological and ecosystem level processes of the subtropical forest.

Possible mechanisms buffering the effects of the rainfall anomaly

The shortage in rainfall was compensated by soil water storage, ground water storage, and down-regulation of transpiration. Since water potentials of soils deeper than 10 cm were higher than -0.4 MPa, the soil still can supply enough water to the plants. Adequate soil water status during the 2010 rainfall anomaly suggests that the cloud forests on Ailao Mountain had sufficient ground water and soil water storage to buffer the shortage of rainfall in the dry season and during the severe rainfall anomaly. A larger decrease in ground water table in 2010 than in previous years suggests that more ground water was used to buffer the effects of the rainfall anomaly, and also suggests that roots can have access to deep water sources even if ground water table was relatively far from the soil surface of the forest.

During this severe rainfall anomaly, many crops, rivers and lakes were completely deprived of water, and some forests showed dieback in SW China (Qiu 2010; Stone 2010; Zang *et al*. 2010). One possible mechanism that allowed the studied cloud forest to maintain good water status is its high water storage capacity, which recently has been shown to be an important factor in determining ecosystem productivity and species composition (Lacambra *et al*. 2010; Piedallu 2011). This primary cloud forest has higher soil water storage capacity than some secondary vegetation types in this region (Fig.

3.10). Soil water storage capacity was mainly determined by soil porosity, organic matter content, and root development (Hursh 1943; Madsen *et al*. 2008; Geroy *et al*. 2011). The higher soil porosity of this primary forest compared to secondary vegetation is probably the result of its highly developed fine root system (Qiu & Xie 1998). Rich soil organic matter (Qiu & Xie 1998) may also contribute to its high soil water storage capacity. In addition, deep leaf litter layer on the forest floor of this primary forest (Qiu & Xie 1998) could help to slow down evaporation from the soil surface evaporation. The difference in response to severe rainfall anomaly between this subtropical cloud forest and the Amazonian rainforest (Lewis *et al*. 2011) could be explained by relatively higher soil water storage capacity, higher soil organic matter, and thicker litter layer of the subtropical forest, as well as relatively lower temperatures of the subtropical forests, particularly during the winter/dry season.

Down-regulation in g_s is a common adaptation of plants in coping with diurnal and seasonal water deficits (Schulze *et al*., 1987), and trees growing in humid environments may close their stomata relatively quickly when VPD decreases (Franks & Farquhar 1999; Cunningham 2004). In spite of lower soil water potential and higher VPD in 2010 compared to 2009, midday leaf water potentials in the 2010 dry season of three tree species were similar to the values in the 2009 dry season. This suggests that these species maintained leaf water potential within a certain range by strong stomatal control during rainless periods. This isohydric behavior is explained by the high sensitivity of canopy conductance to VPD. The relationship between daily average canopy conductance and daily average VPD of the cloud forest was similar to a drought sensitive aspen stand (Bernier *et al*. 2006), but the cloud forest showed an even steeper slope of canopy

conductance versus VPD. This conservative water use strategy helped avoid large transpirational water losses and consequent sharp decreases in soil water content during the rainfall anomaly.

Implications for forest succession and management

Increase in frequency and strength of rainfall anomalies may shift the community composition of forests (Condit 1998; Jentsch *et al*. 2007) by favoring drought adapted species that either can tolerate or avoid water deficits (Condit 1998). Two species that showed the highest decrease in g_s among the species studied also exhibited significantly lower A_{max} in 2010 than in 2009, while the rest did not show a significant difference in A_{max} between 2009 and 2010 (Fig. 3.5b). These two species may be disadvantaged in a prolonged rainfall anomaly event in terms of carbon assimilation. In addition, the tree species varied in pre-dawn leaf water potential during the 2010 rainfall anomaly, suggesting a difference in rooting depth (Fig. 3.4a). Pre-dawn leaf water potential is mainly determined by the water potential of soils where the roots are located (Ritchie & Hinckley 1975; Bucci *et al*. 2005) if there is a water potential equilibrium between the leaves and the soil depths from which the roots are taking water. Tree species with a high investment in deep rooting systems may have an access to deep soil water, which usually tends to be a stable source of water for plant growth, but they may show relatively low growth rates because of less resource allocated to aboveground growth. This type of life history trait will be favored by an environment with increased duration, strength and frequency of drought (Trenberth 1999; Easterling *et al*. 2000; Jentsch *et al*. 2007).

The 2010 SW China rainfall anomaly had a large destructive impact on the regional economy and agriculture (Qiu 2010; Stone 2010). Large scale deforestation in SW China has been suggested to be a factor that exacerbated the effects of the 2010 rainfall anomaly (Qiu 2010). At a landscape level, the primary forests with sufficient soil and ground water storage will not only help to provide water to the trees, but also to the nearby agricultural systems. Our results thus suggest that maintaining relatively large scale primary forests with high water storage will be of importance to enhance the capacity of the region to buffer rainfall anomaly effects. However, primary forests in SW China underwent severe deforestation during the past decades, and are still facing large threats by expanding rubber and eucalyptus plantations (Qiu 2009; Ziegler *et al*. 2010).

In conclusion, the water loss rate of the primary subtropical cloud forest significantly decreased during the 2010 rainfall anomaly compared to normal dry seasons, but the impact of this rainfall anomaly on leaf area index, carbon economy, and tree growth of the forest was limited. Abundant soil water storage, water sources at depth and a lower stomatal and canopy conductance that reduces the rate of water loss were important in avoiding the negative effects of rainfall anomalies at plant and ecosystem levels. Substantial carbon assimilation by the forest during dry seasons and the 2010 rainfall anomaly provides evidence that this subtropical cloud forest has a high capacity to buffer severe rainfall anomalies. The considerable carbon gain by the evergreen broadleaf trees in dry seasons also partially explains the dominance of evergreen species in the subtropical forests of SW China, and the high carbon sink function of these subtropical forests. The results of this study also provide a better mechanistic

understanding of the potential homeostatic responses of Asian subtropical forests to global climate change.

Table 3.1 Nine evergreen broadleaf tree species studied in Chapter 3, their species code used, and family

Species	Species Code	Family
Lithocarpus jingdongensis Y.C.Hsu & H.J.Qian	LJ	Fagaceae
Symplocos sumuntia D. Don	SS	Symplocaceae
Schima noronhae Reinw. ex Blume	SN	Theaceae
Vaccinium delavayi Franch	VD	Vacciniaceae
Manglietia insignis Blume	MI	Magonoliaceae
Lithocarpus hypoviridis Y.C. Hsu, B.S. Sun & H.J. Qian	LH	Fagaceae
Ternstroemia gymnanthera Sprague	TG	Theaceae
Hartia sinensis Dunn	HS	Theaceae
Illicium macranthum A.C. Smith	IM	Illiciaceae

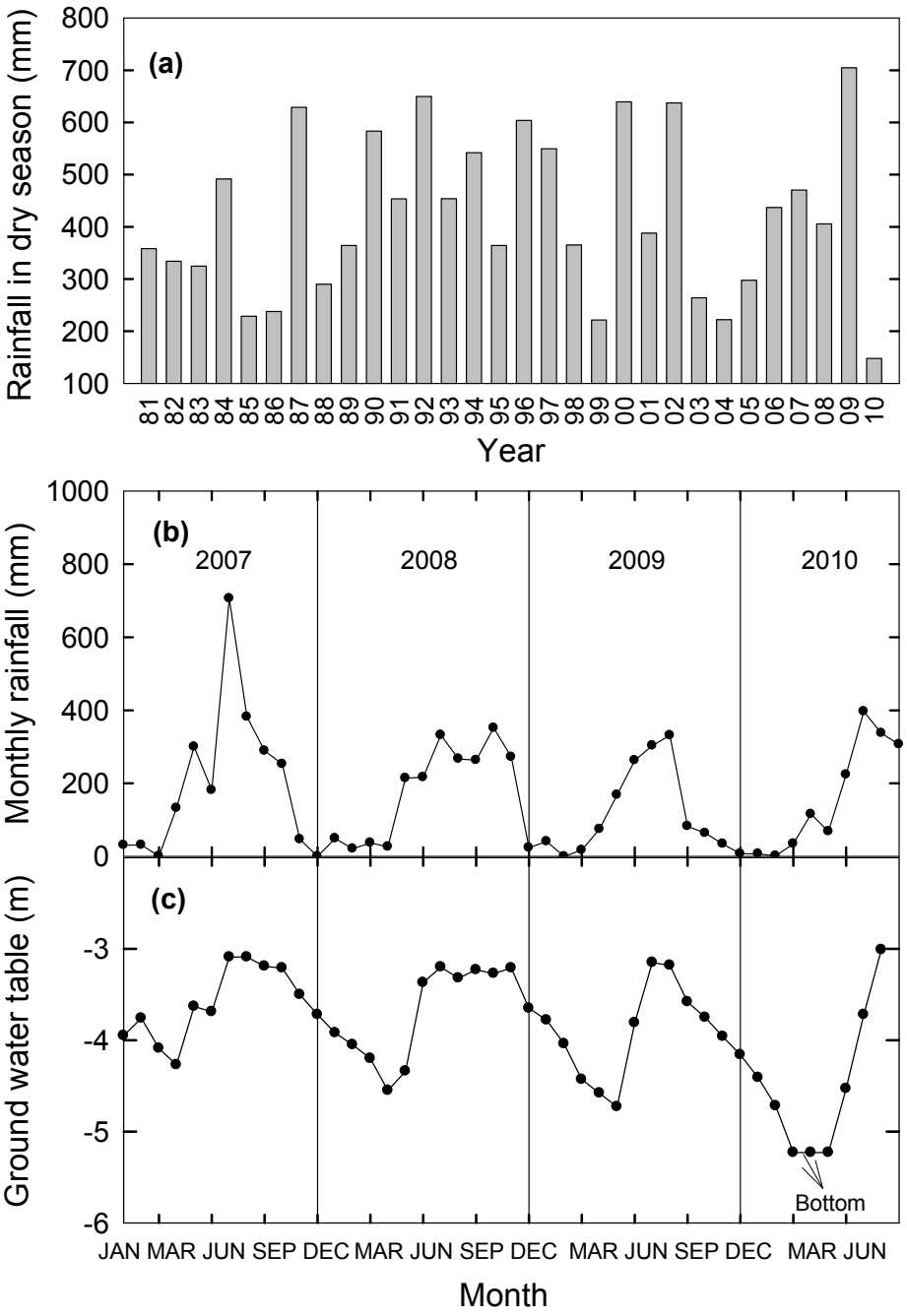

Figure 3.1 (a) Rainfall in dry season from 1980 to 2010, and (b) monthly rainfall and (c) dynamics of ground water table from 2007 to 2010. Data from Ailaoshan Station for Subtropical Ecosystem Studies (Elevation 2460 m).

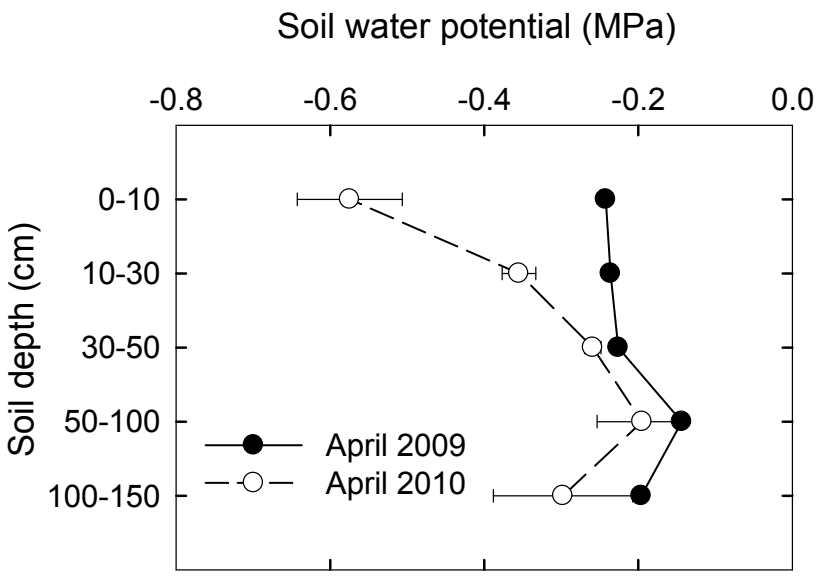

Figure 3.2 Soil water potential of different soil layers at the end of the dry season in 2009 and 2010 (measured on April 15th, right before the beginning of the wet season).

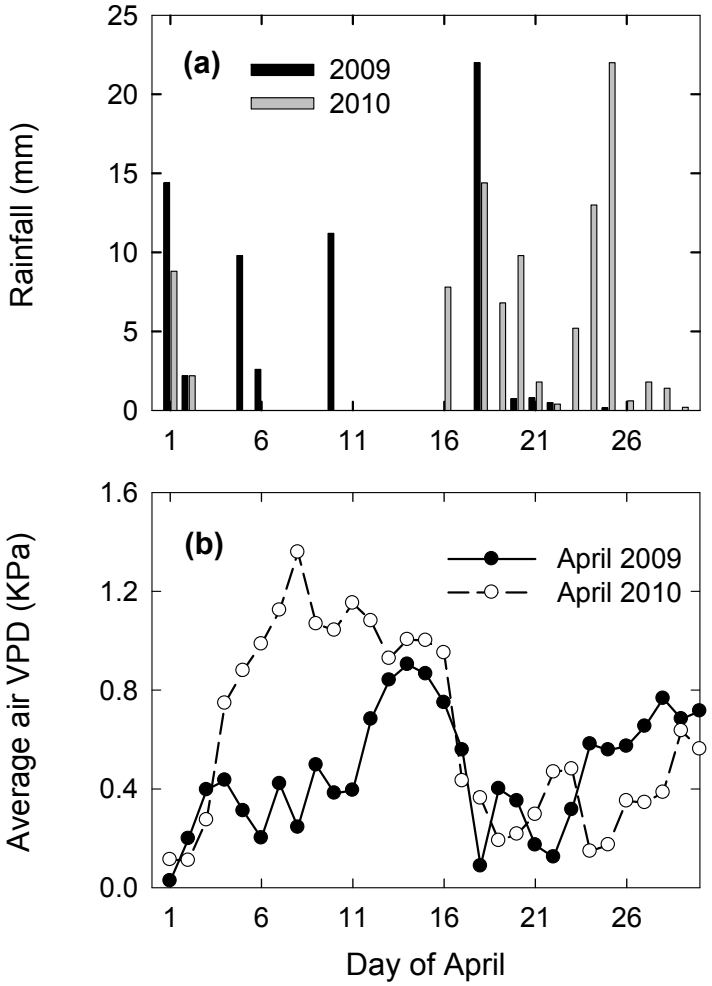

Figure 3.3 (a) daily rainfall and (b) average air VPD at the end of the dry season in 2009 and 2010. Data from Ailaoshan Station for Subtropical Ecosystem Studies (Elevation 2460 m).

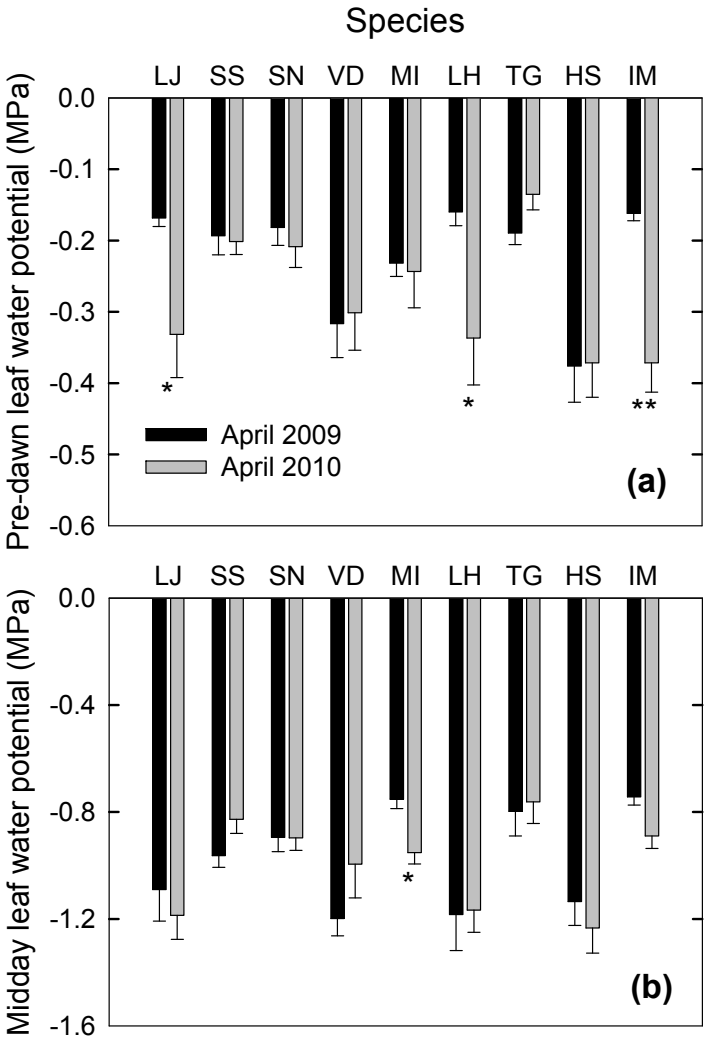

Figure 3.4 Predawn (a) and midday (b) leaf water potential of nine evergreen species at the end of the dry seasons of 2009 and 2010. Bars are means + SE. *, $P < 0.05$; **, $P < 0.01$; ***, $P < 0.001$. Species codes are in table 3.1.

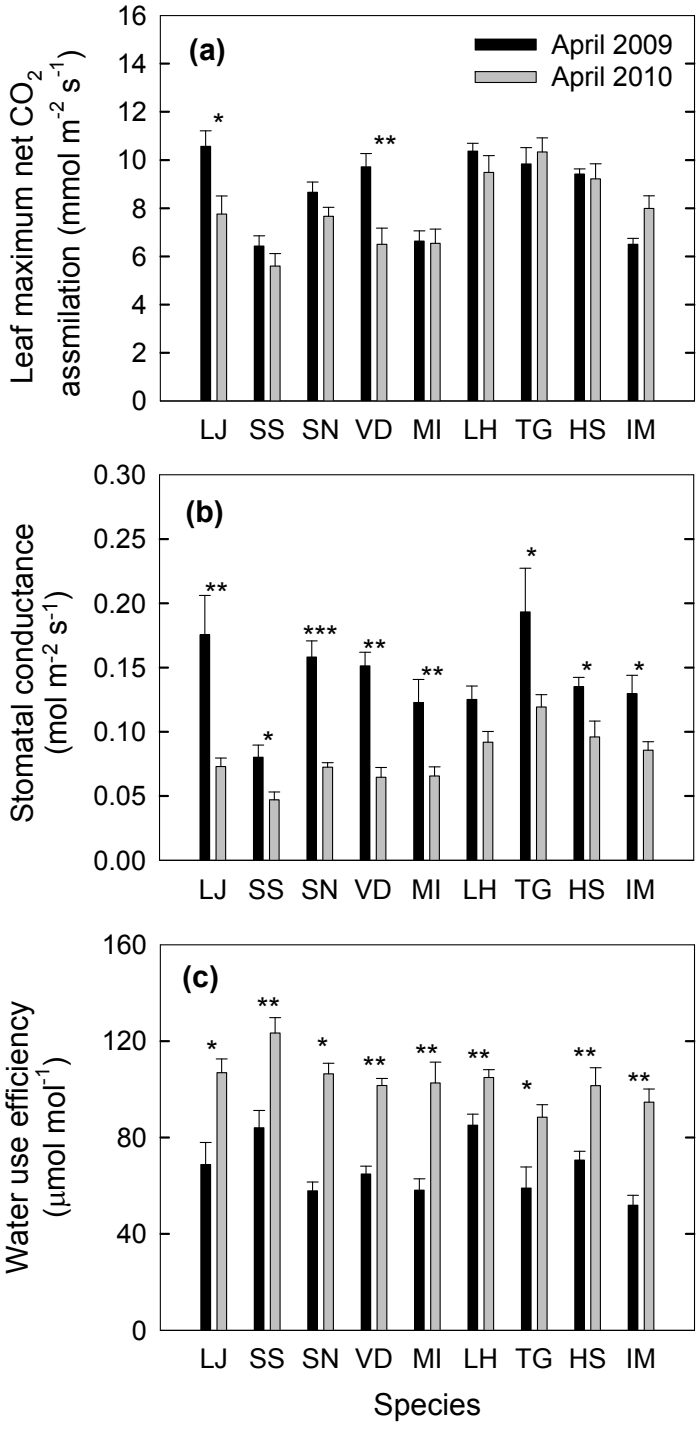

Figure 3.5 The leaf maximum net CO_2 assimilation (a), stomatal conductance (b), and water use efficiency (c) of different tree species in the 2009 and 2010 dry seasons. Bars are means + SE. *, $P < 0.05$; **, $P < 0.01$; ***, $P < 0.001$. Species codes are in table 3.1.

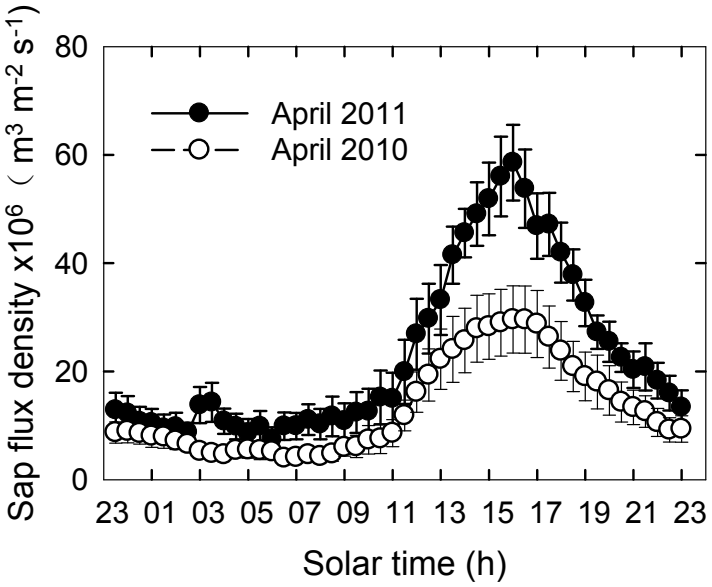

Figure 3.6 Diurnal variation in sap flux density of six trees on sunny days in the dry season of 2010 (the driest year of a century), and 2011 (a normal dry season). Points are means ± SE (n = 10).

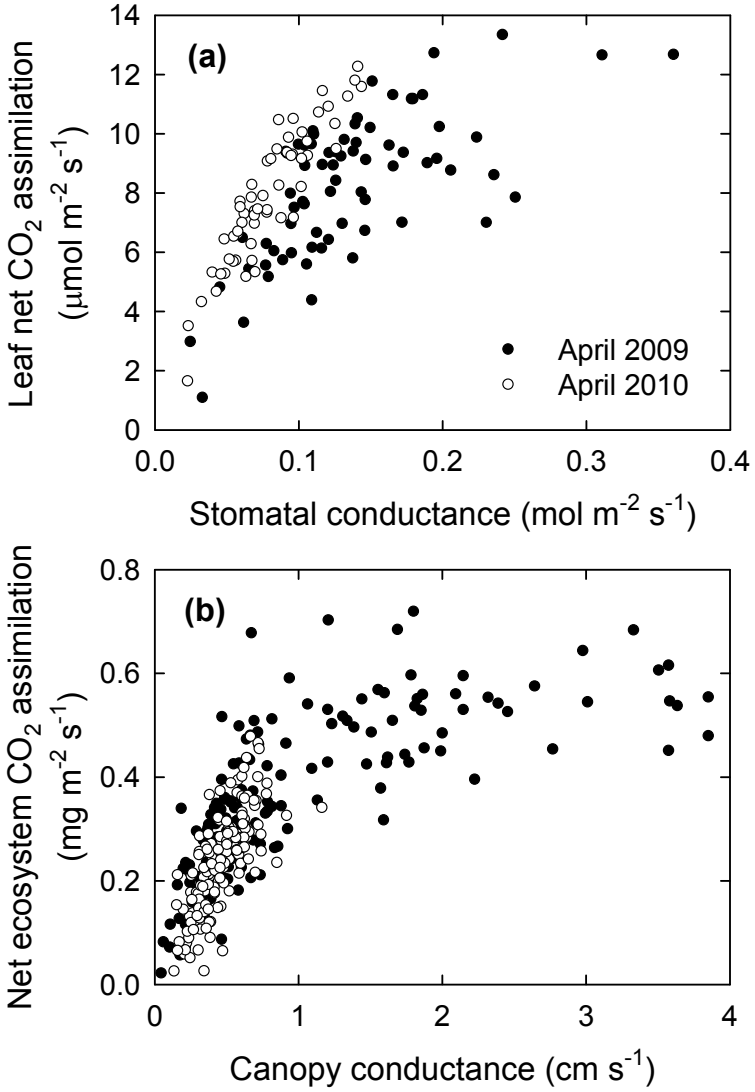

Figure 3.7 The relationship between leaf net CO_2 assimilation and stomatal conductance across species (A), and the relationship between net ecosystem CO2 assimilation and canopy conductance (B) in 2009 and 2010 dry seasons. The points in panel A stand for leaves from different individuals, the points in panel B stand for half hour mean values of the forest canopy during sunny days.

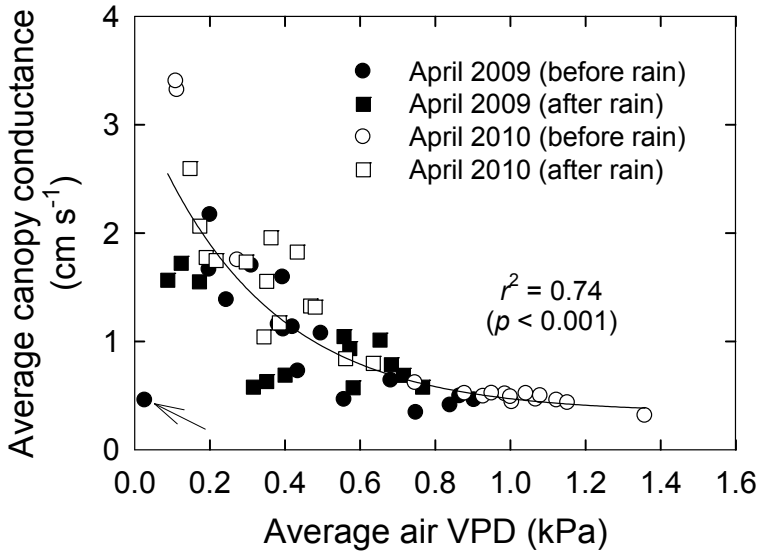

Figure 3.8 The relationship between average daily canopy conductance and daily average VPD in April, 2009 and 2010. Each point represent a day. Open points are days of April 2010, while the closed points represent measurements done in April 2009. Circles are days before the big rain events (April 18th, 2009; April 16th, 2010; representing the coming of the wet season; Fig. 3a), while squares are days after the big rain event. The line is an exponential regression fitted to the data with the day with average VPD close to zero (the point with an arrow) not included.

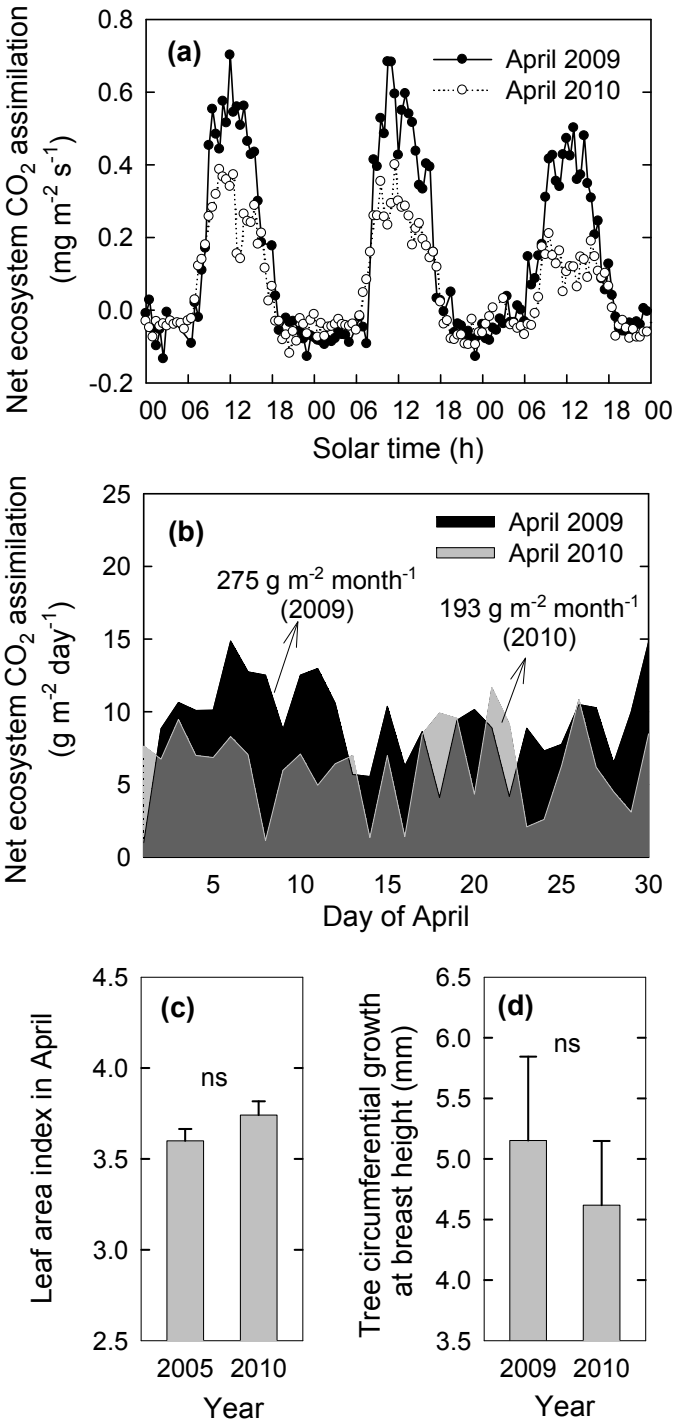

Figure 3.9 (a) Diurnal variations of net ecosystem CO_2 assimilation in three typical sunny days at the end of the dry seasons of 2009 and 2010. (b) Daily net ecosystem CO_2 assimilation in April 2009 and April 2010. (c) Leaf area index in April, 2005 and 2010. (d) Yearly tree circumferential growth at breast height in 2009 and 2010 (n = 102).

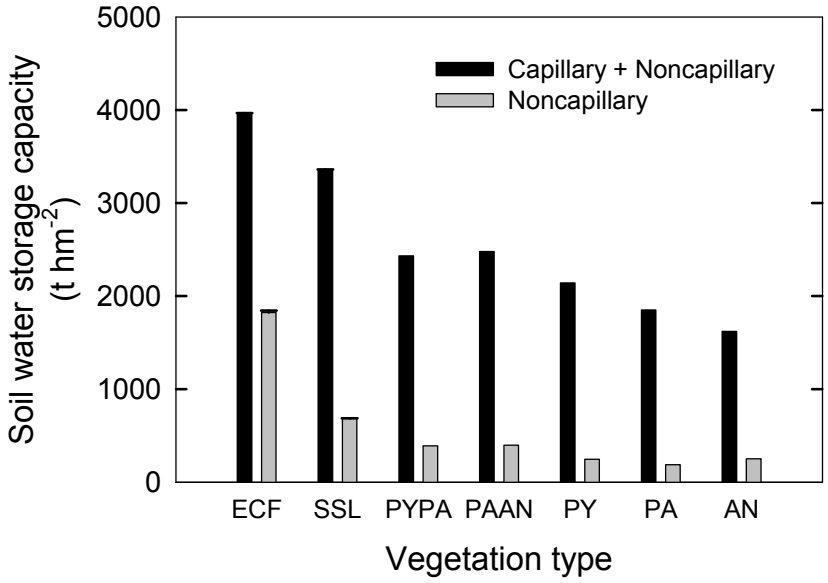

Figure 3.10 Soil water storage capacity (0 – 50 cm) of the Ailao cloud forest and different types of secondary vegetations. ECF stands for evergreen broadleaf cloud forest in Mount Ailao, SSL stands for secondary shrub land in Mount Ailao, PYPA stands for secondary forest mixed with *Pinus yunnanensis* and *Pinus armand* in this region; PAAN stands for secondary forest mixed with *Pinus armandi* and *Alnus nepalens* in this region; PY stands for secondary pure forest of *Pinus yunnanensis* in this region; PA stands for secondary pure forest of *Pinus armandi* in this region; AN stands for secondary pure forest of *Alnus nepalens* in this region. The data of the 5 secondary forests were cited from Peng *et al*. (2005).

CHAPTER 4

Leaf and ecosystem level carbon balances of an Asian subtropical cloud forest: the influences of cloud cover and seasonal low temperatures

Summary

Seasonal dynamics of CO_2 assimilation in subtropical forests are poorly understood. Evergreen broadleaf trees dominate the forests from elevations of 1000 to 2600 m in the subtropical area of SW China despite a pronounced cold-dry season. It is intriguing that evergreen trees are dominant in these forests, because deciduous trees might be expected to outcompete evergreen trees in areas with strong rainfall seasonality and frequent freezing winter temperatures. In order to understand this paradox, seasonal dynamics in the photosynthesis of ten evergreen and five deciduous broadleaf tree species from a montane cloud forest in SW China were studied. Long distance water transport and low temperature effects on photosynthetic system I and II also were studied. Carbon assimilation at the ecosystem level also was studied with eddy covariance methods. Although all 10 evergreen species down-regulated maximum photosynthetic rate by 13 to 53% in winter, they maintained high winter carbon assimilation (5.4 to 8.8 μmol m^{-2} s^{-1}). Trees were able to tolerate the coldest winter season in history. The ecosystem CO_2 assimilation was limited by frequent cloud cover, reduced incoming solar radiation and leaf wetness duration, but by not low winter temperatures. The high winter carbon assimilation of evergreen trees resulted in a higher annual carbon gain than by the deciduous species, which may partially explain why the evergreen trees can establish dominance in these subtropical montane forests. Substantial winter carbon uptake also

allows these forests to sequester relatively high levels of carbon compared to other forest ecosystems.

Background

Temperature is one of the major limiting factors for photosynthesis. Evergreen trees, which maintain leaves in the winter season, are prone to low temperature effects. Low temperatures limit photosynthesis by increasing photoinhibition (Sevanto *et al*. 2006), and impairing enzyme activities (Hammel 1967). In habitats with frequent subzero temperatures, winter photosynthesis could also be limited by a decrease in water supply to leaves. Freeze-thaw cycles could induce embolism (blocking of xylem vessels by air bubbles) in the xylem tissue (Hammel 1967; Sperry & Sullivan 1992; Davis *et al*. 1999; Cavender-Bares & Holbrook 2001; Pittermann & Sperry 2006), which will lower the stem hydraulic conductivity, reduce the supply of water to leaves, and may consequently decrease the stomatal conductance and leaf photosynthetic rates. In a Japanese temperate forest, evergreen broad-leafed trees that exhibited distinct decreases in hydraulic conductivity assimilated little CO_2 during the winter, while evergreen broad-leaf species that could maintain substantial stem water conductance also maintained positive CO_2 assimilation (Taneda & Tateno 2005).

Winter photosynthesis of trees is well studied in boreal, Mediterranean, and temperate forests (*e.g*. Pearcy 1987; Malhi *et al*. 1999). Conifer trees in boreal forests show negligible or even negative net photosynthesis in winter owing to freezing temperatures (Hanninean & Hari 2002; Sevanto *et al*. 2006; Hari & Makela 2003), while shrubs in Mediterranean biomes can maintain considerably high net photosynthesis in

winter because of mild low temperatures (Flexas *et al*. 2001; Oliveira & Penuelas 2004). Trees in temperate forests have different winter photosynthetic performances depending on the temperature regime and the freezing resistance of the species (Taneda & Tateno 2005). Some tree species in temperate forests maintain high winter photosynthetic rates, while some freezing-intolerant trees exhibit negative net photosynthesis (Taneda & Tateno 2005). Trees in forests from subtropical areas, particularly at higher elevations, also are exposed to seasonal low temperatures. It is not known, however, if they can maintain relatively high photosynthetic rates during the winter.

Cloud cover reduces solar radiation, and thereby limits leaf photosynthesis. Cloud cover greatly influences day to day and year to year variation in net ecosystem carbon gain, based on eddy-covariance studies (Hollinger *et al*. 1994; Kellomäki & Wang 2000; Zhang *et al*. 2011). The canopy photosynthesis of trees in lowland tropical forests is limited by cloud cover and light, especially in wet forests (Mulkey *et al*. 1996). Artificial increases in light levels on trees in a Panamanian tropical rainforest increased leaf CO_2 uptake and tree growth (Graham *et al*. 2003). Subtropical zones in East Asia are subject to the influences of monsoons, resulting in a wet season with high rainfall and long duration of cloud cover, as well as a pronounced dry season. Therefore the wet season photosynthesis of trees in the Asian subtropics could be limited by long duration of cloud cover. In contrast, less cloud cover in the dry season may promote leaf CO_2 assimilation by allowing higher incoming solar radiation. However, dry seasons in the Asian subtropics coincide with seasonal low temperatures. A combination of high solar radiation and low temperatures in the dry/winter season could induce severe photo-

inhibition, because low temperatures may reduce light utilization in relation to greater light absorption (Germino & Smith 1999; 2000; Miyazawa *et al*. 2007).

Owing to limited studies in subtropical forests, the contribution of subtropical forests to the global carbon cycle is poorly understood. Subtropical forests could potentially be larger carbon sinks than tropical forests if they maintain relatively high carbon uptake and low respiration rates during the winter. For instance, the annual net ecosystem carbon sequestration of a subtropical evergreen broadleaf forest in SW China is among the highest of old-growth forests (Tan *et al*. 2001). Subtropical forests are mainly distributed in East Asia and South America. Evergreen broadleaf trees dominate the forests from 1000 to 2600 m in the subtropical area of SW China, while subtropical forests from SE China with similar elevations are dominated by deciduous trees. The subtropical area in SW China has milder low temperatures in winter than in SE China, as the Tibet Plateau prevents cold fronts from moving south in western China. The objectives of this study were (1) to assess winter photosynthetic performances of evergreen trees and annual carbon balances of evergreen and deciduous trees near the upper distribution limits of the subtropical zone, (2) to understand the environmental limitations on leaf photosynthesis and ecosystem carbon gain in the subtropics, and (3) to deduce the importance of winter carbon assimilation for evergreen broadleaf trees, which may partially explain their dominance in the subtropical montane forests of SW China.

Materials and methods

Study site and plant materials

This study was performed in a primary evergreen broadleaf forest at the Ailaoshan Station for Subtropical Evergreen Broadleaf Forest Ecosystem Studies (24°32′N, 101°01′E, elevation 2460 m), located on Ailao Mountain, Jingdong County, Yunnan Province, SW China. This mountain stretches for 500 KM, ranging from 23^{o} 35’ to 24^{o}44’N, and from 100^{o} 54’ to 101^{o}30’E. The station is affiliated with Xishugangbanna Tropical Botanical Garden, Chinese Academy of Sciences, and is a member of the Chinese Ecosystem Research Network (CERN), and also the Chinese National Ecosystem Observation and Research Network (CEORN). Annual average temperature at the study site is 11.3 ^{o}C and annual average precipitation is 1931 mm (5 year average; Qiu & Xie 1998). During five months of the year (from November to March), minimum air temperatures are below 0 ^{o}C (Fig. 4.1a). More than 85% of rainfall occurs during the wet season, from May to October, and the dry season extends from November to April. Because of abundant moisture and persistent cloud cover, this forest also has been described as subtropical cloud forest. In the wet season from May to October, the number of days with daytime fog is higher than 20 per month, while the number of rainy days is higher than 14 per month (Fig. 4.1b). Consequently, the sunshine duration in the wet season is substantially lower than that in the dry season (Fig. 4.1c). Photosynthetic photon flux density (PPFD) is higher from February to May than the rest of the year (Fig. 4.1d). Fluctuation in daily PPFD is reduced during the winter season because of lower numbers of foggy and rainy days (Fig. 4.1d). The soils of the study site are loamy yellow-

brown soils. The surface soil layer (0-15 cm) contains 12.15% organic matter, 0.42% total N, and 0.16% total P (Qiu & Xie 1998).

The cloud forests on Ailao Mountain are dominated by evergreen broadleaf tree species, with some deciduous species scattered in the forest (Table 4.1). Fifteen broadleaf tree species in the forest, including 10 evergreen and 5 deciduous species, were selected for the present study (Table 4.1). *Lithocarpus jingdongensis* is the most abundant evergreen species, while *Lyonia ovalifolia* var. *ovalifolia* is the most abundant deciduous species (Table 4.1). Sun-exposed trees (2 to 5-m-high) at the forest edge were used to perform the physiological measurements to avoid shading effects, and to minimize differences in microhabitats.

Gas exchange measurements

Seasonal dynamics in leaf light-saturated net CO_2 assimilation (A_{max}) of the 15 broadleaf tree species were monitored using a portable photosynthesis measurement system (LI-6400XT, LI-COR, Lincoln, NE, USA) from October 2008 to July 2009. Six sun exposed mature leaves from different individuals per species were measured at a saturation photosynthetic photon flux density (1200 mol m^{-2} s^{-1} for evergreen species, and 1500 for deciduous species, based on photosynthetic light response curves) and ambient temperature and ambient CO_2 concentration. Trees were measured on sunny days between 0830 and 1030 h solar time. Some photosynthetic rates of trees during the wet season were measured on cloudy days because there were very few sunny days in the rainy season (Fig. 4.1b). Leaf dark respiration during the night also was measured with

the portable photosynthesis measurement system between 2100 to 2300 h in January and September 2009, under ambient temperatures and ambient CO_2 concentrations.

The leaf photosynthetic light response curves were completed in August, December 2008, and January, March, June 2009 for *Lithocarpus jingdongensis*, and in August, November 2008, and April, June 2009 for *Lyonia ovalifolia* var. *ovalifolia*. Leaves were exposed to a gradient of PPFD ranging from 0 to 2000 μmol m^{-2} s^{-1}, generated by a LED light source (LI-COR, Lincoln, NE, USA) attached to the photosynthetic measurement system. When a steady state net photosynthesis was obtained after exposing the leaf surface to a specific light intensity for about 3 to 5 minutes, the net photosynthetic rate was recorded by the LI-6400 portable photosynthesis measurement system. The relationships between *A* and PPFD were fitted by an exponential equation described by Bassman & Zwier (1991). Leaf daily CO_2 assimilation was estimated by the light response curves, and PPFD data was measured by a Li-190SB PPFD quantum sensor (LI-COR, Nebraska, USA), and recorded by a CR3000 data logger (Campbell Scientific Inc., Logan, UT, USA).

Diurnal changes in leaf actual CO_2 assmilation of *Lithocarpus jingdongensis* were monitored on December 21, 2009 (a typical sunny day). Six-sun exposed leaves from different individuals were marked and their diurnal variations in gas exchange were monitored. The net CO_2 assmilation was recorded by the LI-6400 portable photosynthesis measurement system under actual PPFD, ambient temperature and ambient CO_2 concentration. The measurement was repeated seven times during the day (0800, 1000, 1130, 1330, 1500, 1700, and 1830 h).

Leaf sensitivity to low temperatures

Sensitivity of leaf photosynthetic system I and II (PSI and PSII) to low temperatures was determined in January 2010, when the trees were fully acclimated to winter temperatures. Six sun-exposed mature leaves per species from different individuals were collected in the late afternoon. After dark acclimation in black plastic bags with slightly wet paper towels for 12 h, maximum quantum yield of PSII (F_v/F_m), and maximum P700 changes (P_m; indicating the amount of active PSI complex) were determined with a Dual PAM-100 (Walz, Germany). Leaf F_v/F_m was determined by illuminating the leaf with a saturating light pulse of 1000 μmol m^{-2} s^{-1} for 600 ms (Schreiber *et al*. 1994). For P_m determination, leaves were pre-illuminated with far-red light for 10 seconds; P_m was then measured with a saturation pulse. After measuring the values of F_v/F_m and P_m at room temperatures (about 10 ^oC), leaves were incubated at different temperatures in a freezer (4; 0; -2, -5,-7.5, -10,-12, -15, -17.5, -20, and -23 ^oC) for 30 min. Leaves in the field during the measurement period were exposed to temperatures as low as -5 ^oC, and were assumed to be cold acclimated. After low temperature treatments, they were taken out from the freezer, placed in zip lock clear plastic bags, and illuminated with a weak light (200 mol m^{-2} s^{-1}) for 30 minutes, simulating light condition in the morning on foggy days after night freezing temperatures. After that, the leaves were allowed to thaw and recover in the dark at room temperatures (10 ^oC) for 12 h. Then the F_v/F_m and P_m were measured with the Dual PAM-100. Relative F_v/F_m or P_m was calculated as the percentage of the control values before the low temperature treatment. The relationship between relative F_v/F_m or P_m and the treatment temperature was fitted with a sigmoid function, and the temperature at 50% loss of F_v/F_m or P_m was interpolated. The chlorophyll fluorescence

method is widely used to assess the sensitivity of leaves to low temperatures (e.g., Boorse *et al*. 1998; Sierra-Almeida & Cavieres 2010). The temperature at 50% loss of relative F_v/F_m or P_m was defined as the leaf lethal temperature (LT_{50}).

Stem hydraulic conductivity

Stem hydraulic conductivity was measured for the trees in summer (August) and winter (January), using a hydraulic conductivity measurement system (Tyree & Sperry 1989). Branches about 1.5-m-long were cut from the trees (n = 6) in the early morning, placed in black plastic bags with slightly wet paper towels, and then transported to the lab for measurements. Maximum vessel length in the studied tree species ranged from 23 to 160 cm. After arriving at the laboratory within 15 minutes after cutting the branches, stem segments about 70-cm-long were re-cut under water and attached to the hydraulic conductivity measurement system (Tyree & Sperry 1989). The downstream ends of the stems were connected to measuring pipettes and the flow rates were volumetrically monitored. Following a short equilibration period (about 15 minutes), water flow generated by a constant hydraulic head of 70 cm, was measured. Distilled/de-gassed water was used as the perfusion fluid. Hydraulic conductivity (kg m $s^{-1}MPa^{-1}$) was calculated as:

$$K_h = J_v / (\Delta P/\Delta X) \quad (4.1)$$

where J_v is the flow rate through the stem segment (kg s^{-1}; converted from ml s^{-1}) and $\Delta P/\Delta X$ is the pressure gradient across the stem segment (MPa m^{-1}). Specific hydraulic conductivity (K_s; kg m^{-1} $s^{-1}MPa^{-1}$) was obtained as the ratio of K_h and the cross-sectional

area of the active xylem. Active xylem area was distinguished from heartwood by pushing dye through the stem section.

Tree growth, canopy leaf area index, and leaf wetness

Tree radial growth at breast height of *Lithocarpus jingdongensis*, and *Lyonia ovalifolia* var. *ovalifolia* trees (n = 6) from the forest was monitored using manually constructed stainless steel dendrometer bands installed at ~1.5-m-high. Irregular sections of tree stems were avoided. Data were collected monthly from December 2008 to January 2010. Leaf wetness was monitored by a LWS leaf wetness sensor (Decagon Devices, Pullman, WA, USA) installed at 1.8-m-high at the forest edge. Leaf wetness was measured per second, and 10 minute averages were recorded by a CR3000 datalogger (Campbell Scientific Inc., Logan, UT, USA).

Ecosystem net carbon exchange

Ecosystem carbon assimilation was estimated from eddy flux data. The eddy flux system was installed above the canopy on a canopy tower, at a height of 34 m. The flux system included a CSAT3 three-dimensional sonic anemometer (Campbell Scientific Inc., Logan, UT, USA), and a Li-7500 open-path CO_2/H_2O infrared gas analyzer (Li-Cor Inc., Lincoln, NE, USA). Fluxes were measured every 0.1 s, and the data were recorded by a CR5000 datalogger (Campbell Scientific Inc., Logan, UT, USA). Air humidity and temperature (HMP45C, Vaisala, Helsinki, Finland), wind speed (A100R, Vector Instruments, Denhighshire, UK), and soil heat flux (HFP01, HukseFlux, Delft, the Netherlands) also were recorded every 30 minutes. Data processing and calculation were described by Tan

et al. (2011). The tower for eddy flux measurements was in the same forest stand where leaf and tree level measurements and were obtained.

Leaf and stem total soluble sugar concentrations

Sun-exposed leaf and stem samples (n = 6) were collected in January, March, June, and October 2010 to determine the leaf and stem total soluble sugar concentrations. Samples were collected from the field, immediately transported to the lab, and oven dried at 70 ^{o}C. Sample total soluble sugar concentrations were then measured following the ISO/Coresta method (ISO method no. 15154; Coresta Method no. 38) by an Auto Analyzer 3 (Seal Analytical Ltd., West Sussex, UK). The samples were ground and the powdered material was incubated with HCl at 90 ºC to hydrolyse sucrose and other disaccharides to reducing sugars such as glucose and fructose. Reducing sugars in the extract were then determined by reaction with p-hydroxy benzoic acid hydrazide. In an alkaline medium at 85°C, a yellow osazone was formed the absorbance of which was measured at 420 nm.

Data analysis

The differences between summer and winter K_s, leaf respiration rate, as well as the differences in average K_s, leaf respiration rate, leaf area per branch, leaf area per individual between evergreen and deciduous species were tested by Mann-Whitney U tests. The relationships between relative F_v/F_m or Pm and treatment temperature were fitted by a sigmoid function. The relationships between monthly net ecosystem carbon assimilation and environmental factors were fitted with linear or polynomial regressions (see Fig. 4.8).

Results

All of the 10 evergreen broadleaf tree species down-regulated leaf maximum carbon assimilation (A_{max}) by 13 to 53% in winter (January) compared to that in summer, depending on species (Fig. 4.2). However, all of the trees maintained high winter carbon assimilation, ranging from 5.4 to 8.8 μmol m^{-2} s^{-1} in January (Fig. 4.2). Deciduous species had higher A_{max} than evergreen species in the summer (Fig. 4.2). The leaf life span of the evergreen species ranged from 0.9 to 2.4 years. The deciduous tree species had substantially shorter leaf life spans.

The lethal temperatures (LT_{50}) of PSII (indicated by F_v/F_m) ranged from -10.0 to -15.1 ^oC, all of which were lower than the minimum air temperature of the 2009-2010 winter season (-5.7 ^oC), and the historical minimum air temperature (-9.0 ^oC; Fig. 4.3). The lethal temperature of PSI (indicated by P_m) ranged from -8.2 to -14.4 ^oC, lower than the minimum air temperature for the 2009-2010 winter season (-5.7 ^oC). The lethal temperature of PSI in *Lyonia ovalifolia* var. *lanceolata* was higher than the historical minimum air temperature (-9.0 ^oC), while PSI of other species can tolerate -9.0 ^oC. In six evergreen tree species (*S. sumuntia, S. noronhae, V. delavayi, L. hypoviridis, T. gymnanthera, L. ovalifolia* var. *ovalifolia*), PSI was more prone to freezing damage than PSII, and the LT_{50} of PSII was 1.3 to 2.4 ^oC lower than that of PSI (Fig. 4.3). The temperatures at which F_v/F_m or P_m started to decrease in the six tree species were above the minimum air temperature of the 2009-2010 winter season, and near the historical minimum recorded air temperature (Fig. 4.3), suggesting that leaves of these tree species may be damaged by freezing in very cold winters.

Stem xylem specific hydraulic conductivity (K_s) was significantly lower in winter than in summer in only three evergreen species, while the rest of the evergreen species and deciduous species did not differ in K_s between summer and winter (Fig. 4.4a). Overall, the K_s of the deciduous species in the summer were about two times higher than the evergreen species (Fig. 4.4a). The respiration rates of the evergreen species in the winter were less than half of that in the summer (Fig. 4.4b). Summer respiration rates in three deciduous species were significantly higher than for the evergreen species (Fig. 4.4b).

Annual estimated carbon assimilation per leaf area was higher in the most abundant evergreen species, *Lithocarpus jingdongensis*, than the most abundant deciduous species, *Lyonia ovalifolia* var. *ovalifolia* (109 versus 83 mol m^{-2} y^{-1}; Fig. 4.5a; 4.5b). *Lithocarpus jingdongensis* also had a longer duration of tree radial growth than *L. ovalifolia* var. *ovalifolia*. The radial growth of *Lithocarpus jingdongensis* was initiated in April while that of the *Lyonia ovalifolia* was initiated in June (Fig. 4.5c). *In situ* diurnal CO_2 assimilation was depressed at mid-day, therefore the diurnal CO_2 assimilation estimation based on PPFD and light response curves was higher than that from *in situ* gas exchange measurements for *L. jingdongensis* (Fig. 4.5d).

The cloud forest on Ailao Mountain was a carbon sink during the entire year because the net carbon gain was always positive (Fig. 4.6a). The net ecosystem carbon gain (estimated by the eddy covariance method) from June to October (part of the summer/wet season) was slightly lower than the rest of the year (Fig. 4.6a). The percent time that leaves were wet was lower from February to May compared to the rest of the year (Fig. 4.6b). The leaf and stem total soluble sugar concentrations in *L. jingdongensis* and

Manglietia insignis were highest in January, and lowest in June (Fig. 4.7c; 4.7d). The leaf and stem total soluble sugar concentrations of these two species were slightly higher in March than that in October (Fig. 4.6c; 4.6d).

Monthly net ecosystem carbon assimilation was positively correlated with sunshine duration (Fig. 4.7a), monthly PPFD (Fig. 4.7e), and negatively correlated with leaf wetness duration (Fig. 4.7b), number of foggy days per month (Fig. 4.7c), and marginally negatively correlated with monthly rainfall (Fig. 4.7f). The relationship between monthly net ecosystem carbon assimilation and monthly mean air temperature was described by a second-order polynomial equation (Fig. 4.7d).

Discussion

Our results reveal substantial winter carbon gain at leaf and ecosystem levels in a subtropical montane cloud forest at an elevation of 2460 m. This elevation is close to the upper distribution limit of evergreen broadleaf trees in subtropical zones of SW China. Our results also suggest that cloud cover constrains the leaf and ecosystem CO_2 assimilation in the summer/wet season in these subtropical forests. Higher winter CO_2 assimilation in the evergreen broadleaf species resulted in a higher annual carbon gain in the evergreen than the deciduous species, which have higher photosynthetic capacity during the summer. This helps to explain the dominance of evergreen broadleaf trees at the high elevations of subtropical forests in SW China. Carbon sequestration during the entire year also makes this subtropical forest a great carbon sink (Tan *et al*. 2011).

Low temperature effects on photosynthesis of evergreen species

Winter photosynthesis in the evergreen species was not limited by leaf water supply. Although there is a pronounced dry season according to the rainfall seasonal patterns, the trees maintained adequate water balance in the winter/dry season owing to sufficient water supply from the soil (Chapter 3). Photosynthesis during the winter also could be limited by freeze-thaw induced embolism (Taneda & Tateno 2005). Three evergreen species significantly decreased their xylem hydraulic conductivity (K_s) in winter. Despite a decrease in K_s, these tree species were similar in photosynthetic capacity (A_{max}) during the winter compared to other evergreen species, suggesting that xylem water transport efficiency is not the major constraint on carbon assimilation. Winter photosynthesis of evergreen trees may be more constrained by low temperature-induced photo-inhibition or decreased enzyme activities (Hammel 1967; Sevanto *et al*. 2006).

Leaves of all the evergreen trees were able to tolerate low temperatures in winter without unrecoverable freezing damage. The substantial freezing tolerance found in all of the evergreen tree species allows leaves to maintain active metabolism and considerably high carbon assimilation (5.4 to 8.8 μmol m^{-2} s^{-1}) in winter. Among the evergreen species, only *Lyonia ovalifolia* var. *lanceolata* would experience unrecoverable damage under historical minimum temperatures. This species is phylogenetically closely related to one of the deciduous species studied (*Lyonia ovalifolia* var. *ovalifolia*), and could be considered a leaf exchanger (all previous years leaves senesced when new leaves were expanding; Kikuzawa & Lechowicz 2011). Therefore this species does not need to protect its leaves from freezing damage because all the leaves will be exchanged.

Sensitivities of PSI and PSII to chilling (metabolic disruption by above zero low temperatures) are different for the same species (Terashima *et al*. 1994; Havaux & Davaud 1994; Huang *et al*. 2010), while the contrasting sensitivity of PSI and PSII to subzero temperatures of freezing tolerant plants has not been studied. The evergreen species studied in the present study are not chilling sensitive, and our results suggest that sensitivities of PSI and PSII to subzero temperatures are different in some species. In *L. jingdongensis, H. sinensis, I. macranthum,* and *M. insignis*, PSI and PSII performed the same at freezing temperatures, while in *S. sumuntia, S. noronhae, V. delavayi, L. hypoviridis, T. gymnanthera*, and *L. ovalifolia var. lanceolata*, the LT_{50} of PSII was 2.4 ^{o}C lower than that of PSI.

Comparative yearly carbon gain between evergreen and deciduous species

Leaf life span is negatively correlated with A_{max} per unit mass (Reich *et al*. 1991; 1992; 1997; Wright *et al*. 2004), therefore deciduous species with shorter leaf life spans generally have higher A_{max} per unit mass than evergreen species. One physiological mechanism that can explain this difference is that deciduous species allocate more N to photosynthesis than evergreen species because of less N partitioning to persistent leaves (Takashima *et al*. 2004). Deciduous species in the cloud forest assimilated more CO_2 during the summer than the evergreen species. However, because of high winter CO_2 assimilation by the evergreen species, the annual leaf level CO_2 assimilation of the deciduous species was lower than that of the evergreen species. Significantly lower respiration rates of the evergreen species in winter than in summer also helps them maintain a positive carbon balance in the winter. In addition, plants in general can lose

30% of the carbohydrates from photosynthesis in photorespiration (Monteith 1977), and the photorespiration loss of photosynthates increases as temperature increases (Long *et al*. 2006). Lower temperatures in winter result in lower photorespiration and promote winter carbon accumulation for the evergreen species.

Higher annual carbon gain of the evergreen species may partially explain the dominance of evergreen broad leaf trees in the high elevation subtropical forests in SW China (Wu 1980). Notably, the most abundant deciduous species in the cloud forest extended its leaf life span for two months of the winter season with substantial carbon assimilation, which may contribute to its success in this forest compared to other deciduous species (Chapter 5). Belowground carbon allocation may be also an important factor in explaining the relative success of these two different life history traits under a particular environment (Givnish 2002). Another factor that may influence the relative abundance of these two distinct growth forms under a particular environment is their difference in reproductive biology. Seed dispersal and seedling establishment should be studied to obtain a more comprehensive understanding of the relative dominances of evergreen and deciduous species in the subtropical forests of China.

Light rather than temperature constrains carbon assimilation

There is less cloud cover and substantially more sunshine duration in winter than in summer, and the detrimental effects of low temperature on photosynthesis appears to be compensated by relatively high levels of incoming solar radiation. Cloud cover in tropical rainforests reduces irradiance and constrains leaf CO_2 assimilation and tree growth (Graham *et al*. 2003). In addition, frequent rainfall and longtime fog persistence in the

summer wets the leaf surface, decreases CO_2 diffusion into the leaves and consequently decreases the photosynthetic carbon uptake, even under high light. Dew events depressed photosynthetic gas exchange by 77% in alpine and subalpine plants with wettable leaves (Smith & McClean 1989), and the negative effects on photosynthesis can last for 24 h after drying the leaf surface in control experiments with beans (Ishibashi & Terashima 1995; Ishibashi, Usuda & Terashima 1996). Species with unwettable leaf surfaces may not decrease in photosynthesis during natural dew events or mist spray (Smith & McClean 1989; Hanba *et al*. 2004). However, all the evergreen species studied in this research have wettable surfaces (unpublished data, YJZ). Therefore, the relative contribution of winter carbon assimilation to the whole year carbon budget may be as important as, or even more important than summer carbon gain because fog substantially decreases CO_2 uptake during the summer in subtropical forests of SW China.

Even though, at the leaf level, photosynthetic net CO_2 assimilation is lower in the winter than in the summer, at the ecosystem level, net ecosystem carbon assimilation is higher in the winter than during the summer. One possible explanation for this apparent discrepancy between results at leaf and ecosystem levels is that the leaf-level CO_2 assimilation in the summer was overestimated because the fog and rain effects on leaf surface wetness has not been taken into account. Another plausible explanation is the extremely low winter ecosystem respiration compared to that of the summer season (Tan *et al*. 2011). At the ecosystem level, the respiration rates of roots, soils, soil decomposing organisms, and tree stems also will be lower in the winter than in the summer/wet season. Lower ecosystem respiration, together with higher solar radiation, makes ecosystem net CO_2 assimilation in winter higher than that in the summer/wet season.

The positive correlation between net ecosystem carbon gain and sunshine duration, as well as the negative relationships between net ecosystem CO_2 assimilation and number of foggy days (observed days with daytime fog) and leaf wetness duration, suggest that cloud cover is a major constraint on ecosystem carbon gain. Rainfall and temperature are two major factors limiting ecosystem productivity (Lieth 1975; Law *et al*. 2002). However, strong temperature and rainfall limitations on carbon gain of this cloud forest were not detected. Ecosystem net carbon gain reached a maximum when monthly air temperature reached 11^{o}C, and increases in rainfall even had a negative effect on carbon gain (Fig 4.8f). The optimum air temperature for ecosystem net carbon gain of this subtropical cloud forest is similar to that of an alpine forest in the European Alps, and a Russian spruce forest with annual mean air temperatures around 7 ^{o}C (Niu *et al*. 2012). The seasonal dynamics in leaf and stem total soluble sugar concentrations were consistent with the ecosystem net carbon gain. The concentration of total soluble sugars indicates the balance between photosynthetic carbon gain and the carbon utilized for growth and metabolism (Sala *et al*. 2011). Higher stem and leaf total soluble sugar concentrations in January and March could be explained by lower tree growth rates than in June, but it also suggests that the carbohydrate accumulation from photosynthesis in winter was not diminished.

In conclusion, our study suggests that evergreen broadleaf trees in subtropical areas of SW China down-regulated photosynthetic rates in winter, but still maintained high CO_2 assimilation. The CO_2 assimilation of this subtropical cloud forest was constrained by incoming solar radiation in the summer, while the low temperature effects on photosynthesis were compensated by higher solar radiation, and lower ecosystem

respiration rate during the winter. The high winter carbon assimilation of evergreen broadleaf trees in this area may confer them advantages over deciduous trees and help them establish dominance. High CO_2 assimilation throughout the year also allows these forests to be large carbon sinks.

Table 4.1 Fifteen broadleaf tree species studied in Chapter 4, their species code used, family and relative dominance in the forest. Dominance data are from a forest survey by Qiu & Xie (1998), '-' indicates not found in the survey

Species	Code	Family	Dominance (%)
Evergreen			
Lithocarpus jingdongensis Y.C. Hsu & H.J. Qian	LJ	Fagaceae	17.9
Symplocos sumuntia D. Don	SS	Symplocaceae	-
Schima noronhae Reinw. ex Blume	SN	Theaceae	9.9
Vaccinium delavayi Franch	VD	Vacciniaceae	2.4
Manglietia insignis Blume	MI	Magonoliaceae	2.0
Lithocarpus hypoviridis Y.C. Hsu, B.S. Sun & H.J. Qian	LH	Fagaceae	-
Ternstroemia gymnanthera Sprague	TG	Theaceae	< 0.1
Lyonia ovalifolia Drude var. *lanceolata* Hand.-Mazz.	LOv	Ericaceae	-
Hartia sinensis Dunn	HS	Theaceae	3.1
Illicium macranthum A.C. Smith	IM	Illiciaceae	1.3
Deciduous			
Lyonia ovalifolia Drude var. *ovalifolia*	LO	Ericaceae	2.0
Betula alnoides Hamilt.	BA	Betulaceae	-
Populus yunnanensis Dode	PY	Salicaceae	-
Alnus nepalensis D. Don	AN	Betulaceae	-
Clethra brammeriana Hand.-Mazz.	CB	Clethraceae	-

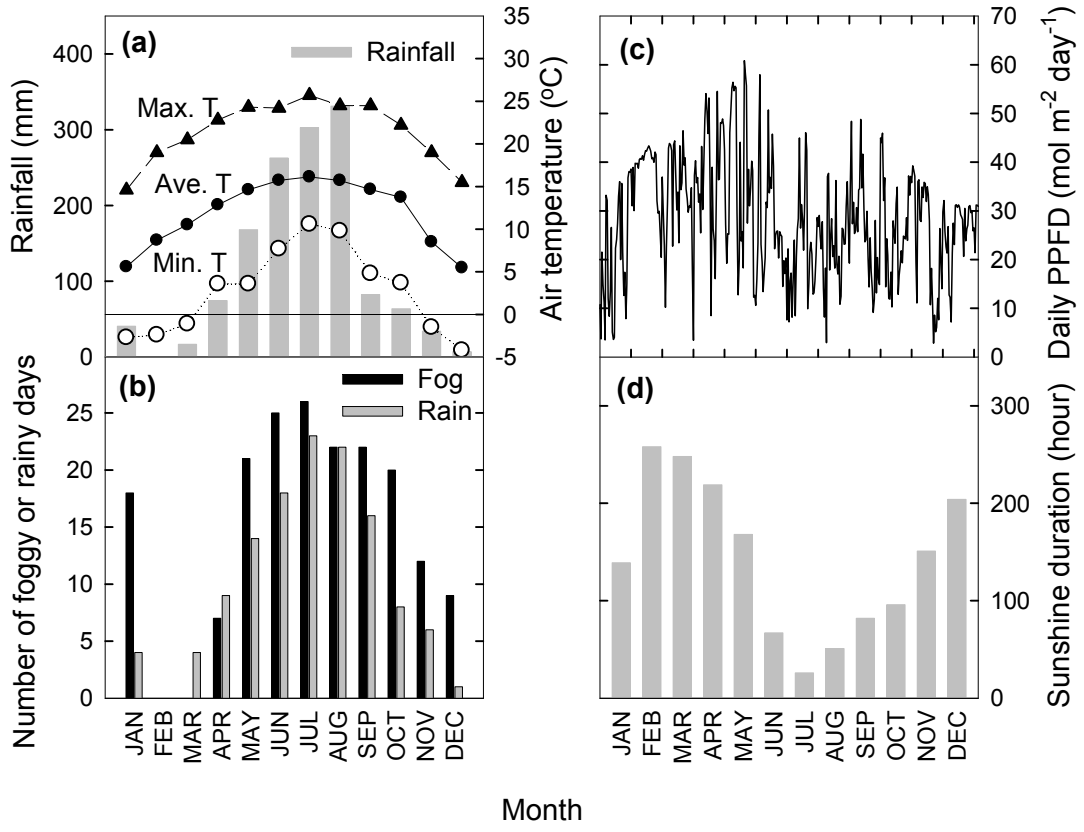

Figure 4.1 Mean monthly rainfall, maximum, minimum mean temperatures (a), and monthly number of foggy or rainy days (b), Daily PPFD (c), and sunshine duration (d) in Mount Ailao for 2009 (Data from Ailaoshan Station for Subtropical Forest Ecosystem Studies; elevation 2460 m). Foggy days are defined as days with fog observed during the day time.

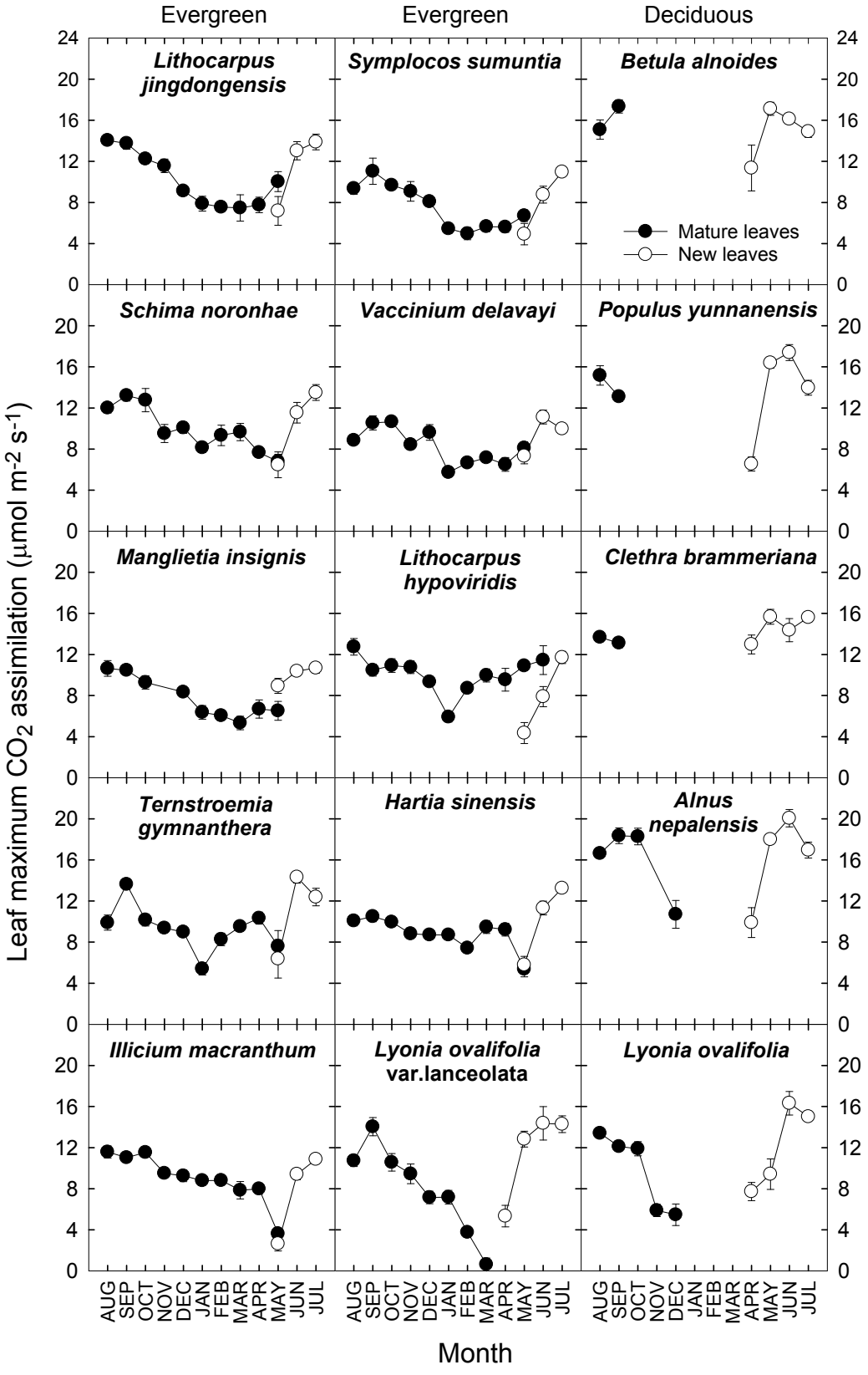
Evergreen
Evergreen
Deciduous
Lithocarpus jingdongensis
Symplocos sumuntia
Betula alnoides
Mature leaves
New leaves
Schima noronhae
Vaccinium delavayi
Populus yunnanensis
Manglietia insignis
Lithocarpus hypoviridis
Clethra brammeriana
Ternstroemia gymnanthera
Hartia sinensis
Alnus nepalensis
Illicium macranthum
Lyonia ovalifolia var.lanceolata
Lyonia ovalifolia
Leaf maximum CO2 assimilation (μmol m-2 s-1)
AUG SEP OCT NOV DEC JAN FEB MAR APR MAY JUN JUL
Month

Figure 4.2

Figure 4.2 Seasonal dynamics of leaf maximum CO_2 assimilation in 5 deciduous and 10 evergreen broadleaf tree species. Points are means ± SE. The open symbols are new expanding leaves while the closed symbols are leaves that were fully expanded mature leaves in August that started to develop around May 2008 for the evergreen trees and on April 2008 for the deciduous trees.

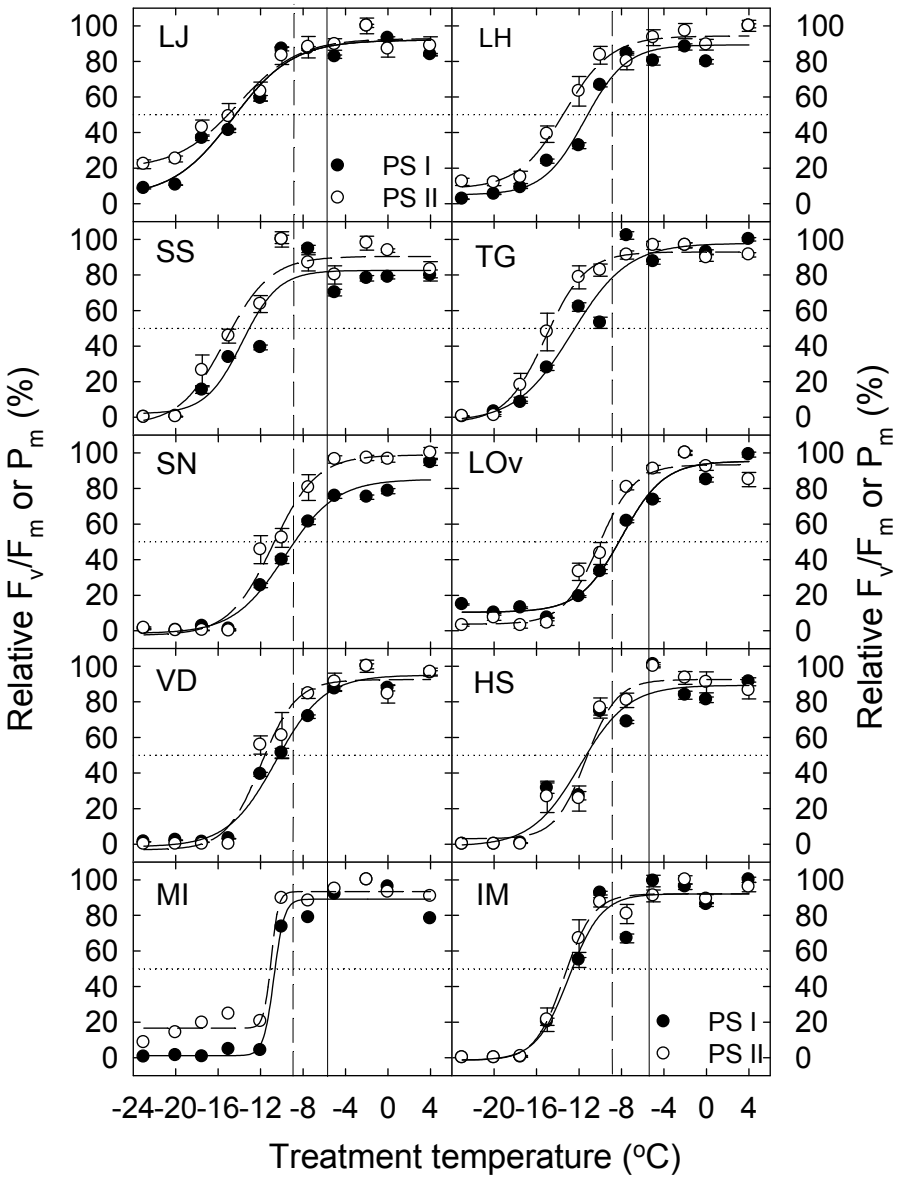

Figure 4.3 Relative F_v/F_m and P_m (percentage of control values before treatment) as a function of treatment temperature. Dotted lines indicate the lethal temperature at which 50% damage occurred (LT_{50}); vertical dashed lines indicate historical minimum air temperature; solid lines indicate minimum air temperatures in January 2010. Sigmoid functions were fitted to the data, and *P* values of all the regressions were < 0.001. Species codes are in Table 4.1.

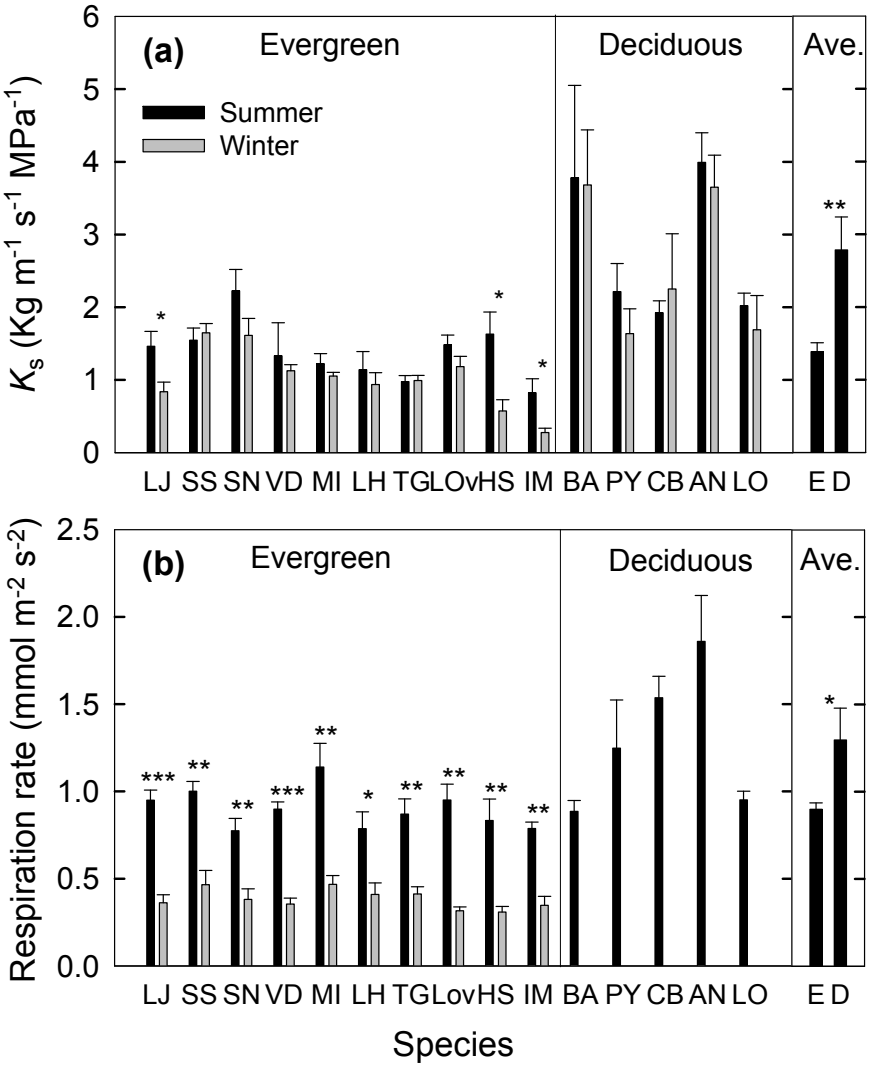

Figure 4.4 Summer and winter stem xylem hydraulic conductivity (Ks; a), and leaf respiration rate of in 5 deciduous and 10 evergreen broadleaf trees. Bars are means + SE. *, $P < 0.05$; ** $P < 0.01$, *** $P < 0.001$. E stands for evergreen, and D stands for deciduous. Species codes are in Table 4.1.

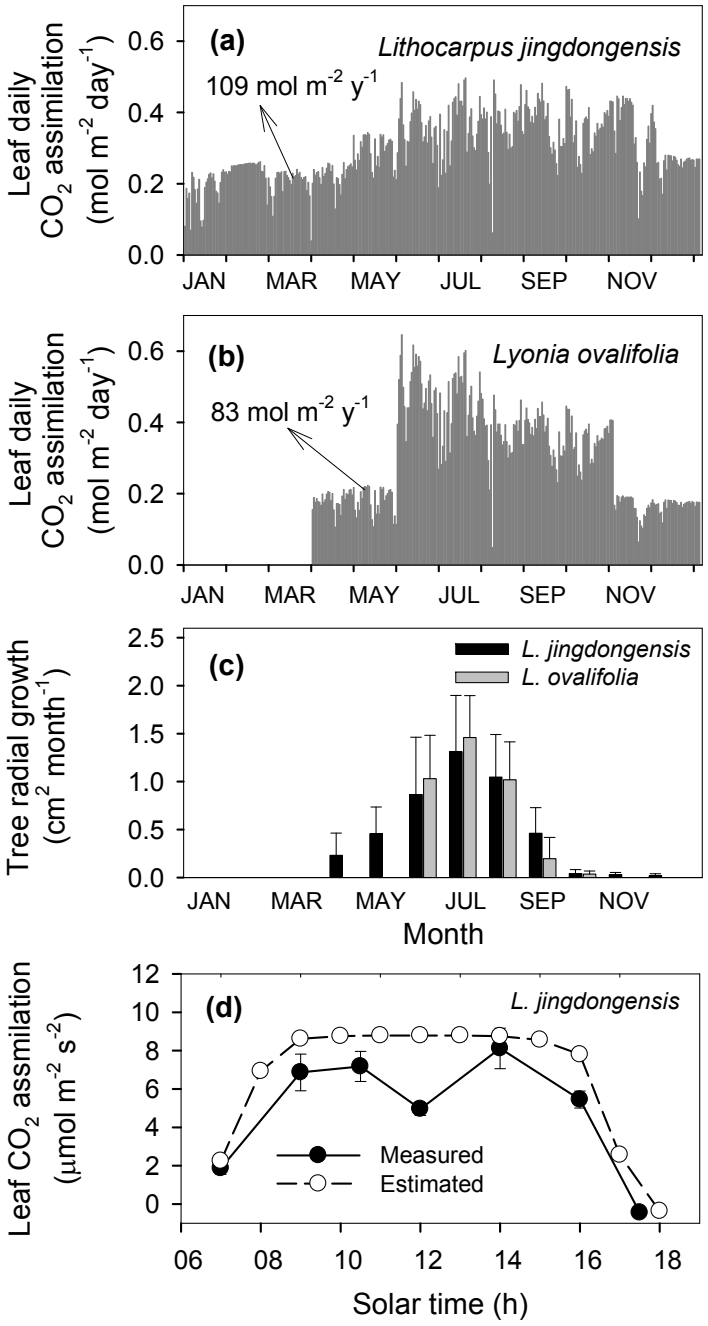

Figure 4.5 Seasonal dynamics in leaf daily CO_2 assimilation of *Lithocarpus jingdongensis* (a), and *Lyonia ovalifolia* (b), seasonal dynamics of tree radial growth of *L. jingdongensis* and *L. ovalifolia* (c), and diurnal changes in leaf CO_2 assimilation of *L. jingdongensis*. Bars in (c) are menas + SE. Open symbols in (d) are data estimated from photosynthetic response curve and PPFD data, while the closed points are directly measured CO_2 assimilation.

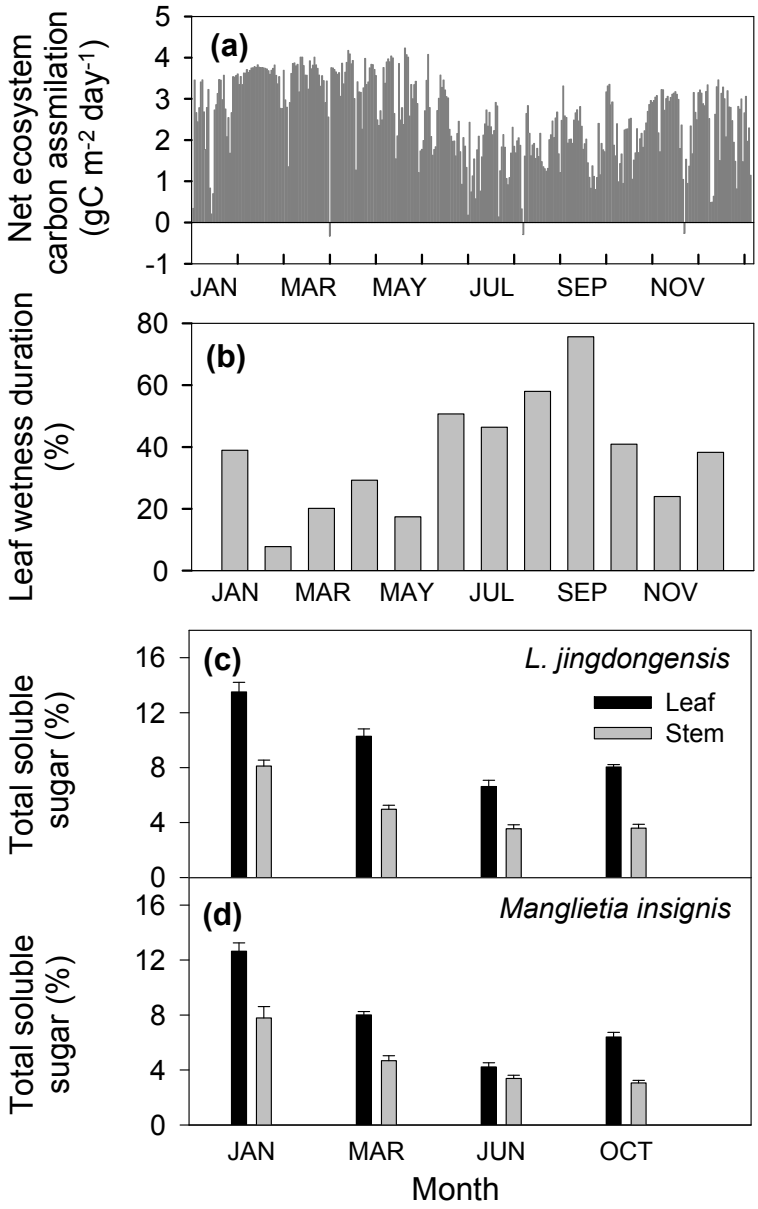

Figure 4.6 Seasonal dynamics of net ecosystem CO_2 assimilation (a), leaf wetness duration (b), and total leaf and stem soluble sugar concentration in *Lithocarpus jingdongensis* (c), and *Lyonia ovalifolia* (d). Bars in (c) and (d) are means + SE. Fig. 7a is adapted from Tan *et al*. (2011).

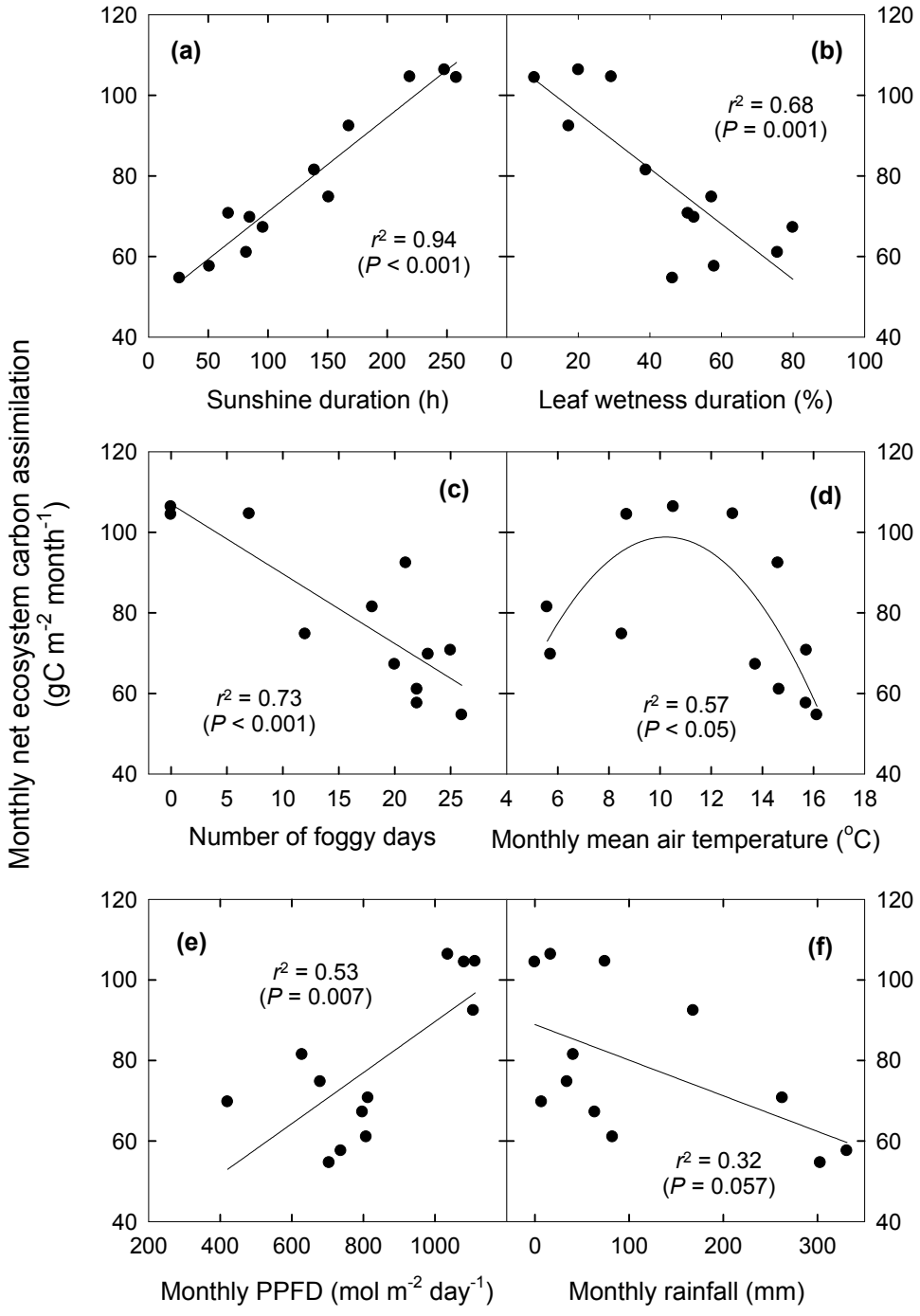

Figure 4.7 Monthly net ecosystem carbon assimilation in relation to monthly sunshine duration (a), leaf wetness duration (b), number of foggy days (c), mean air temperature (d), PPFD (e), rainfall (f). Lines are linear (a; b; c; e; f; g) or polynomial (d) regressions fitted to the data.

CHAPTER 5

Winter photosynthesis in red leaves of a subtropical deciduous species: importance of winter carbon assimilation and the role of anthocyanins

Summary

The relative advantages of being deciduous or evergreen in high elevation subtropical forests are not well understood. A deciduous species (*Lyonia ovalifolia*) from a subtropical montane cloud forest in SW China maintains red senescing leaves for a long time in the winter while he co-occurring deciduous tree species remain leafless for about 4 to 5 months. The aim of this study was to understand whether red senescing leaves of this species were able to assimilate carbon in winter, to assess the importance of maintaining positive winter carbon assimilation in this forest, and to understand the role of anthocyanins in leaf photo-protection and nutrient resorption. The red senescing leaves of *L. ovalifolia* could assimilate considerable carbon during part of the winter. Anthocyanins in senescing leaves may play a role in protecting leaves from photo-damage. *L. ovalifolia* leaves also acclimate to cold temperatures: winter red leaves had substantially higher freezing resistance than the summer, green leaves. Leaf N and P resorption efficiency of *L. ovalifolia* was higher than that of co-occurring non-anthocyaninic deciduous species, supporting the hypothesis that anthocyanin accumulation helps in nutrient resorption. Extending the carbon assimilation period into the winter months has the advantage that the incoming solar radiation is greater than during the summer. Acclimation to low freezing temperatures, efficient nutrient resorption, and additional months of carbon assimilation may explain the success of *L.*

ovalifolia versus that of the other deciduous species in the subtropical cloud forests of SW China.

Background

Deciduous trees remain completely leafless for a certain period of time during the year (for a review see: Kikuzawa & Lechowicz 2011). The habit of deciduousness originated in the Cretaceous period when angiosperms spread from low latitude to mid-latitude regions (Axelrod 1966; Wolfe 1987). Deciduousness is thought to be an adaptation to the seasonal low temperatures in the mid-latitude region of the northern hemisphere, or to the seasonal drought in some tropical or subtropical regions (Givnish 2002). Being deciduous avoids the investment in low temperature (or drought) resistance, at a cost of a relatively short period of carbon assimilation (Givnish 2002). Therefore, whether the unfavorable season allows evergreen trees to assimilate considerable carbon is an important factor in determining the relative dominance of evergreen or deciduous trees in a forest ecosystem. The influence of an unfavorable season on tree carbon assimilation has been investigated in tropical, temperate, boreal, and Mediterranean forests/shrublands (Malhi*et al*. 1999; Oliveira & Penuelas 2004; Taneda & Tateno 2005). Subtropical forests also are exposed to seasonal water deficits and low temperatures. The winter and the rainy season occur at different times of the year in the Asian subtropics. Therefore, tree photosynthesis and growth might be negatively affected by low temperatures in winter and high cloud cover (low incoming solar radiation) in summer. The relative advantages of being deciduous or evergreen in subtropical forests are poorly understood.

China harbors the largest area of subtropical broadleaf forests in the world (Wu 1980; Song *et al*. 2005). Evergreen broadleaf trees dominate the forests from 1000 to 2600 m in the subtropical area of SW China, while subtropical forests from SE China with similar elevations are dominated by deciduous trees (Wu 1980). The subtropical area in SW China has milder temperatures in winter than SE China because Tibetan Plateau prevents cold fronts from moving south in western China. If the medium and high elevation subtropical forests in SW China are dominated by evergreen broadleaf trees owing to a mild winter, it is reasonable to hypothesize that some coexisting deciduous species will extend their leaf life spans to partially utilize autumn and winter solar energy.

Many deciduous species show anthocyanin accumulation during leaf senescence (*e.g.* Matile 2000; Field *et al*. 2001; Lee *et al*. 2003). Although the role of anthocyanins in leaf functioning has recently received great attention (Gould 2004; Archetti *et al*. 2009; Hughes 2011), some key issues remain unclear. There is some evidence showing that anthocyanins in leaves can act as a light-attenuation screen (Feild *et al*. 2001; Gould *et al*. 2002; Gould 2004; Hughes *et al*. 2005) or antioxidants (Hoch *et al*. 2001; Neill *et al*. 2002; Neill & Gould 2003; Kytridis & Manetas 2006) to reduce photo-inhibition and photo-oxidation. Since the leaves will senesce anyway, anthocyanin synthesis for photo-protection would be costly and without an apparent adaptive value. One hypothesis proposed to explain the adaptive significance of anthocyanin synthesis in senescing leaves is that anthocyanins will reduce photo-damage to protect the physiological processes of nutrient resorption (Feild *et al*. 2001; Lee *et al*. 2003; Hoch *et al*. 2003). That contention mainly is based on the reasoning that free radicals induced by photo-oxidation will oxidize the products of chlorophyll degradation (Matile *et al*. 1999),

thereby interrupting the resorption process of nutrients. This hypothesis was supported by two studies. Three anthocyanic deciduous woody species recycle more N than acyanic mutants (Hoch *et al*. 2003), and leaf anthocyanin content was negatively correlated with leaf N concentration in senescent leaves of deciduous species in New England (Lee *et al*. 2003). Photo-protection by anthocyanins in senescing leaves also will allow senescing leaves to maintain some degree of carbon assimilation, at least during the early stage of leaf senescence. The carbon assimilation of senescing leaves has not been investigated, probably because the senescence process is usually short. Carbon assimilation by senescing leaves, however, could be of importance to some deciduous species showing prolonged senescence.

Lyonia ovalifolia Drude var. *ovalifolia* (Ericaceae), the most common deciduous tree species in the subtropical evergreen broadleaf forest of Ailao Mountain of SW China (Qiu & Xie 1998), maintains red leaves on trees for a long period in winter (more than two months) while other deciduous trees are leafless. The objectives of this study were (1) to assess the winter photosynthetic performance of *Lyonia ovalifolia* red leaves and the relative contribution of winter carbon assimilation to the yearly carbon balance; (2) to determine the importance of winter carbon assimilation for trees in this region, which may help to explain the dominance of evergreen broadleaf trees in subtropical montane forests of SW China; (3) to understand the role of anthocyanins in reducing photo-inhibition, in enhancing leaf freezing resistance, and in protecting the nutrient resorption process of senescing leaves.

Materials and methods

Study site

This study was performed in an evergreen broad leaf forest at the Ailaoshan Station for Subtropical Evergreen Broadleaf Forest Ecosystem Studies (24°32′N, 101°01′E, elevation 2460 m), located at Ailao Mountain, Jingdong County, Yunnan Province, SW China. The station is part of the Chinese Ecosystem Research Network (CERN), and belongs to the Chinese National Ecosystem Observation and Research Network (CEORN). Annual average temperature at the study site is 11.3^{o}C, and annual average precipitation is 1931 mm (5 year average; Qiu & Xie 1998). The climate of 2009, when we conducted the present study, is shown in Fig. 1. Sunshine duration in the summer/wet season is much lower than that in the winter season (Fig. 1). Because of abundant moisture and persistent cloud cover, this forest is known as a subtropical cloud forest. The soils of the study site are loamy yellow-brown soils. The surface soil layer (0-15 cm) contains 12.15% organic matter, 0.42% total N, and 0.16% total P (Qiu & Xie 1998). This forest is dominated by evergreen broadleaf trees, with some deciduous species occasionally scattered in the forest. Our plant material in the present study, *Lyonia ovalifolia* Drude var. *ovalifolia* (Ericaceae), is the most successful deciduous tree species in terms of relative abundance and importance values (Qiu & Xie 1998). The leaf life span can be as long as 11 months but during the last two months, before the trees are completely leafless, only a few leaves remain on the trees. The leaves of *L. ovalifolia* turn red at the end of October or the beginning of November. The red leaves are maintained on the *L. ovalifolia* trees in November and December, and a small portion of the red

leaves last on some of the trees until February, about a month before the new leaves flush in March. Nutrient resorption efficiencies of four co-occurring deciduous tree species (*Alnus nepalensis* D. Don, *Betula alnoides* Hamilt, *Populus yunnanensis* Dode, *Clethra brammeriana* Hand.-Mazz.) were also studied for comparison. These four deciduous species do not show leaf redness during senescence, and leaves drop in October or early November. Sun-exposed trees (2 to 3-m-high) on the forest edges were chosen for the physiological measurements and to minimize shading effects. We performed the physiological measurements from April 2009 to February 2010.

Gas exchange measurements

Six sun-exposed leaves from different *L. ovalifolia* individuals were chosen for gas exchange measurement. Maximum (light-saturated) photosynthetic rate (A_{max}) was measured by a LI-6400 portable photosynthetic measurement system (LI-COR, Nebraska, USA) under a saturation photosynthetic photon flux density (PPFD; 1200 μmol m^{-2} s^{-1}), ambient temperatures, and ambient CO_2 concentrations. Gas exchange measurement was repeated monthly from April to December. In January and February, gas exchange measurement was not performed because only few leaves remained on some of the trees. Gas exchange was measured at 900 to 1100 h on typical sunny days from September to December, and occasionally on cloudy days from April to August, when typical sunny days were rare.

The leaf photosynthetic light response curves were determined in August, and November, 2009. Each leaf was exposed to a gradient of PPFD ranging from 0 to 2000 μmol m^{-2} s^{-1}, generated by a LED light source (LI-COR, Nebraska, USA) attached to the

photosynthetic measurement system. When a steady state of net photosynthesis was obtained after exposing the leaf surface to a specific light intensity for about 3 to 5 minutes, the net photosynthetic rate was recorded by the LI-6400 portable photosynthetic measurement system. The relationship between A and PPFD was fitted with an exponential equation described by Bassman & Zwier (1991). Then A_{max}, dark respiration rate (R_d), apparent quantum yield (AQY), light saturation point (LST) and light compensation point (LCT) were calculated (Bassman & Zwier 1991). AQY is the light utilization efficiency by photosynthesis (Evans 1989). Leaf daily CO_2 assimilation was estimated by the light response curve and PPFD data. PPFD was measured by a Li-190SB PPFD quantum sensor (LI-COR, Nebraska, USA) every second, and one hour averages were recorded by a CR3000 datalogger (Campbell Sci., Logan, UT, USA).

Leaf mass per area and leaf pigment concentration

Six sun-exposed leaves of *Lyonia ovalifolia* from different individuals were collected in August (green leaf stage) and November (red leaf stage) to measure leaf mass per area (LMA), leaf chlorophyll *a*, chlorophyll *b*, and carotene concentrations. For LMA determinations, leaf areas were measured by a LI-3000A area meter (LI-COR, Nebraska, USA), then the leaves were oven-dried at 70 °C to constant weight, and weighed. Leaf pigment concentrations were determined using the wet chemical method (Arnon 1949). After pigment extraction using 99% ethanol, spectrophotometric determination was conducted using a UV 2501 spectrophotometer (Shimadzu, Japan).

Leaf reflectance and transmission spectrum

A USB-4000 fiber optic spectrum meter (Ocean Optics Inc., U.S.A) attached to an integrating sphere by fiber optics was used to study the leaf spectral reflectance and transmittance at wavelengths from 400 to 740 nm, setting integration time at 4 ms, and light source at 100%. Dark and reference scans were conducted before sample measurement. During measurement, dark reflectance was autocorrected for each measurement. A modified normalized difference vegetation index NDVI, which is strongly correlated with leaf chlorophyll content (Gamon *et al*. 1997; Gamon & Surfus 1999) was calculated. Leaf anthocyanin concentration was estimated by an anthocyanin reflectance index (ARI), which has been shown to be well correlated with leaf anthocyanin concentration (Gitelson *et al*. 2001). The calculations were:

$$\text{NDVI (chlorophyll)} = (R_{750}-R_{705}) / (R_{750}+R_{705}) \quad (5.1)$$

$$\text{ARI} = (R_{550})^{-1}-(R_{700})^{-1} \quad (5.2)$$

In the equations, R refers to reflectance, and the subscripts refer to a specific wavelength. Leaf light absorbance was calculated as (1 – reflectance – transmittance).

Leaf freezing resistance

Leaf freezing resistance was determined for green (August) and red (January) *L. ovalifolia* leaves using the Chlorophyll fluorescence method (Boorse *et al*. 1998). Sun-exposed leaves from different individuals (n = 6) were collected in the late afternoon, and then kept in black plastic bags with slightly moist paper towels for 12h for dark adaptation. Maximum quantum yield of PSII (F_v/F_m) of the leaves were then determined with a Dual PAM-100 (Walz, Germany). Leaf F_v/F_m was determined by illuminating the

leaf with a saturating light pulse with a photon flux density of 1000 mol m^{-2} s^{-1} for 600 ms (Schreiber *et al*., 1994). After measuring the control value of F_v/F_m (before low temperature treatment), leaves were treated with different temperatures generated by a freezer (10; 5; 2.5; 0; -2.5, -5,-7.5, -10,-12.5, -15, -17.5, -20, -22.5, and -25 ^oC) for 30 min. The temperature was monitored with copper-constantan thermocouples and a CR1000 datalogger (Campbell Sci., Logan, UT, USA) connected to a computer. After the different low temperature treatments, leaf samples were removed from the freezer, and the leaves were allowed to thaw in the dark at room temperature (15^oC) for 12h. Leaves were kept in plastic bags with wet paper tower to avoid losing water. Then the leaf F_v/F_m was re-measured with the Dual PAM -100. Relative F_v/F_m was calculated as the percentage of the control values before low temperature treatment. The relationship between relative F_v/F_m and treatment temperature was fitted with a sigmoid function, and the temperature at 50% loss of F_v/F_m was interpolated. The chlorophyll fluorescence method is widely used to assess the sensitivity of leaves to low temperatures (*e.g*. Boorse *et al*. 1998; Sierra-Almeida & Cavieres 2010), and the temperature at 50% loss of F_v/F_m was defined as the leaf lethal temperature (LT_{50}).

Leaf nutrient concentration and nutrient resorption efficiency

Sun-exposed mature leaves of *L. ovalifolia* and the four co-occurring deciduous species were collected in the field in August to determine foliar nutrient concentrations (n = 6). Leaves of the deciduous species in the cloud forest reached peak photosynthetic rates along their leaf life spans in June or July, so we collected leaves in August for nutrient concentration determination to make sure the leaves were fully mature. Leaves of *L.*

ovalifolia were also collected in September, November, and January. Recently senesced tree leaves of those species were collected at different times, depending on the species. Senesced leaves of *L. ovalifolia* were collected in January and those of other species were collected in October or early November. We collected senesced leaves when leaves dropped on windy days so that we could distinguish them among different individuals. Leaves were oven-dried at 70°C for 48 h and analyzed for total N, and P. Leaf total N concentration was determined using a Vario MAX CN auto element analyzer (Elementar Analysensysteme, Hanau, Germany). Leaf P concentration was measured using an inductively coupled plasma atomic-emission spectrometer (IRIS Advantage-ER, Thermo Jarrell Ash Corporation, MA, USA) after the samples were digested with concentrated HNO_3–$HClO_4$. Leaf N or P resorption efficiency was calculated as the percentage of total nutrient recycled after senescence by using leaf N or P concentration of mature green leaves as 100%.

Data analysis

The differences in mean A_{max}, R_d, LSP, LCP between August green leaves and November red leaves were tested by One-way ANOVA. The differences in mean Chl *a* + *b*, Chl *a*, Chl *b*, Car, Cha *a*/*b* between August green leaves and November red leaves were tested by the Mann-Whitney U test, because variances were not homogenous.

Results

The leaves of *Lyonia ovalifolia* reached the yearly highest maximum photosynthetic rate (A_{max}; 15.0 μmol CO_2 m^{-2} s^{-1}) in June, and then started to decrease (Fig. 5.2a). The A_{max} of *L. ovalifolia* leaves decreased sharply to 5.9 μmol CO_2 m^{-2} s^{-1} when the leaves turned red in November, and this A_{max} was maintained in December (Fig. 5.2a). In January and February, only few leaves remain on some of the trees. The A_{max}, R_d, AQY, LCP, and LSP of the winter red leaves (November) were significantly lower than those of the August green leaves (Fig. 5.2b; Table 5.1). Daily net CO_2 assimilation (estimated from light response curves and daily PPFD) in red leaves was lower than that of the green leaves (Fig. 5.3). However, daily net CO_2 assimilation of red leaves showed less temporal fluctuation compared to green leaves (Fig. 5.3), probably owing to fewer rainfall events and less cloud cover in winter. Estimated monthly CO_2 assimilation in red leaves was close to half of that in green leaves (Fig. 5.3).

Anthocyanin reflectance index (ARI) in *L. ovalifolia* leaves was zero in August, September, and October, while it reached a value of 0.09 in November, and tended to increase slightly in December, January, and February. The ARI of *L. ovalifolia* leaves in February was 0.11 (Fig. 5.4a). In contrast, the Chlorophyll reflectance index (NDVI) of *L. ovalifolia* leaves was around 0.46 in August, September and October, and it decreased to 0.26 in November, and maintained this value in December, January, and February (Fig. 5.4b). Relative total visible light absorptance (400-740) of *L. ovalifolia* leaves tended to decrease from August to February, but no sharp change was found when leaves turned red in November (Fig. 5.4c). The total chlorophyll concentration (Chl *a* + *b*), Chl *a* concentration, Chl *a*/*b* ratio and carotene concentration of *L. ovalifolia* red leaves

(November) were significantly lower than those of the green leaves (Table 5.2). The total chlorophyll concentration and carotene concentration of the red leaves were half of those of the green leaves. However, no significant difference was found in Chl *b* concentration between green and red leaves (Table 5.2). Red and green leaves did not differ significantly in LMA (Table 5.2).

Winter red leaves resisted freezing temperatures more than the summer leaves (Fig. 5.5). Relative PSII quantum efficiency (F_v/F_m) started to decrease at -2.5 ^oC in green leaves, while it started to decrease at -10^oC in red leaves. The decrease in relative F_v/F_m of the green leaves was very sharp, and 100% loss of relative F_v/F_m occurred at -7.5 ^oC. The decrease in relative F_v/F_m of the red leaves was relatively gradual, and 100% loss of relative F_v/F_m occurred at -22.5 ^oC. The 50% loss of relative F_v/F_m occurred at -7.5 ^oC in green leaves, and at -13.5 ^oC in red leaves (Fig. 5.5).

Leaf total N concentration of *L. ovalifolia* leaves was about 13.5 g Kg^{-1} in August and September, and it decreased to 10.3 g Kg^{-1} in November and to 7.4 g Kg^{-1} in January (Fig 5.6a). Total P concentration of *L. ovalifolia* leaves was about 0.98 g Kg^{-1} in August and September, and it decreased to 0.87 g Kg^{-1} in November and to 0.51 g Kg^{-1} in January (Fig 5.6b). Nutrient resorption efficiency of *L. ovalifolia* was higher than that of four co-ocurring deciduous tree species (Table 5.3).

Discussion

Our results reveal that a deciduous species from a subtropical evergreen forest can use red senescing leaves to assimilate substantial amounts of carbon in two months of the winter season. Senescing leaves of some deciduous tree species can be maintained on

plants for as long as three weeks, such as red-osier dogwood (Feild *et al*. 2001), while *L. ovalifolia* could maintain red leaves for more than two months. Substantial winter carbon assimilation would allow *L. ovalifolia* to reach a higher yearly carbon gain than other co-occurring deciduous tree species, which may potentially contribute to its ecological success in this subtropical cloud forest dominated by evergreen broadleaf trees. Photoprotection related to anthocyanin accumulation may help winter CO_2 assimilation. We also observed continuing nutrient resorption in *L. ovalifolia* during the red leaf stage, and a higher nutrient resorption efficiency than for co-occurring deciduous species, supporting the hypothesis that anthocyanin accumulation in senescing leaves protects the nutrient resorption process (Feild *et al*. 2001; Lee *et al*. 2003; Hoch *et al*. 2003).

Winter carbon assimilation

The photosynthetic rate of *L. ovalifolia* winter red leaves was substantially lower than that of the summer green leaves, but the red leaves still maintained high winter CO_2 assimilation in November and December. The substantial down-regulation in photosynthetic capacity is partially the result of a significant decrease in Chl *a* concentration, and a significant decrease in apparent quantum yield, compared to summer green leaves (Table 5.1; 5.2). Carbon assimilation in red leaves was facilitated by higher solar energy in winter than in the summer/wet season (Fig. 5.1b). A significantly lower leaf respiration rate in red leaves compared to the green leaves (Table 5.1) also promoted carbon assimilation during the red leaf stage. The relative contribution of red leaf carbon assimilation could be underestimated because fog and rain effects on the leaf surface have not been considered in the present study. Frequent rain events and longtime fog

persistence in the summer season will wet the leaf surface, decrease CO_2 diffusion into the leaves and consequently decrease the photosynthetic carbon exchange, even given suitable light exposure. Winter carbon assimilation could at least partially compensate for the disadvantage of being deciduous: a shortened time period for carbon assimilation (Givnish 2002).

The considerably high winter carbon assimilation of *L. ovalifolia* may provide advantages over other deciduous trees, which dropped leaves in October or early November, in terms of their yearly carbon balances. This could be one of the reasons why *L. ovalifolia* is the most successful deciduous species in this subtropical evergreen forest (Qiu & Xie 1998). Duration and capacity of winter carbon assimilation in *L. ovalifolia*, however, were lower than for co-occurring evergreen broadleaf species (Chapter 4). This could be in part the reason that the abundance of *L. ovalifolia* in this forest is lower than the dominant evergreen broadleaf trees (Qiu & Xie 1998). The elevation (2460 m) of the study site is close to the upper distribution limits of evergreen broadleaf forests in subtropical zones of SW China, and it is unclear why evergreen broadleaf trees are able to dominate at high elevations in subtropical zones of SW China with a conspicuous winter season. The importance of utilizing winter solar energy for this deciduous species provides indirect evidence for the dominance of evergreen species in this high elevation subtropical site.

Interestingly, this deciduous species has a variant, *Lyonia ovalifolia* Drude var. *lanceolata* Hand.-Mazz., which is an evergreen species in the cloud forest. Therefore, *Lyonia ovalifolia* var. *ovalifolia* could be a transition form from deciduous species to evergreen species, which was able to partially utilize the winter solar energy for carbon

assimilation. In addition, *L. ovalifolia* var. *ovalifolia* loses the life history trait of deciduousness under warmer environmental conditions. *Lyonia ovalifolia* var. *ovalifolia* seedlings also exhibited red senescing leaves, and show a leafless period at the study site. When transplanted to a warmer low elevation site, however, *L. ovalifolia* var. *ovalifolia* seedlings produced no anthocyanin and were not deciduous (unpublished data, YJZ). This suggests that the habit of deciduousness is switchable when the plants are exposed to different climate regimes. A switch from evergreen to deciduous is found in *Hevea brasiliensis*, the rubber tree, when transplanted from its native habitat (*i.e.* Brazil; typical tropical area) to the northern limits of the tropics (*i.e.* Xishuangbanna, China).

Cold resistance and photoprotection in red leaves

CO_2 assmilation in *L. ovalifolia* senescing leaves is facilitated by cold acclimation and athocyanin accumulation. Considerable cold acclimation was found in deciduous *L. ovalifolia*: winter red leaves of *L. ovalifolia* resisted freezing substantially more than summer green leaves (Fig. 5.5). Evergreen species are known to undergo structural and physiological changes to help in cold acclimation during the transition from warm to cold seasons, enhancing the resistance to subzero temperatures (for reviews see Thomashow1999; Xin & Browse 2000). Since freezing events frequently occur in this high elevation subtropical forest, development of freezing resistance in *L. ovalifolia* allowed red leaves to remain metabolically active in winter.

Anthocyanins may play a role in photoprotection in red senescing leaves of *L. ovalifolia*. Cold could induce photoinhibition and photooxidation even under normal or low light conditions because low temperatures affect light utilization more than light

absorption (Germino & Smith 1999; 2000; Long *et al*. 2000; Miyazawa *et al*. 2007). The photosynthetic capacity of *L. ovalifolia* decreased substantially after turning red, which further increased the excess of photon flux for photosynthesis. Anthocyanins strongly absorb blue-green light (Harborne 1988; Neill & Gould 1999; Smillie & Hetherington 1999; Barnes *et al*. 2000; Merzlyak & Chivkunova 2000), which would potentially reduce the photons captured by chlorophylls and carotenoids. Therefore light attenuation by anthocyanins has been supported by some studies (Smillie 1999; Feild *et al*. 2001; Gould *et al*. 2002; Gould 2004; Hughes *et al*. 2005; Hughes & Smith 2007). In addition, anthocyanins attenuate light that might over-saturate the xanthophyll cycle because xanthophyll equilibrium is sensitive to the wavelength that anthocyanins absorb (Gamon, Filella & Penuelas 1993; Gamon, Serrano & Surfus 1997). Xanthophyll cycle-dependent thermal dissipation is an important mechanism preventing photodamage (Demmig-Adams & Adams 1992). Anthocyanins also can attenuate light that photoactivates the high active chlorophyll intermediates during degradation such as red Chl catabolite (RCC), which has a peak absorbance in the wavelengths that anthocyanins absorb (Engel *et al*., 1991; Iturraspe, Engel & Gossauer, 1993; Mur *et al*., 2010).

Leaf senescence and nutrient resorption

Cold acclimation and photo-protection by anthocyanins during the autumn and winter facilitated carbon assimilation, and also promoted nutrient resorption by *L. ovalifolia*. Nutrient resorption efficiency is an important functional trait of plants, and nutrient resorption during leaf senescence is important for reproduction and leaf production during the following growing season (Aerts 1996; Killingbeck 1996; Matile *et al*. 1999;

Matile 2000; Bogard *et al*. 2011). Anthocyanin synthesis in autumn leaves was hypothesized to protect the nutrient resorption process (Field *et al*. 2001; Lee *et al*. 2003; Hoch *et al*. 2003). In the present study, leaf N and P resorption efficiency of anthocyaninic *L. ovalifolia* leaves were higher than for four co-occurring non-anthocyanic deciduous tree species. The enhanced leaf resorption efficiency in *L. ovalifolia* may result from the protection effects of anothocyanins for the nutrient resorption process, and may also be promoted by a prolonged time period of leaf senescence.

Leaf N and P concentrations decrease continuously during leaf senescence (Fig. 6), but chlorophyll concentration (indicated by NDVI) remained constant during this time period, suggesting that the nutrients recycled did not result from continuous degradation of chlorophylls. Since 90% of the nitrogen resorbed by plants during leaf senescence is from the degradation of stroma proteins and thylakoid membranes (Evans 1983), the nutrients recycled during this period were unlikely from degradation of other leaf components. Therefore, we suggest that the nutrient resorption process possibly needs a relatively long time to achieve a high efficiency, and that an extended leaf senescence duration can promote leaf nutrient recycling. Nutrient resorption by grain in winter wheat is related to the duration of leaf senescence (Bogard *et al*. 2011).

In conclusion, the deciduous species *L. ovalifolia* used red senescing leaves to assimilate considerable carbon during part of the winter season. Cold acclimation and photoprotection related to anthocyanin accumulation facilitated CO_2 assimilation during the winter. That leaf N and P concentrations during the red leaf stage were decreasing through time, as well as higher nutrient resorption efficiency in *L. ovalifolia* compared to

co-occurring non-anthocyaninic deciduous species, suggest that photoprotection by anthocyanins and/or a prolonged leaf senescence duration may facilitate nutrient resorption. Acclimation to low freezing temperatures, efficient nutrient resorption and additional months of carbon assimilation may explain the success of *L. ovalifolia* compared to other deciduous tree species in the subtropical cloud forests of SW China. To extend the carbon assimilation period to the winter months has the advantage that the incoming solar radiation is higher than during the summer. The importance of winter carbon gain to this deciduous species also provides indirect evidence for the dominance of evergreen species in this high elevation subtropical cloud forest.

Table 5.1 Maximum photosynthetic rate (A_{max}), dark respiration rate (R_d), apparent quantum yield (AQY), light compensation point (LCP), light saturation point (LSP) of green (August) and red (November) leaves. Values are means ± SE. Values followed by the same letter do not differ significantly between red and green leaves

	A_{max} μmol m^{-2} s^{-1}	R_d μmol m^{-2} s^{-1}	AQY	LCP μmol m^{-2} s^{-1}	LSP μmol m^{-2} s^{-1}
Green leaf	12.6±0.5a	0.84±0.14a	0.052±0.001a	16.1±2.6a	1011±60a
Red leaf	5.7±0.6b	0.22±0.06b	0.032±0.002b	7.1±2.1b	718±64b

Table 5.2 Leaf mass per area (LMA), total leaf chlorophyll concentration (Chl *a*+*b*), chlorophyll a concentration (Chl *a*), chlorophyll *b* concentration (Chl *b*), chlorophyll *a*/*b* ratio (Chl *a*/*b*), and carotene concentration (Car) of green (August) and red (November) leaves. Values are means ± SE. Values followed by the same letter do not differ significantly between red and green leaves

	LMA g m^{-2}	Chl *a*+*b* mg g^{-1}	Chl *a* mg g^{-1}	Chl *b* mg g^{-1}	Chl *a*/*b*	Car mg g^{-1}
Green leaf	94.6±3.9a	3.62±0.46a	2.71±0.36a	0.91±0.11a	2.96±0.17a	0.58±0.07a
Red leaf	92.9±5.1a	1.88±0.18b	0.98±0.12b	0.90±0.09a	1.10±0.11b	0.29±0.03b

Table 5.3 Leaf N and P resorption efficiency of *L. ovalifolia* and four co-occurring deciduous tree species. Values are means ± SE

Resorption	*L. ovalifolia*	*B. alnoides*	*C. brammeriana*	*P. yunnanensis*	*A. nepalensis*
N (%)	46.5 ± 6.4	28.3 ± 4.2	10.2 ± 4.6	34.7 ± 3.3	17.7 ± 2.6
P (%)	48.5 ± 7.9	25.4 ± 7.9	20.1 ± 3.0	26.6 ± 4.5	41.7 ± 7.6

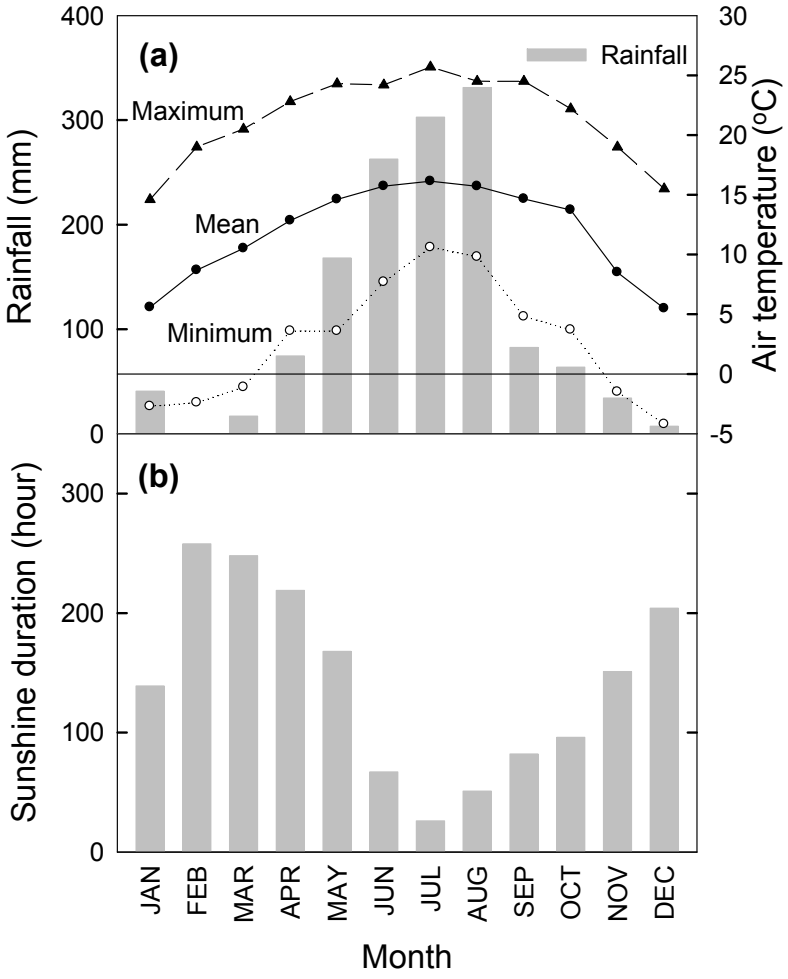

Figure 5.1 (a) Mean monthly rainfall (bars), maximum, minimum, and mean temperatures, and (b) sunshine duration in Ailao Mountain for 2009 (Data from Ailaoshan Station for Subtropical Forest Ecosystem Studies; elevation 2460 m).

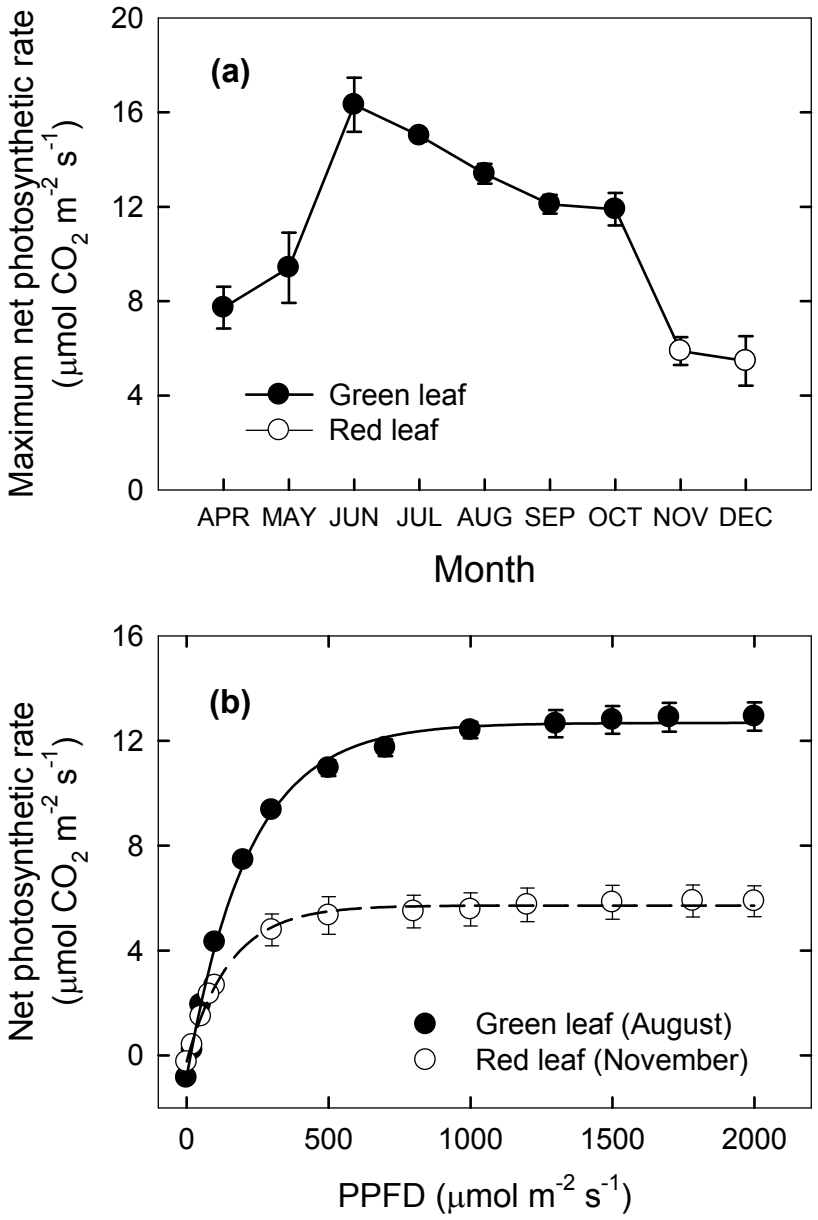

Figure 5.2 (a) Seasonal dynamic in maximum photosynthetic rates (A_{max}) of *Lyonia ovalifolia*, and (b) light response curves of *Lyonia ovalifolia* green (August) and red (November) leaves. Closed symbols represent green leaves, and open symbols represent red leaves. Data are means ± SE (n = 6).

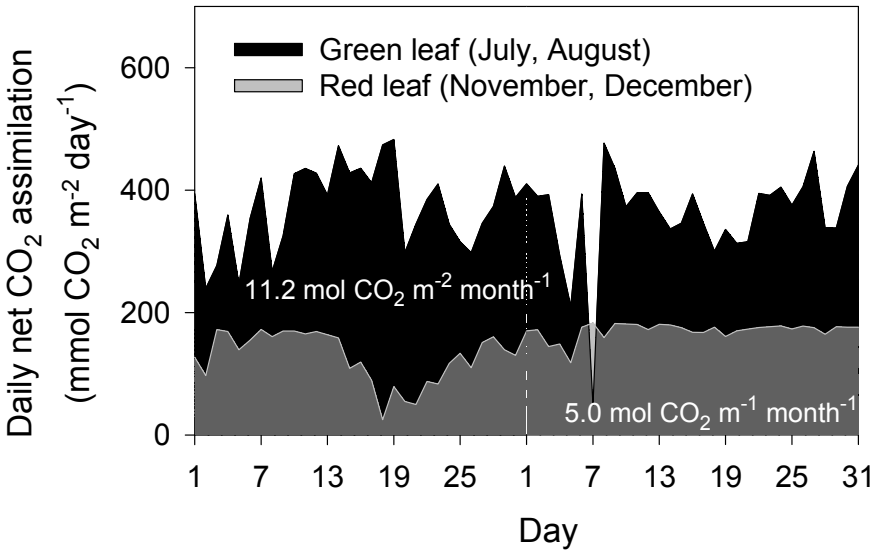

Figure 5.3 Daily net carbon assimilation of *Lyonia ovalifolia* green (July, and August) and red (November and December) leaves.

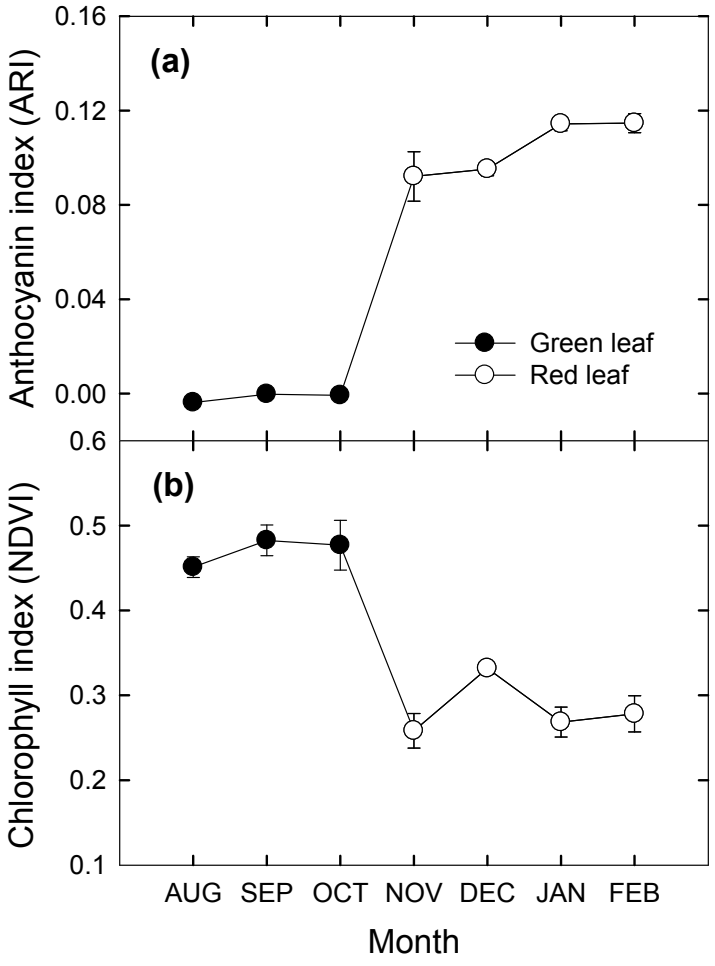

Figure 5.4 Seasonal dynamics in (a) Anthocynin reflectance index (ARI) and (b) NDVI of *Lyonia ovalifolia* leaves. Closed symbols represent green leaves, and open symbols represent red leaves. Data are means ± SE (n = 6).

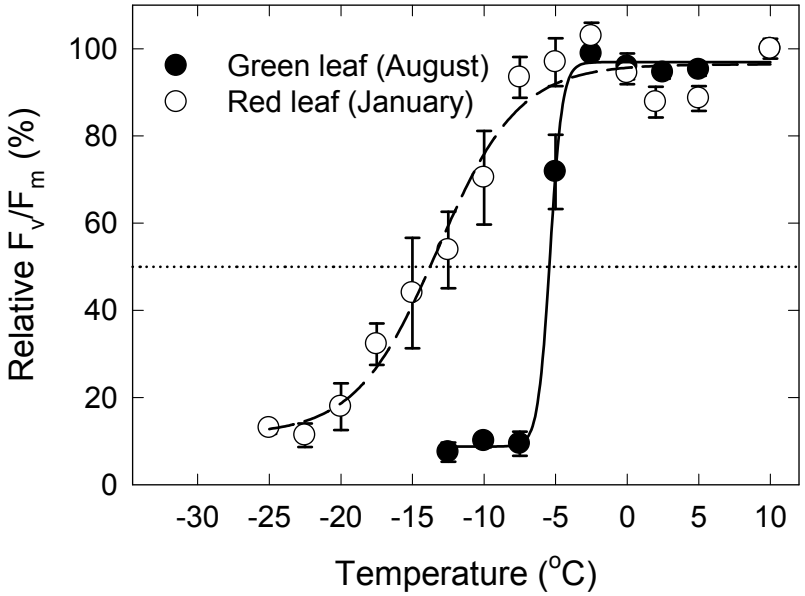

Figure 5.5 Freezing resistance of green (August), and red (January) *Lyonia ovalifolia* leaves. Closed symbols represent green leaves, and open symbols represent red leaves. Data are means ± SE (n = 6).

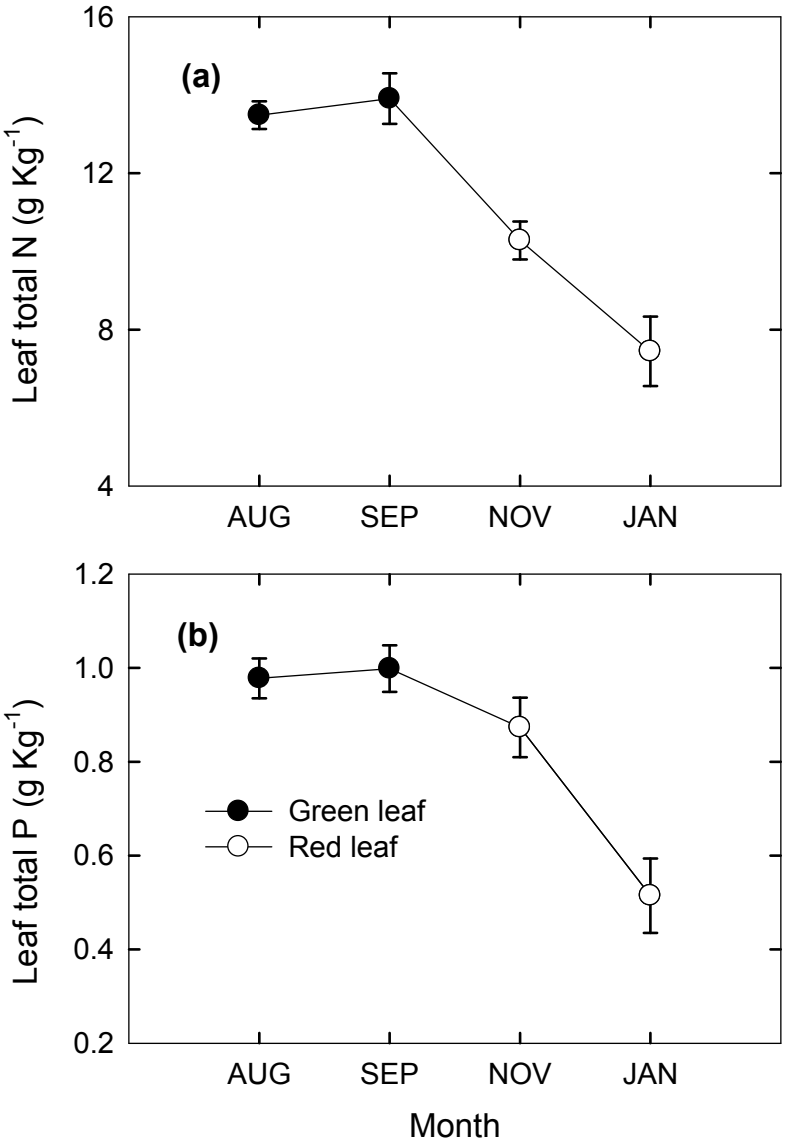

Figure 5.6 Seasonal dynamics in leaf total C, N, and P concentrations of *Lyonia ovalifolia*. Closed symbols represent green leaves, and open symbols represent red leaves. Data are means ± SE (n = 6).

CHAPTER 6

Conclusions

By comparing the water relations and carbon assimilation of deciduous and evergreen broadleaf trees, as well as assessing the environmental constraints on leaf and ecosystem level carbon assimilation in a subtropical montane cloud forest in Southwest China, this dissertation provides understanding about the tradeoffs between being deciduous and evergreen and the climatic determinants of tree water and carbon balances in subtropical cloud forest habitats. This dissertation also provides an eco-physiological and mechanistic explanation of the dominance of evergreen broadleaf trees in the montane subtropical forests in Southwest China in terms of water and carbon economy. In addition, this dissertation reveals some insights concerning the hydraulic determinants of midday stomatal conductance (g_s), the coordination between stem and leaf hydraulics, and the adaptive significance of midday depression in g_s.

Daily water and carbon balances in deciduous and evergreen trees

Deciduous species had significantly higher stem hydraulic conductivity and greater daily reliance on stem capacitance than evergreen species. Higher stem hydraulic conductivity and hydraulic capacitance allowed deciduous species to maintain higher stem water potential and g_s at midday than evergreen species. Higher midday g_s resulted in a higher daily carbon gain in deciduous species than in evergreen species during the summer. In addition, midday g_s was more associated with midday stem water status than with leaf

water status, suggesting that the functional significance of stomatal regulation in the broadleaf tree species is mainly for preventing stem xylem dysfunction.

Limited impacts of seasonal water deficits and rainfall anomalies on the subtropical cloud forests

The evergreen trees in the subtropical montane cloud forest maintained good water status and substantial carbon assimilation during the dry season and during the 2010 rainfall anomaly, suggesting that the subtropical cloud forests in this region have a high capacity to buffer the effects of regular seasonal water deficits and rainfall anomalies. The water loss of the cloud forest significantly decreased during the 2010 rainfall anomaly compared to normal dry seasons, but the impact of this rainfall anomaly on leaf area index, carbon economy, and tree growth of the forest was limited. Abundant soil water storage, water sources at depth, and lower leaf and canopy water loss rates avoided the negative effects of rainfall anomalies at plant and ecosystem levels. The considerable carbon gain by the evergreen broadleaf trees in the dry season partially explains the dominance of evergreen species in the subtropical forests of SW China, and the large carbon sink function of these subtropical forests.

The effects of cloud cover and seasonal low temperatures

All of the evergreen species studied were able to tolerate the coldest winter season in history, and were able to maintain high carbon assimilation (5.4 to 8.8 μmol m^{-2} s^{-1}) during the winter. The ecosystem CO_2 assimilation was limited by frequent cloud cover, reduced incoming solar radiation, and leaf wetness duration, but by not low temperatures during the winter. The considerable amount of winter carbon gain of evergreen trees

resulted in a higher yearly carbon assmilation than by the deciduous species, which may partially explain why the evergreen trees can establish dominance in these subtropical montane forests. Substantial carbon uptake throughout the year also allows this forest to be one of the largest carbon sinks among old-growth forests.

Winter photosynthesis in red leaves of a deciduous species

The most abundant deciduous species in the forest (*Lyonia ovalifolia* Drude var. *ovalifolia*) extended its leaf life span, and used red senescing leaves to assimilate a considerable amount of carbon during part of the winter season. Anthocyanin accumulation may play a role in protecting *L. ovalifolia* leaves from photodamage. *Lyonia ovalifolia* leaves also acclimate to cold temperatures: winter red leaves had substantially higher freezing resistance than the summer, green leaves. Extended leaf senescence duration also promoted leaf nutrient recycling in *L. ovalifolia*. Extending the carbon assimilation period into the winter months has the advantage that the incoming solar radiation is greater than during the summer. Acclimation to low freezing temperatures, efficient nutrient resorption, and additional months of carbon assimilation may explain the success of *L. ovalifolia* compared to other deciduous species. The importance of utilizing winter solar energy for this deciduous species provides indirect evidence for why evergreen species dominate the subtropical forests in SW China.

General conclusion

To sum up, seasonal water deficits and low temperatures have limited impacts on leaf and ecosystem level carbon assimilation of a subtropical cloud forest in Southwest China.

Although deciduous species had higher stem hydraulic conductivity, hydraulic capacitance, photosynthetic capacity, and daily carbon gain than evergreen species during the summer/wet season, high carbon assimilation during the winter/dry season resulted in a higher yearly carbon gain by evergreen species than the deciduous species. The constraint of cloud cover on carbon assimilation during the summer further reduces the advantage of deciduous species having higher summer photosynthetic capacities. Therefore, this dissertation provided a potential explanation for the dominance of evergreen trees in the subtropical forests of Southwest China in terms of carbon balance. The presence of cloud forests in the subtopics of China is not known or very little known to the international academic community. This dissertation puts the Chinese cloud forests on the world map and provides a mechanistic understanding of the selective pressures operating in subtropical cloud forests. The results of this dissertation also reveal the hydraulic and photosynthetic adaptations of evergreen and deciduous tree species growing in subtropical cloud forests.

REFERENCES

Aerts R. (1995) The advantages of being evergreen. *Trends of Ecology and Evolution* **10**, 402–407.

Aerts R. (1996) Nutrient resorption from senescing leaves of perennials: are there general patterns? *Journal of Ecology* **84**: 597–608.

Allen C.D. (2009) Climate-induced forest dieback: an escalating global phenomenon? *Unasylva* **231/232**, 43–49.

Allen C.D., Macalady A.K., Chenchouni H., Bachelet D., McDowell N., Vennetier M., Kitzberger T., Rigling A., Breshears D.D., Hogg E.H. (Ted), Gonzalez P., Fensham R., Zhang Z., Castro J., Demidova N., Lim J.H., Allard G., Running S.W., Semerci A. & Cobb N. (2010) A global overview of drought and heat-induced tree mortality reveals emerging climate change risks for forests. *Forest Ecology and Management* **259**, 660–684.

Archetti M., Doring T.F., Hagen S.B., Hughes N.M., Leather S.R., Lee D.W., Lev-Yadun S., Manetas Y., Ougham H.J., Schaberg P.G. & Thomas H. (2009) Adaptive explanations for autumn colours: an interdisciplinary approach. *Trends in Ecology and Evolution* **24**, 166–173.

Arnon D.I. (1949) Copper enzymes in isolated chloroplasts. Polyphenoloxidase in Beta vulgaris. *Plant physiology* **24**, 1–15.

Axelrod D.I. (1966) Origin of deciduous and evergreen habit in temperate forests. *Evolution* **20**,1–15.

Bachelet D., Neilson R.P., Lenihan J.M. & Drapek R.J. (2001) Climate change effects on vegetation distribution and carbon budget in the United States. *Ecosystems* **4**, 164–185.

Bassman J. & Zwier J.C. (1991) Gas exchange characteristics of *Populus trichocarpa*, *Populus deltoides* and a *Populus trichocarpa* x *P. deltoides* clone. *Tree Physiology* **8**, 145–149.

Begg J.E. & Turner N.C. (1970) Water potential gradients in field tobacco. *Plant Physiology* **46**, 343–346.

Bernier P.Y., Bartlett P., Black T.A., Barr A., Kljun N. & McCaughey J.H. (2006) Drought constraints on transpiration and canopy conductance in mature aspen and jack pine stands. *Agricultural and Forest Meteorology* **140**, 64–78.

Bogard M., Jourdan M., Allard V. Martre P., Perretant M.R., Ravel C., Heumez E., Orford S., Snape J., Griffiths S., Gaju O., Foulkes J. & Le Gouis J. (2011). Anthesis date mainly explained correlations between post-anthesis leaf senescence, grain yield, and grain protein concentration in a winter wheat population segregating for flowering time QTLs. *Journal of Experimental Botany* **62**, 3621–3636.

Boorse G.C., Gartman T.L., Meyer A.C., Ewers F.W. & Davis SD. (1998) Comparative methods of estimating freezing temperatures and freezing injury in leaves of chaparral shrubs. *International Journal of Plant Science* **159**, 513–521.

Breda N., Huc R., Granier A. & Dreyer E. (2006) Temperate forest trees and stands under severe drought: a review of ecophysiological responses, adaptation processes and long-term consequences. *Annals of Forest Science* **63**, 625–644.

Borchert R. (1994) Soil and stem water storage determine phenology and distribution of tropical dry forest trees. *Ecology* **75**, 1437–1449.

Brodribb T.J. & Feild T.S. (2000) Stem hydraulic supply is linked to leaf photosynthetic capacity: evidence from New Caledonian and Tasmanian rainforests. *Plant Cell and Environment* **23**, 1381–1388.

Brodribb T.J., Feild T. & Jordan G. (2007) Leaf maximum photosynthetic rate and venation are linked by hydraulics. *Plant Physiology* **144**, 1890–1898.

Brodribb T.J. & Holbrook N.M. (2003) Stomatal closure during leaf dehydration, correlation with other leaf physiological traits. *Plant Physiology* **132,** 2166–2173.

Brodribb T.J. & Holbrook N.M. (2004a) Diurnal depression of leaf hydraulic conductance in a tropical tree species. *Plant, Cell and Environment* **27**, 820–827.

Brodribb T.J. & Holbrook N.M. (2004b) Stomatal protection against hydraulic failure: a comparison of coexisting ferns and angiosperms. *New Phytologist* **162**, 663–670.

Brodribb T.J., Holbrook N.M., Edwards E.J. & Gutierrez, M.V. (2003) Relation between stomatal closure, leaf turgor and xylem vulnerability in eight tropical dry forest trees. *Plant, Cell Environment* **26**, 443–450.

Brodribb T.J., Holbrook N.M. & Gutierrez M.V. (2002) Hydraulic and photosynthetic coordination in seasonally dry tropical forest trees. *Plant, Cell and Environment* **25**, 1435–1444.

Brodribb T.J., Holbrook N.M. & Hill R.S. (2005) Seedling growth in conifers and angiosperms: impacts of contrasting xylem structure. *Australian Journal of Botany* **53**, 749–755.

Brodribb T.J. & Jordan G. J. (2008) Internal coordination between hydraulics and stomatal control in leaves. *Plant, Cell and Environment* **31**, 1557–1564.

Bucci S.J., Scholz F.G., Goldstein G., Meinzer F.C. & Sternberg L. Da S.L. (2003) Dynamic changes in hydraulic conductivity in petioles of two savanna tree species: factors and mechanisms contributing to the refilling of embolized vessels. *Plant, Cell and Environment* **26**, 1633–1645.

Bucci S.J., Scholz F.G., Goldstein G., Meinzer F.C., Hinojosa J.A., Hoffmann W.A. & Franco, A.C. (2004) Processes preventing nocturnal equilibration between leaf and soil water potential in tropical savanna woody species. *Tree Physiology* **24**, 1119–1127.

Bucci S.J., Goldstein G., Meinzer F.C., Franco A.C., Campanello P. & Scholz F.G. (2005) Mechanisms contributing to seasonal homeostasis of minimum leaf water potential and predawn disequilibrium between soil and plants in Neotropical savanna trees. *Trees* **19**, 296–304.

CERN Science Commission. (2007) *Protocols for Standard Water Environmental Observation and Measurement in Terrestrial Ecosystems*. Beijing: China Environmental Science Press.

Campanello P.I., Gatti M.G. & Goldstein G. (2008) Coordination between water-transport efficiency and photosynthetic capacity in canopy tree species at different growth irradiances. *Tree Physiology* **28**, 85–94.

Cavender-Bares J. & Holbrook N.M. (2001) Hydraulic properties and freezing-induced cavitation in sympatric evergreen and deciduous oaks with contrasting habitats. *Plant, Cell and Environment* **24**, 1243–1256.

Choat B., Ball M.C., Luly J.G. & Holtum J.A.M. (2005) Hydraulic architecture of deciduous and evergreen dry rainforest tree species from north-eastern Australia. *Trees* **19**, 305–311.

Close D.C., Beadle C.L. & Brown P.H. (2000) Cold-inducedphotoinhibition affects establishment of *Eucalyptus nitens* (Deane and Maiden) Maiden and *Eucalyptus globulus* Labill. *Trees* **15**, 32–41.

Condit R. (1998) Ecological implication of changes in drought patterns: shifts in forest composition in Panama. *Climatic Change* **39**, 413–427.

Cunningham S. (2004) Stomatal sensitivity to vapour pressure deficit of temperate and tropical evergreen rainforest trees of Australia. *Trees* **18**, 399–407.

Davis S.D., Sperry J.S. & Hacke U.G. (1999) The relationship between xylem conduit diameter caused by freeze-thaw events. *American Journal of Bot*any **86**, 1341–1355.

Dixon H.H. & Joly J. (1894) On the ascent of sap. *Annals of Botany* **8**, 468–470.

Eamus D. (1999) Ecophysiological traits of deciduous and evergreen woody species in the seasonally dry tropics. *Trends of Ecology and Evolution* **14**, 11–16.

Easterling D.R., Meehl G.A., Parmesan C., Changnon S.A., Karl T.R. & Mearns L.O. (2000) Climate extremes: observations, modeling, and impacts. *Science* **289**, 2068–2074.

Engel N., Jenny T.A., Mooser V. & Gossauer A. (1991) Chlorophyll catabolism in *Chlorella protothecoides*. Isolation and structural elucidation of a red bilin derivative. *Federation of European Biochemical Societies Letters* **293**, 131–133.

Engelbrecht B.M.J., Comita L.S., Condit R., Kursar T.A., Tyree M.T., Turner B.L. & Hubbell S.P. (2007) Drought sensitivity shapes species distribution patterns in tropical forests. *Nature* **447**, 80–82.

Evans J.R. (1989) Photosynthesis-the dependence on nitrogen partitioning. In *Causes and Consequences of Variation in Growth Rate and Productivity of Higher Plants*. Lambers H., Cambridge M.L., Konings H.& Pons T.L., Eds. SPB The Hague: Academic publishing, pp 159–174.

Feild T.S., Lee D.W. & Holbrook N.M. (2001) Why leaves turn red in autumn. The role of anthocyanins in senescing leaves of Red-Osier dogwood. *Plant Physiology* **127**, 566–574.

Fisher R.A., Williams M., Do Vale R.L., Da Costa A.L. & Meir P. (2006) Evidence from Amazonian forests is consistent with isohydric control of leaf water potential. *Plant, Cell and Environment* **29**, 151–165.

Flexas J., Gulias J., Jonasson S., Medrano H. & Mus M. (2001) Seasonal patterns and control of gas exchange in local populations of the Mediterranean evergreen shrub *Pistacia lentiscus* L. *Acta Oecologica* **22**, 33–43.

Franks P.J., Cowan I.R., Tyerman S.D., Cleary A.I., Lloyd J. & Farquhar G.D. (1995) Guard-cell pressure aperture characteristics measured with the pressure probe. *Plant Cell and Environment* **18**, 795–800.

Franks P.J. & Farquhar G.D. (1999) A relationship between humidity response, growth form and photosynthetic operating point in C_3 plants. *Plant, Cell and Environment* **22**, 1337–1349.

Gamon J.A., Filella I., & Penuelas J. (1993) The dynamic 531-nanometer Delta reflectance signal: a survey of twenty Angiosperm species. In *Photosynthetic Responses to the Environment*. Yamamoto H.Y. & Smith C.M., EDs. American Society of Plant Physiologists, pp. 172–177.

Gamon J.A., Serrano L. & Surfus J.S. (1997) The photochemical reflectance index: an optical indicator of photosynthetic radiation use efficiency across species, functional types, and nutrient levels. *Oecologia* **112**, 492–501.

Gamon J.A. & Surfus J.S. (1999) Assessing leaf content and activity with a reflectometer. *New Phytologist* **143**, 105–117.

Gartner B.L., Bullock S.H., Mooney H.A., Brown V.B. & Whitbeck, J.L. (1990) Water transport properties of vine and tree stems in a tropical deciduous forest. *American Journal of Botany* **77**, 742–74.

Germino M.J. & Smith W.K. (1999) Sky exposure, crown architecture, and low-temperature photoinhibition in conifer seedlings at alpine treeline. *Plant, Cell and Environment* **22**, 407–415.

Germino M.J. & Smith W.K. (2000) Differences in microsite, plant form, and low-temperature photosynthesis in alpine plants. *Arctic, Antarctic, and Alpine Research* **32**, 388–396.

Geroy I.J., Gribb M.M., Marshall H.P., Chandler D.G., Benner S.G. & McNamara J.P. (2011) Aspect influences on soil water retention and storage. *Hydrological Process* **25**, 3836–3842.

Gitelson A.A., Merzlyak M.N. & Chivkunova O.B. (2001) Optical properties and nondestructive estimation of anthocyanin contentin plant leaves. *Photochemstiry Photobiol*ogy **74**:38–45.

Givnish T.J. (2002) Adaptive significance of evergreen vs. deciduous leaves: solving the triple paradox. *Silva Fennica* **36**, 703–743.

Goldstein G., Andrade J.L., Meinzer F.C., Holbrook N.M., Cavelier J., Jackson P. & Celis A. (1998) Stemwater storage and diurnal patterns ofwater use in tropical forest canopy trees. *Plant, Cell and Environment* **21**, 397–406.

Goldstein G., Rada F. & Catalan A. (1987) Water transport efficiency in stems of evergreen and deciduous savanna trees. *Proceedings of the international conference on measurement of soil and plant water status.* Utah: Utah State University.

Goldstein G., Rada F., Rundel P., Azocar A. & Orozco A. (1990) Gas exchange and water relations of evergreen and deciduous tropical savanna trees. *Annals of Forest Science* **46**, S448–S453.

Gould K.S. (2004) Nature's swiss army knife: the diverse protective roles of anthocyanins in leaves. *Journal of Biomedicine and Biotechnology* **5**, 314–320.

Gould K.S., Vogelmann T.C., Han T. & Clearwater M.J. (2002) Profiles of photosynthesis within red and green leaves of *Quintinia serrata*. *Physiologia Plantarum* **116**, 127–133.

Graham E.A., Mulkey S.S., Kitajima K., Philips N.G. & Wright J. (2003) Cloud cover limits net CO2 uptake and growth of a rainforest tree during tropical rainy seasons. *Proceedings of the National Academy of Sciences, USA* **100**, 572–576.

Granier A. (1985) Une nouvelle méthode pour la mesure du flux de sève brute dans le tronic des arbres. *Annals of Forest Science* **42**, 193–200.

Granier A. (1987) Evaluation of transpiration in a Douglas-fir stand by means of sap flow measurements. *Tree Physiology* **3**, 309–320.

Granier A., Reichstein M., Bréda N., Janssens I.A., Falge E., Ciais P., Grünwald T., Aubinet M., Berbigier P., Bernhofer C., Buchmann N., Facini O., Grassi G., Heinesch B., Ilvesniemi H., Keronen P., Knohl A., Köstner O.B., Lagergren F., Lindroth A., Longdoz B., Loustau D., Mateus J., Montagnani L., Nys C., Moors E., Papale D., Peiffer M., Pilegaard K., Pita G., Pumpanen J., Rambal S., Rebmann C., Rodrigues A., Seufert G., Tenhunen J., Vesala T. & Wang Q. (2007) Evidence for soil water control on carbon and water dynamics in European forests during the extremely dry year: 2003. *Agricultural and Forest Meteorology* **143**, 123–145.

Grassi G., Ripullone F., Borghetti M., Raddi S. & Magnani F. (2009) Contribution of diffusional and non-diffusional limitations to midday depression of photosynthesis in Arbutus unedo L. *Trees* **23**, 1149–1161.

Hacke U.G. & Sperry J.S. (2003) Limits to xylem refilling under negative pressure in *Laurus nobilis* and *Acer negundo*. *Plant, Cell and Environment* **26**, 303–311.

Hao G.-Y., Hoffmann W.A., Scholz F. G., Bucci S. J., Meinzer F. C., Franco A. C., Cao, K.-F. & Goldstein G. (2008) Stem and leaf hydraulics of congeneric tree species from adjacent tropical savanna and forest ecosystems. *Oecologia* **155**, 405–415.

Hammel H.T. (1967) Freezing of xylem sap without cavitation. *Plant Physiology* **42**, 55–66.

Hanba Y.T., Moriya A. & Kimura K. (2004) Effect of leaf surface wetness and wettability on photosynthesis in bean and pea. *Plant, Cell and Environment* **27**, 413–421.

Hanninen H. & Hari P. (2002) Recovery of photosynthesis of boreal conifers during spring: a comparison of two models. *Forest Ecology and Management* **169**, 53–64.

Happer J.L. (1977) *Population biology of plants*. London: Academic Press.

Hari P. & Makela A. (2003) Annual pattern of photosynthesis in Scots pine in the boreal zone. *Tree physiology* **23**, 145–155.

Havaux M. & Davaud A. (1994) Photoinhibition of photosynthesis in chilled potato leaves is not correlated with a loss of photosystem II activity—preferential inactivation of photosystem I. *Photosynthesis Research* **40**, 75–92.

Huang W., Zhang S.-B. & Cao K.-F. (2010) The different effects of chilling stress under moderate light intensity on photosystem II compared with photosystem I and subsequent recovery in tropical tree species I and subsequent recovery in tropical tree species. *Photosynthesis Research* **103**, 175–182.

Hoch W.A., Zeldin E.L. & Mcgown B.H. (2001) Physiological significance of anthocyanins during autumnal leaf senescence. *Tree Physiology* **21**, 1–8.

Hoch W.A., Singsaas E.L. & McCown B.H. (2003) Resorption protection. Anthocyanins facilitate nutrient recovery in autumn by shielding leaves from potentially damaging light levels. *Plant Physiology* **133**, 1296–1305.

Hollinger D.Y., Kelliher F.M., Byers J.N., Hunt J.E., McSeveny T.M. & Weir P.L. (1994) Carbon dioxide exchange between an undisturbed old-growth temperate forest and the atmosphere. *Ecology* **75**, 134–50.

Hughes N.M. (2011) Winter leaf reddening in 'evergreen' species. *New Phytologist* **190**, 573–581.

Hughes N.M., Burkey K.O. & Neufeld H.S. (2005) Functional role of anthocyanins in high-light winter leaves of the evergreen herb, *Galax urceolata*. *New Phytologist* **168**, 575–587.

Hughes N.M. & Smith W.K. (2007) Attenuation of incident light in *Galax urceolata* (Diapensiaceae): concerted influence of adaxial and abaxial anthocyanic layers on photoprotection. *American Journal of Botany* **94**, 784–790.

Hursh CR. (1943) Water storage limitations in forest soil profiles. *Soil science society proceedings* **8**, 412–414.

Iio A., Fukasawa H., Nose Y. & Kakubari Y. (2004) Stomatal closure induced by high vapor pressure deficit limited midday photosynthesis at the canopy top of *Fagus crenata* Blume on Naeba mountain in Japan. *Trees* **18**, 510–517.

Ishibashi M. & Terashima I. (1995) Effects of continuous leaf wetness on photosynthesis: adverse aspects of rainfall. *Plant, Cell and Environment* **18**, 431–438.

Ishibashi M., Usuda H. & Terashima I. (1996) The loss of ribulose-1,5-bisphosphate carboxylase/oxygenase caused by 24-hour rain treatment fully explains the decrease in the photosynthetic rate in bean leaves. *Plant Physiology* **111**, 635–640.

Iturraspe J., Engel N. & Gossauer A. (1994) Chlorophyll catabolism. Isolation and structure elucidation of chlorophyll b catabolites in *Chlorella protothecoides*. *Phytochemistry* **35**, 1387–1390.

James S.A., Clearwater M.J., Meinzer F.C. & Goldstein. G. (2002) Heat dissipation sensors of variable length for the measurement of sap flow in trees with deep sapwood. *Tree Physiology* **22**, 277–283.

Jentsch A., Kreyling J. & Beierkuhnlein C. (2007) A new generation of climate-change experiments: events, not trends. *Frontiers in Ecology and the Environment* **5**, 365–374.

Johnson D.M., McCulloh K.A., Woodruff D.R. & Meinzer F.C. (2011a) Evidence for xylem embolism as a primary factor in dehydration-induced decline in leaf hydraulic conductance. *Plant cell and Environment* **35**, 760–769

Johnson D.M., McCulloh K.A., Meinzer F.C., Woodruff D.R. & Eissenstant D.M. (2011b) Hydraulic patterns and safety margins, from stem to stomata, in three eastern US tree species. *Tree Physiology* **31**, 659–668.

Johnson D.M. & Smith W.K. (2006) Low clouds and cloud immersion enhance photosynthesis in understory species of a southern Appalachian spruce-fir forest (USA).*American Journal of Botany* **93**, 1625–1632.

Ke G., & Weger M.J.A. (1999) Different responses to shade of evergreen and deciduous oak seedlings and the effect of acorn size. *Acta Oecologia* **20**: 579–586.

Kellomäki S. & Wang K.-Y. (2000) Short-term environmental controls on carbon fluxes above a boreal coniferous forest: model computation compared with measurements by eddy correlation. *Ecological Modeling* **128**, 63–88.

Kikuzawa K. (1991) A cost-benefit analysis of leaf habit and leaf longevity of trees and their geographical pattern. *American Naturalist* **138**, 1250–1263.

Kikuzawa K. & Lechowicz M.J. (2011) *Ecology of leaf longevity*. Berlin Heidelberg New York, Springer.

Killingbeck K.T. (1996) Nutrients in senesced leaves: keys to the search for potential resorption and resorption proficiency. *Ecology* **77**, 1716–1727

Koch G.W., Amthor J.S. & Goulden M.L. (1994) Diurnal patterns of leaf photosynthesis, conductance and water potential at the top of a lowland rainforest in Cameroon: measurements from the Radeu de Cimes. *Tree Physiology* **14**, 347–360.

Kosugi Y. & Matsuo N. (2006) Seasonal fluctuations and temperature dependence of leaf gas exchange parameters of co-occurring evergreen and deciduous trees in a temperate broad-leaved forest. *Tree Physiology* **26**, 1173–1184.

Krishnan P., Black T.A., Grant N.J., Barr A.G., Hogg E.T.H., Jassal R.S. & Morgenstern K. (2006) Impact of changing soil moisture distribution on net ecosystem productivity of a boreal aspen forest during and following drought. *Agricultural and Forest Meteorology* **139**, 208–223.

Kyparissis A., Grammatikopoulos G. & Manetas Y. (2007) Leaf morphological and physiological adjustments to the spectrally selective shade imposed by anthocyanins in *Prunus cerasifera*. *Tree Physiology* **27**, 849–857.

Lacambra J.L.C., Blanco Andray A. & Santos France´s F. (2010) Influence of the soil water holding capacity on the potential distribution of forest species. A case study: the potential distribution of cork oak (Quercus suber L.) in central-western Spain. *European Journal of Forest Research* **129**, 111–117.

Law B., Falge E., Gu L., Baldocchi D.D., Bakwin P., Berbigier P., Davis K.J., Dolman A.J., Falk M., Fuentes J.D., Goldstein A.H., Granier A., Grelle A., Hollinger D., Janssens I.A., Jarvis P.G., Jensen N.O., Katul G., Mahli Y., Matteucci G., Meyers T., Monson R.K., Munger J.W., Oechel W., Olson R., Pilegaard K., Paw U.K.T., Thorgeirsson H., Valentini R., Verma S., Vesala T., Wilson K. & Wofsy S. (2002) Environmental controls over carbon dioxide and water vapor exchange of terrestrial vegetation. *Agricultural and Forest Meteorology* **113**, 97–120.

Lee D.W., O'Keefe J., Holbrook N.M. & Feild T.S. (2003) Pigment dynamics and autumn leaf senescence in a New England deciduous forest, eastern USA. *Ecological Research* **18**, 677–694.

Lewis S.L., Brando P.M., Phillips O.L., van der Heijden G.M.F. & Nepstad D. (2011) The 2010 Amazon drought, *Science* **331**, 554.

Li S. G., Eugster W., Asanuma J., Kotani A., Davaa G., Oyunbaatar D. & Sugita M. (2006), Energy partitioning and its biophysical controls above a grazing steppe in central Mongolia, *Agricultural and Forest. Meteorology* **137**, 89–835.

Lieth H. (1975) Modeling the primary productivity of the world. In: *Primary productivity of the world.* Leith H. & Whittaker R.H., EDs. Heidelberg: Springer-Verlad, pp. 237–283.

Long S.P., Humpheries S. & Falkowski P.G. (1994) Photoinhibition of photosynthesis in nature. *Annual Review of Plant Physiology and Plant Molecular Biology* **45**, 633–662.

Madsen M.D., Chandler D.G. & Belnap J. (2008) Spatial gradients in ecohydrologic properties within a Pinyon-Juniper ecosystem. *Ecohydrology* **1**: 349–360.

Malhi Y., Baldocchi D.D. & Jarvis P.G. (1999) The carbon balance of tropical temperate and boreal forests. *Plant, Cell and Environment* **22**, 715–740.

Marengo J.A., Nobre C.A., Tomasella J., Oyama M.D., Oliveira G.S., de Oliveira R., Camargo H., Alves L.M. & Brown I.F. (2008) The drought of Amazonia in 2005. *Journal of. Climate* **21**, 495–516.

Matile R., Hörtensteiner S. & Thomas H. (1999) Chlorophyll degradation. *Annual Review of Plant Physiology and Plant Molecular Biology* **50**, 67–95.

Matile P. (2000) Biochemistry of Indian summer: physiology of autumn leaf coloration. *Experimental Gerontology* **35**, 145–158

Meinzer F.C., James S.A., Goldstein G. & Woodruff, D.R. (2003) Whole-tree water transport scales with sapwood capacitance in tropical forest canopy trees. *Plant, Cell and Environment* **26**, 1147–1155.

Meinzer F.C., Woodruff D.R., Domec J.-C., Goldstein G., Campanello P.I., Gatti M.G. & R. Villalobos-Vega. (2008) Coordination of leaf and stem water transport properties in tropical forest trees. *Oecologia* **156**, 31–41.

Meinzer F.C., Johnson D.M., Lachenbruch B., McCulloh K.A. & Woodruff D.R. (2009) Xylem hydraulic safety margins in woody plants: coordination of stomatal control of xylem tension with hydraulic capacitance. *Functional Ecology* **23**, 922–930.

Miyazawa Y. & Kikuzawa K. (2005) Winter photosynthesis by saplings of evergreen broad-leaved trees in a deciduous temperate forest. *New Phytologist* **165**, 857–866.

Miyazawa Y., Kikuzawa K. & Otsuki K. (2007) Decrease in the capacity for RuBP carboxylation and regeneration with the progression of cold-induced photoinhibition during winter in evergreen broadleaf tree species in a temperate forest. *Functional Plant Biology* **34**, 393–401.

Monteith J.L. (1977) Climate and the efficiency of crop production in Britain. *Philosophical Transactions of the Royal Society of London* **281**, 277–294.

Mueller R.C., Scudder C.M., Porter M.E., Trotter R.T., Gehring C.A., & Whitham T.G. (2005) Differential tree mortality in response to severe drought: evidence for long term vegetation shifts. *Journal of Ecology* **93**, 1085–1093.

Mulkey S.S., Kitajima K. & Wright S.J. (1996) Plant physiological ecology of tropical forest canopies. *Trends in Ecology and Evolution* **11**, 408–412.

Mur L.A.J., Aubry S., Mondhe M., Kingston-Smith A., Gallagher J., Timms-Taravella E., James C., Papp I., Hortensteiner S., Thomas H. & Ougham H. (2010) Accumulation of chlorophyll catabolites photosensitizes the hypersensitive response elicited by Pseudomonas syringae in Arabidopsis. *New Phytologist* **188**, 161–174.

Nagel J. F. (1956) Fog precipitation on Table Mountain. *Quarterly Journal of the Royal .Meteorological Society* **82**, 452–460.

Nardini A. & Salleo S. (2000) Limitation of stomatal conductance by hydraulic traits: sensing or preventing xylem cavitation? *Trees* **15**, 14–24.

Nardini A., Tyree M.T. & Salleo S. (2001) Xylem cavitation in the leaf of *Prunus laurocerasus* and its impact on leaf hydraulics. *Plant Physiology* **125**, 1700–1709.

Nardini A., Lo Gullo M.A. & Salleo S. (2011) Refilling embolized xylem conduits: is it a matter of phloem unloading? *Plant Science* **180**, 604–611.

Niu S., Luo Y., Fei S., Yuan W., Schimel D., Law B. E., Ammann C., Altaf Arain M., Arneth A., Aubinet M., Barr A., Beringer J., Bernhofer C., Andrew Black T., Buchmann N., Cescatti A., Chen J., Davis K. J., Dellwik E., Desai A. R., Etzold S., Francois L., Gianelle D., Gielen B., Goldstein A., Groenendijk M., Gu L., Hanan N., Helfter C., Hirano T., Hollinger D. Y., Jones M. B., Kiely G., Kolb T. E., Kutsch W. L., Lafleur P., Lawrence D. M., Li, L., Lindroth A., Litvak M., Loustau, D., Lund M., Marek M., Martin T. A., Matteucci G., Migliavacca M., Montagnani L., Moors E., William Munger J., Noormets A., Oechel W., Olejnik J., U, K. T. P., Pilegaard K., Rambal S., Raschi A., Scott R. L., Seufert G., Spano D., Stoy P., Sutton M. A., Varlagin A., Vesala T., Weng E., Wohlfahrt G., Yang B., Zhang Z.& Zhou X. (2012) Thermal optimality of net ecosystem exchange of carbon dioxide and underlying mechanisms. *New Phytologist*, doi: 10.1111/j.1469-8137.2012.04095.x.

Oliveira G. & Penuelas J. (2004) Effects of winter cold stress on photosynthesis and photochemical efficiency of PSII of the Mediterranean *Cistus albidus* L. and *Quercus ilex* L. *Plant Ecology* **175**, 179–191.

Osmond C.B. (1994) What is photoinhibition? Some results from comparisons of shade and sun plants. In: *Photoinhibition and photosynthesis: from molecular mechanisms to the field*. Baker N.R. & Bowyer J.R., EDs. Oxford: BIOS Scientific Publishers, pp. 1–24.

Pearcy R.W. (1987) Photosynthetic gas exchange responses of Australian tropical forest trees in canopy, gap, and understory micro-environments. *Functional Ecology* **1**, 169–178.

Peng M.J., Lang N.J., Wen S.L., Guo Y.Q., Jiang Q. C., Yang X., Zheng K., Guo Y.H. & Zhang L.X. (2005) Soil properties and water conservation function of different forest types in Jinshajiang River watershed. *Journal of Soil and Water Conservation* **19**, 106–109.

Piedallu C., Gégou t J.C., Bruand A. & Seynave I. (2011) Mapping soil water holding capacity over large areas to predict potential production of forest stands. *Geoderma* **160**, 355–366.

Pittermann J. & Sperry J.S. (2006) Analysis of freeze-thaw embolism in conifers: the interaction between cavitation pressure and tracheid size. *Plant Physiology* **140**, 374–382.

Pockman W.T., Sperry J.S. & O'leary J.W. (1995) Sustained and significant negative water pressure in xylem. *Nature* **378**, 715–716.

Qiu J. (2009) Where the rubber meets the garden. *Nature* **457**, 246–247.

Qiu J. (2010) China drought highlights future climate threats. *Nature* **465**, 142–143.

Qiu X.-Z. & Xie S.-C. (1998) *Studies on the forest ecosystem in Ailao Mountains Yunnan, China*. Kunming: Yunnan Science and Technology Press.

Rammig A., Jupp T., Thonicke K., Tietjen B., Heinke J., Ostberg S., Lucht W., Cramer W., Cox P. (2010) Estimating the risk of Amazonian forest dieback. *New Phytologist* **187**, 694–706.

Raschke K. & Resemann A. (1986) The midday depression of CO_2 assimilation in leaves of *Arbutus unedo* L.: diurnal changes in photosynthetic capacity related to changes in temperature and humidity. *Planta* **168**, 546–558.

Reich P.B., Uhl C., Walters M.B. & Ellsworth D.S. (1991) Leaf lifespan as a determinant of leaf structure and function among 23 Amazonian tree species. *Oecologia* **86**, 16–24.

Reich P.B., Walters M.B. & Ellsworth D.S. (1992) Leaf lifespan in relation to leaf, plant, and stand characteristics among diverse ecosystems. *Ecological Monographs* **62**, 365–392.

Reich P.B., Walters M.B. & Ellsworth D.S. (1997) From tropics to tundra: global convergence in plant functioning. *Proceedings of the National Academy of Sciences, USA* **94**, 13730–13734.

Ritchie G.A. & Hinckley T.M. (1975) The pressure chamber as an instrument for ecological research. *Advances in Ecological Research* **9**,165–254.

Sack L., Cowan P.D., Jaikumar N. & Holbrook N.M. (2003) The 'hydrology' of leaves: coordination of structure and function in temperate woody species. *Plant Cell Environment* **26**, 1343–1356.

Sala A., Fouts W. & Hoch G. (2011) Carbon storage in trees: does relative carbon supply decrease with tree size? In: Meinzer F.C., Lachenbruch B., Dawson T.E., EDs. *Size- and age-related changes in tree structure and function*. Dordrecht: Springer.

Santiago L.S., Goldstein G., Meinzer F.C., Fisher J.B., Machado K., Woodruff D. & Jones T. (2004) Leaf photosynthetic traits scale with hydraulic conductivity and wood density in Panamanian forest canopy trees. *Oecologia* **140**, 543–550.

Schreiber U., Bilger W. & Neubauer C. (1994) Chlorophyll fluorescence as a nonintrusive indicator for rapid assessment of in vivo photosynthesis. In *Ecophysiology of photosynthesis*. Schulze E.D. & Caldwell M.M., EDs. Berlin Heidelberg New York: Springer, pp 49–70.

Schulze E.-D., Lange O.L., Evenari M., Kappen L. & Buschbom U. (1974) The role of air humidity and leaf temperature in controlling stomatal resistance of *Prunus armeniaca* L. under desert conditions. I. A simulation of daily course of stomatal resistance. *Oecologia* **17**, 159–170.

Schulze E.-D., Turner N.C., Gollan T. & Shackel K.A. (1987) Stomatal responses to air humidity and to soil drought. In Z Zeiger, GD Farquhar, IR Cowan, EDs, *Stomatal Function*. CA: Stanford University Press, pp 311–321.

Scholz F.G., Bucci S.G., Goldstein G., Meinzer F.C., Franco A.C. & Miralles-Wilhelm F. (2007) Biophysical properties and functional significance of stem water storage tissues in Neotropical savanna trees. *Plant, Cell and Environment* **30**, 236–248.

Sellin A. & Kupper P. (2007) Temperature, light and leaf hydraulic conductance of little-leaf linden (*Tilia cordata*) in a mixed forest canopy. *Tree Physiology* **27**, 679–688.

Sevanto S., Suni T., Pumpanen J., Grönholm T., Kolari P., Nikinmaa E., Hari P. & Vesala T. (2006) Wintertime photosynthesis and water uptake in a boreal forest. *Tree Physiology* **26**, 749–57.

Sobrado M.A. (1993) Trade-off between water transport efficiency and leaf life span in a tropical dry forest. *Oecologia* **96**, 19–23.

Sobrado M.A. (1997) Embolism vulnerability in drought-deciduous and evergreen species of a tropical dry forest. *Acta Oecologia* **18**, 383–391

Sierra-Almeida A. & Cavieres L.A. (2010) Summer freezing resistance in high-elevation plants exposed to experimental warming in the central Chilean Andes. *Oecologia* **163**, 267–276.

Smillie R.M. & Hetherington S.E. (1999) Photoabatement by anthocyanin shields photosynthetic systems from light stress. *Photosynthetica* **36**, 451–463.

Smith W.K. & McClean T.M. (1989) Adaptive rrelationship between leaf water repellency, stomatal distribution, and gas exchange. *American Journal of Botany* **76**, 465–469.

Song Y.-C., Chen X.-Y. & Wang X.-H. (2005) Studies of evergreen broad-leaved forests of China: a retrospect and prospect. *Journal of East China Normal University*. **1**, 1–8. (In Chinese with English Abstract)

Sperry J.S. (1995) Limitations on stem water transport and their consequences. In: Plant stems. *Physiology and functional morphology,* B.L. Gartner, ED. San Diego: Academic Press, pp. 105–124.

Sperry J.S. & Sullivan J.E. (1992) Xylem embolism in response to freeze-thaw cycles and water stress in ring-porous, diffuse-porous, and conifer species. *Plant Physiology* **100**, 605–613.

Stone R. (2010) Severe drought puts spotlight on Chinese dams. *Science* **327**, 1311–1311.

Sun Y.H., Zhang H.J., Cheng J.H., Wang Y.J., Shi J. & Cheng Y.. (2006) Soil characteristics and water conservation of different forest types in Jinyun Mountain. *Journal of Soil and Water Conservation* **20**, 106–109.

Tan Z.-H., Zhang Y.-P., Schaefer D., Yu G.-R., Liang N. & Song Q.-H.. (2011) An old-growth subtropical Asian evergreen forest as a large carbon sink. *Atmospheric Environment* **45**, 1548–1554.

Taneda H. & Tateno M. (2005) Hydraulic conductivity, photosynthesis and leaf water balance in six evergreen woody species from fall to winter. *Tree physiology* **25**, 299–306.

Takashima T., Hikosaka K. & Hirose T. (2004) Photosynthesis or persistence: nitrogen allocation in leaves of evergreen and deciduous Quercus Species. *Plant Cell and Environment* **27**, 1047–1054.

Tenhunen J.D., Pearcy R.W. & Lange O.L. (1987) Diurnal variations in leaf conductance and gas exchange in natural environments. In *Stomatal Function*, pp. 323–351.Eds E. Zeiger, G.D. Farquhar and I.P. Cowan. Stanford, CA, USA: Stanford University Press.

Terashima I., Funayama S. & Sonoike K. (1994) The site of photoinhibition in leaves of *Cucumis-sativus* L. at low temperatures is photosystem I, not photosystem II. *Planta* **193**, 300–306.

Thomashow M.F. (1999) Plant cold acclimation: Freezing tolerance genes and regulatory mechanisms. *Annual Review of Plant Physiology and Plant Molecular Biology* **50**, 571–599.

Trenberth K.E. (1999) Conceptual framework for changes of extremes of the hydrological cycle with climate change. *Climatic Change* **42**, 327–339.

Tucci M.L.S, Erismann N.M., Machado E.C. & Ribeiro R. (2010) Diurnal and seasonal variation in photosynthesis of peach palms grown under subtropical conditions. *Photosynthetica* **48**, 421–429.

Tyree M.T. & Richter H. (1981) Alternative methods of analyzing water potential isotherms: some cautions and clarifications. *Journal of Experimental Botany* **32**, 643–653.

Tyree M.T. & Sperry J.S. (1989) Vulnerability of xylem to cavitation and embolism. *Annual Review of Plant Physiology and Molecular Biology* **40**, l9–38.

Tyree M.T. & Zimmermann M.H. (2002) *Xylem structure and the ascent of sap*. Springer, New York Berlin Heidelberg.

Wilner J. (1960) Relative and absolute electrolytic conductance tests for frost hardiness of apple varieties. *Canadian Journal of Plant Science* **40**, 630–637.

Wolfe J.A. (1987) Late Cretaceous-Cenozoic history of deciduousness and the terminal Cretaceous event. *Paleobiology* **13**, 215–226.

Woodruff D.R., Mcculloh K.A., Warren J.M., Meinzer F.C. & Lachenbruch, B. (2007) Impacts of tree height on leaf hydraulic architecture and stomatal control in Douglas-fir. *Plant, Cell and Environment* **30**, 559–569.

Wright I.J., Reich P.B., Westoby M., Ackerly D.D., Baruch Z., Bongers F., Cavender-Bares J., Chapin T., Cornelissen J.H.C., Diemer M., Flexas J., Garnier E., Groom P.K., Gulias J., Hikosaka K., Lamont B.B., Lee T., Lee W., Lusk C., Midgley J.J., Navas M.L., Niinemets U., Oleksyn J., Osada N., Poorter H., Poot P., Prior L., Pyankov V.I., Roumet C., Thomas S.C., Tjoelker M.G., Veneklaas E.J. & Villar R. (2004) The worldwide leaf economics spectrum. *Nature*, **428**, 821–827.

Wu Z.-Y. (1980) *The vegetation of China*. Beijing: Science Press.

Xin Z. & Browse J. (2000) Cold comfort farm: the acclimation of plants to freezing temperatures. *Plant, Cell and Environment* **23**, 893–902.

Zang W.B., Ruan B.Q., Li J.G. & Huang S.F. (2010). Analysis of extraordinary meteorological drought in Southwest China by using TRMM precipitation data. *Journal of China Institute of Water Resources amd Hydropower Research* **8**, 97–106.

Ziegler A.D., Fox J.M. & Xu J. (2010) The rubber juggernaut. *Science* **324**, 1024–1025.

Zhang J.-L. & Cao K.-F. (2009) Stem hydraulics mediates leaf water status, carbon gain, nutrient use efficiencies and plant growth rates across dipterocarp species. *Functional Ecology* **23**, 658–667.

Zhang M., Yu G.-R., Zhuang J., Gentry R., Fu Y.-L., Sun X.-M., Zhang L.-M., Wen X.-F., Wang Q.-F., Han S.-J., Yan J.-H., Zhang Y.-P., Wang Y.-F. & Li Y.-N. (2011) Effects of cloudiness change on net ecosystem exchange light use efficiency, and water use efficiency in typical ecosystems of China. *Agricultural and Forest Meteorology* **151**, 803–16.

Zhang Y.-J., Meinzer F.C., Hao G.-Y., Scholz F.G., Bucci S.J., Takahashi F.S., Villalobos-Vega R, Giraldo J.P., Cao K-F., Hoffmann W.A. & Goldstein G. (2009) Size-dependent mortality in a Neotropical savanna tree: the role of height-related adjustments in hydraulic architecture and carbon allocation. *Plant, Cell and Environment* **32**, 1456–66.

Zufferey V., Cochard H., Ameglio T., Spring J.L. & Viret O. (2011) Diurnal cycles of embolism formation and repair in petioles of grapevine (*Vitisvinifera* cv. *Chasselas*). *Journal of Experimental Botany* **62**, 3885–3894.

Zwieniecki M.A. & Holbrook N.M. (2009) Confronting Maxwell's demon: biophysics of xylem embolism repair. *Trends in Plant Science* **14**, 530–534.